

GENE-TERATOGEN INTERACTION IN INSULIN-INDUCED
MOUSE EXENCEPHALY

A thesis submitted to the School of Graduate Studies in
partial fulfillment of the requirements for the degree of
Master of Science.

by

Wendy Anne Cole

Department of Biology
McGill University
Montreal, Canada
December, 1978

ABSTRACT

When a teratogen is administered to an organism heterozygous for a mutant gene the resulting modification can resemble the phenotype normally found in the mutant homozygote. The mutant gene, in a single dose, and the teratogen potentiate the phenotypic trait; that is to say, there is a gene-teratogen interaction. Two autosomal dominant genes of the mouse, Crooked-tail (Cd) and Rib fusions (Rf) yield spontaneous exencephaly in their homozygous form, the heterozygotes remaining unaffected. Two strains of inbred females, A/J and SWV, were crossed to heterozygote and wild-type males, and treated with insulin, known to induce exencephaly. The nonparallelism of the dose-response curves indicated a gene-teratogen interaction. Severe twisting of the hindbody was present in some of the early exencephalic embryos from the treated heterozygote crosses. Such kinking of the hindbody is normally seen spontaneously only among mutant homozygotes, suggesting that the insulin and mutant gene interacted in the heterozygote to form a phenocopy. The stress placed on the neural folds by this twisting prevented fusion and led to the condition of exencephaly. It was suggested.

RESUME

Quand un tératogène est administré à un organisme hétérozygote pour un gène, la modification résultante peut ressembler au phénotype normalement retrouvé chez le mutant homozygote. Le gène mutant, en dose simple et le tératogène donnent de la force au trait phénotypique; c'est-à-dire une action réciproque entre le gène et le tératogène. Deux gènes autosomals dominants "Crooked-tail" (Cd) et "Rib fusions" (Rf) produisent l'exencephalie spontanée dans leur forme homozygote, les hétérozygotes demeurant sans affectation. Deux lignées de femelles consanguines, A/J et SWV, furent croisées à des mâles hétérozygotes et de type sauvage, et traitées avec de l'insuline, reconnue pour induire l'exencephalie. Le non-parallélisme des courbes dose-réaction indique une action réciproque gène-tératogène. Une torsion sévère de la partie postérieure du corps était présente chez quelque-uns des premiers embryons exencephaliques des croisements hétérozygotes traités. Un tel tortillement de la partie postérieure du corps n'est ordinairement observé spontanément que chez les mutants homozygotes, suggérant que l'insuline et le gène mutant ont agi un sur l'autre dans l'hétérozygote pour former une phénocopie. La tension placée sur les pîs neurax par cette torsion a prévenu le fusionnement et a mené à la condition d'exencephalie.

ACKNOWLEDGEMENTS

I would like to thank my advisor, Dr. D. G. Traylor, for encouragement, advice, and helpful suggestions given during the course of my work. I would also like to thank the other members of my committee, Dr. F. C. Fraser and Dr. J. Matrakos, for many stimulating discussions of the data.

My thanks to Dr. F. G. Biddle and Dr. D. M. Juriloff for their generous expenditure of time, knowledge, and effort in teaching me the applications of probit analysis to the field of teratology.

I am grateful to Mr. R. Lamarche for demonstrating the necessary photographic techniques to me, and to Ms. L. Ohannessian for invaluable assistance with laboratory techniques.

My thanks to Dr. B. Taylor and Dr. K. Sittmann for advice on statistical analyses, to Mr. J. Bolvin for assistance with the computer programs, and to Ms. M. Machado and Mr. J. Sproule for useful discussions of my experiments.

A special note of thanks to Ms. R. Bayreuther for drawing the figures.

TABLE OF CONTENTS

<u>Contents</u>	<u>page</u>
Abstract	i
Resume	ii
Acknowledgements	iii
Table of Contents	iv
List of Figures	vii
List of Tables	ix
 Introduction.....	 1
A. Literature Review	4
1. Early embryological development in the mouse	4
2. Abnormal neural tube development	8
3. Spontaneous exencephaly in the mouse	13
4. Induced exencephaly in the mouse	17
5. Anencephaly	21
6. Gene-teratogen interaction	26
B. Materials and Methods	36
1. General	36
2. The dose-response experiments	37
i) A/J dams	37
ii) SVV dams	41

3.	Probit analysis	44
4.	Morphological rating	48
5.	Log-linear analysis	53
6.	Histology	55
7.	Protection with glucose	56
C.	Results	58
1.	Induced exencephaly; A/J dams	58
2.	Induced exencephaly; SWV dams	63
3.	Analysis of the stained skeletons	72
4.	Resorption data; A/J dams	78
5.	Resorption data; SWV dams	82
6.	Common slopes: A comparison of the calculated probit regressions	85
7.	Analysis of the morphological data	90
8.	Analysis of the histology	111
9.	Effectiveness of glucose supplements	130
D.	Discussion	133
1.	Gene-teratogen interaction in insulin-induced exencephaly and resorption	133
2.	The teratogenicity of insulin	140
3.	The underlying biological mechanisms of the interaction	146

E.	Summary	155
	Appendix	158
	Bibliography	159

LIST OF FIGURES

<u>Figure</u>		<u>page</u>
B1	Time-response curves of insulin-induced exencephaly for the crosses with the A/J dams.	40
B2	Time-response curves of insulin-induced exencephaly for the crosses with the SWV dams.	43
C1	Independently fitted probit dose-responses of insulin-induced exencephaly for the A x Cd/+ and A x +/-Cd crosses.	60
C2	Independently fitted probit dose-responses of insulin-induced exencephaly for the A x Rf/+, A x +/-Rf, and A x A crosses.	61
C3	Independently fitted probit dose-responses of insulin-induced exencephaly for the crosses with the A/J dams.	62
C4	Independently fitted probit dose-responses of insulin-induced exencephaly for the SWV x Cd/+ and SWV x +/-Cd crosses.	69
C5	Independently fitted probit dose-responses of insulin-induced exencephaly for the SWV x Rf/+, SWV x +/-Rf, and SWV x SWV crosses.	70
C6	Independently fitted probit dose-responses of insulin-induced exencephaly for the crosses with the SWV dams.	71
C7	Independently fitted probit dose-responses of resorption for the crosses with the A/J dams (corrected for spontaneous resorption).	79

C8	Independently fitted probit dose-responses of resorption for the crosses with the A/J dams (corrected for spontaneous resorption).	80
C9	Independently fitted probit dose-responses of resorption for the crosses with the SWV dams (corrected for spontaneous resorption).	86
C10	Independently fitted probit dose-responses of resorption for the crosses with the SWV dams (corrected for spontaneous resorption).	87
C11 - C34	Photographs of normal and exencephalic embryos	102 - 105
C35	Histological section of abnormal neural tissue	127
Series C1	Histological sections of normal and abnormal neural and somite tissue	128- 129
Figure D1	Dosage-tolerance distributions of insulin-induced exencephaly for the crosses with the A/J dams	135

LIST OF TABLES

<u>Table</u>	<u>page</u>
B1 Insulin time response data; A/J dams	39
B2 Insulin time response data; SWV dams	42
B3 System used for morphological ratings of D8-10 embryos	50
B4 Stages of neural tube closure	51
B5 Stages of turning of the embryo	52
C1 Insulin dosage-response data; A/J dams	59
C2 ED ₅₀ 's and common and independently fitted slopes of probit regressions for insulin-induced exencephaly in A/J and SWV crosses	64
C3 Tests of parallelism; dose-response data	65
C4 Insulin dosage-response data; SWV dams	67
C5 Frequency of vertebral and rib malformations among D18 control embryos; SWV dams	74
C6 Frequency of vertebral and rib malformations among D18 embryos from the dose-response data; SWV dams	75
C7 Spontaneous resorption data; A/J and SWV dams	81
C8 ED ₅₀ 's and common and independently fitted slopes of probit regressions for insulin-induced resorptions in A/J and SWV crosses.	83
C9 Tests of parallelism; resorption data	84

C10	Tests of parallelism; analysis of the calculated common slopes for the induced exencephaly (dose-response) and resorption data	89
C11	Fisher's exact test; A/J and SWV dams, a comparison of the frequency of exencephaly for the dose-response (collected on D14 and D18) and the morphological data (collected on D9/12, D9/18, and D10/6)	91
C12	Analysis of the morphological data from the treated mutant and nonmutant crosses into normal, delayed, or abnormal turning classifications	95
C13	Tests of partial and marginal associations for the variables of the morphological analysis	107-108
C14	Mean mitotic indices for the neuroectoderm of the cephalic neural tube region of embryos from treated and control mutant crosses	113
C15	Mean mitotic indices for the neuroectoderm of the cephalic neural tube region of embryos from treated and control nonmutant crosses	114
C16	Mean mitotic indices for the mesoderm of the cephalic neural tube region of embryos from treated and control mutant crosses	116
C17	Mean mitotic indices for the mesoderm of the cephalic neural tube region of embryos from treated and control nonmutant crosses	117
C18	Mean mitotic indices for the neuroectoderm and mesoderm of the cephalic neural tube region of exencephalic embryos with a normal hindbody shape from treated mutant crosses	119

C19	Tests of partial and marginal associations for the variables of the mitotic index analysis	123
C20	Frequencies of exencephaly in the mutant and nonmutant crosses treated with insulin or insulin + glucose	131
Appendix 1	List of genotypes of the embryos comprising the mitotic index analysis	158

INTRODUCTION

One of the first major morphological processes to occur in the embryological development of the mouse is closure of the neural tube. Failure of complete neural fold closure in the cephalic region leads to the malformation known as exencephaly. It is characterized by an extruding mass of histologically normal neural tissue resting on top of a rudimentary skull. This malformation is present in the human population as anencephaly. In this highly prevalent and lethal birth defect of the central nervous system the exposed brain undergoes extensive degeneration, due to the length of the gestational period; hence at birth the fetus is born without a brain. An increased alpha-fetoprotein level in the amniotic fluid serves as the method of detecting affected fetuses. Recently, this same increased level has been found in rats and mice, suggesting the use of a small mammal as an animal model for human exencephaly (anencephaly).

Experimental studies on the morphological events leading to the formation of exencephaly have resulted in conflicting concepts to explain its occurrence. Basically advocating either the failure of the neural tube to close or the reopening of a closed neural tube, the hypotheses include neural overgrowth, spinal retroflexion, insufficient amounts of neural tissue, and increased intraluminal pressure. These postulated underlying mechanisms that produce such a severe morphological change have sometimes been traced to ultrastructural alterations and necrosis in specific cells of the affected tissue.

Exencephaly in the mouse is inherited in certain mutant strains of mice, and it is also induced by a variety of substances, known as teratogens for their ability to disrupt normal development. It was felt that the administration of a teratogen known to induce exencephaly to a strain of mice that developed the defect spontaneously could result in a 'gene-teratogen interaction'. This interaction would involve not only an increase in the frequency of exencephalic fetuses, but the action of gene and teratogen would be to affect the same developmental process in such a way as to change the quality as well as the quantity of the response. The term interaction implies the formation of a unique relationship between gene and teratogen, acting on some event in a unified and specific manner. In the past the establishment of an interaction has rested on the delineation of this unique underlying mechanism, although it has not always been possible to isolate and characterize it. Recent work on genotype-teratogen interactions has advocated the use of probit analysis to statistically define an interaction.

In this study two autosomal dominant genes, Crooked-tail (Cd) and Rib fusion (Rf) were used. These genes yield spontaneous exencephaly in their homozygous form, but the heterozygotes remain unaffected. Unrelated normal inbred females were crossed to heterozygous males and treated with insulin, known to induce exencephaly. The dose-response curves for the induction of

exencephaly with insulin in these mice were established. These were then analyzed for the presence of a gene-teratogen interaction. Treated and control embryos were compared for the morphological changes that occur during normal and exencephalic brain formation in order to find criteria for discriminating between the two states. Light microscopic examination of treated and untreated embryological neural tissue was also undertaken to further elucidate the underlying mechanism(s) functioning in the production of exencephaly. Preliminary work was done to separate the teratogenic effects of insulin administration and maternal hypoglycemia, the physiological state caused by the treatment. Glucose was administered to counteract the severe drop in the blood sugar level, and its resultant effect on the induction of exencephaly was noted.

A. Literature Review

1. Early embryological development in the mouse

The development of the mouse embryo has been studied extensively (Adelmann, 1925; Theller, 1972) and the following is a brief discussion of the events prior to neural tube closure. By day 5 of gestation the embryo has implanted in the lining of the uterine wall. The uterine mucosa reacts with the growth of a deciduous capsule separating the embryo from the uterine cavity and forcing it to continue deriving nutrients from the yolk sac. The yolk sac is replaced by a true, visceral placenta on day 10. At that time the mucosal lining of the mesometrial uterine region, the decidua basalis, fuses with the chorion and the allantois, linking the embryo to the maternal blood supply. The inner cell mass or egg cylinder of the embryo has, by day 6, separated into an outer layer of extraembryonic ectoderm, an underlying layer of embryonic ectoderm, and a central core of endoderm. The latter gives rise to Reichert's membrane, which effectively joins with the yolk sac in maintaining the embryo as an autonomous unit until the true placenta is formed. The extraembryonic ectoderm gives rise to outer membranes (chorion and allantois), the inner ectoderm to neural structures, and the endoderm to gastrointestinal structures. The primitive streak, which marks the primary axis of the embryo, begins at the posterior region of the egg cylinder as a thickening of the inner ectoderm. Also at this time the mesenchyme is proliferating laterally between the primitive streak and the endoderm.

At day 7 of gestation the ectoderm in the ventral margin of the egg cylinder begins to thicken, forming a projection known as the head process. Above this region the endoderm, in forming the foregut, begins to move the anterior end of the embryo above the rudimentary heart, until the head process becomes a head fold. The notochord is formed from endoderm lying under the head process, and with continued proliferation of mesoderm the first structures of the three germ layers continue to differentiate. By late day 7, migrating mesoderm begins to aggregate into paired somites adjacent to the notochord, the actual number increasing with continued development. Somite number is thus considered to be a reliable index of embryonic age.

The development of the neural tube is first noticed on day 7, when the ectoderm above the primitive streak begins to thicken and form the neural plate. By early day 8 one can see at least four pairs of somites and a deepening depression in the neural plate, the neural groove, accompanies the formation of neural folds. When the number of somite pairs has increased to 8 (day 8/12 hours) these folds fuse at the level of the fifth somite.

Up to this point the embryo has maintained an S-shaped body configuration, with a concave mid-region. However, due to the rapid growth of the foregut, the embryo must now change from this lordotic curvature to a kyphotic one. The head and tail folds begin a clockwise rotation, with the

trunk area initially remaining stationary due to its firm attachment to the yolk sac. Before completion of rotation, the midgut region does turn, and in doing so, causes the relative position of the placenta, previously ventral, to become dorsal. The turning procedure is completed by early day 9, at which time the embryo possesses a convex dorsal flexion, with the hindbody lying to the right side of the head.

After the initial fusion of the neural folds closure progresses rapidly in both cephalad and caudad directions (Geelen and Langman, 1977). The head fold shows primitive signs of differentiation into a fore (prosencephalon), mid (mesencephalon), and hindbrain (rhombencephalon). Closure at the middle of the prosencephalon also occurs at D8/12 (D = day), and proceeds in both directions until the entire prosencephalic region of the neural tube is closed by D8/18. By early D9 (at the 15-18 somite stage) the closure of the neural tube has progressed to the caudal end of the mesencephalon, also known as the anterior neuropore. By D 9/12 (22-28 somites) closure is incomplete only over the roof of the rhombencephalon and at the posterior neuropore. Therefore incipient exencephaly may be identified by early D 9, if the anterior neuropore has remained open. The posterior neuropore closes by early D 10 (30-34 somites), completing neural tube closure.

The sequence of events in neural tube closure has also been examined at a cellular level in chicks (Langman et al, 1966) and hamsters (Marín-Padilla, 1970). The neural folds are a complex tissue composed of an outer ectoderm and an inner neuroectoderm, supported by an underlying layer of mesoderm. Presumptive neural-crest cells aggregate between the surface ectoderm and neuroectoderm. At the time of fusion it is these cells that make the initial contact. The ectodermal cells fuse next, and establish a continuous surface layer. The neural-crest cells, proliferating rapidly, form a wedge of cells that prevents fusion of the neuroectodermal layer. It is only when the neural-crest cells migrate laterally that the neuroectoderm cells make initial contact, fusing along their internal (ependymal) surface. As the neuroectoderm completes fusion, forming a closed neural tube, the mesodermal cells then occupy the space that has developed between this layer and the surface ectoderm.

The final stages of brain development involve changes in shape and size due to the production of cerebrospinal fluid (Coulombre and Coulombre, 1958). Upon closure of the neural tube neuroepithelial cells secrete cerebrospinal fluid into a sealed compartment. Overproduction of cerebrospinal fluid has been isolated as a cause of hydrocephalus in dogs (James et al, 1977) and its removal, by intubation, from developing chick embryo brains resulted in greatly reduced

cavity volumes (Desmond and Jacobson, 1977). Therefore cerebrospinal fluid pressure may be considered a mechanical force acting on the neural tube after its closure, with any malfunction potentiating the occurrence of a neural tube defect.

2. Abnormal neural tube development

Exencephaly is characterized by the presence of the neural tissue of the brain on the exterior of the cranial cavity. It can be defined as a 'small cranial aperture with intact overlying tissues' (Lemire et al, 1978). By day nine of gestation in the mouse, failure of closure of the anterior neuropore region in the brain is indicative of impending exencephaly. Although the minimum requirement for classification as such is a failure of fusion in the mesencephalic region, generally the prosencephalon (composed of diencephalon and telencephalon) remains open as well. Therefore only the rhombencephalic area will have fused completely. Examination of exencephaly in the rat (Giroud and Martinet, 1957) has shown that regional histological differentiation continues to proceed, despite the exposure of the neural tissue to the amniotic fluid. Thickening of the lateral walls of the telencephalon gives rise to hemispheres. The optic and otic vesicles, olfactory lobes, and neurohypophysis also begin to take form. The diencephalon radiates out along its dorsal surface, and its abnormal,

everted position causes the cerebral hemispheres to develop under this surface. The choroid plexus tissue, as the roof of the diencephalon, is now contiguous with the hemispheres as the brain continues to grow in an everted, reverse arrangement. The corpora striata, normally one of the innermost tissues of the brain, fuses with the thin covering of surface ectoderm. By day 13 the brain is now an overgrown mass of neural tissue spilling out over a rudimentary cranial base. The epithelium is thinly stretched over the cerebrovascular tissue, and the cranial base is poorly formed. The presence of pyknotic nuclei and hemorrhagic patches indicates the commencement of cell death, which ultimately would lead to complete degeneration of the exposed tissue, a condition known as anencephaly. However, the gestational period of the rat, like the mouse, is sufficiently short-term so as to yield preserved specimens of exencephaly prior to a stage of extensive necrosis.

The pathogenesis of exencephaly has been closely examined in an attempt to explain the malfunction (s) responsible for its formation. The more popular concept (Marín-Padilla, 1966) is that the neural tube fails to close, but there is an alternate postulate based on the premise of a reopened neural tube. The latter is advocated by Gardner (1961, 1977), who proposes an increase in intraluminal pressure as the mechanical factor that forces a closed neural tube to split open. This pressure is caused by the production of cerebrospinal fluid by

the neuroepithelial cells, and its great increase must somehow be due to abnormal absorption of the fluid. Murakami et al (1972), tested this hypothesis in rats by injecting vincristine intraperitoneally after the period of neural tube closure. This caused distension and eventually the formation of elevated blebs on the surface of the neural tube. Histological examination revealed that the neural fold tissue showed signs of early necrosis, similar to that found in exencephalic brain tissue. Sundt et al (1976) reported similar findings after injection of a cadmium sulphate solution.

The preferred hypothesis, supported by a large amount of experimental evidence, is that of a failure of the neural tube to close. Several theories, based on mechanical interference of the closure process, have been advocated to explain nonclosure.

The first theory is one of neural overgrowth, resulting from a study on caudal myelochisis in young human embryos (Patten, 1952). Areas of tissue degeneration corresponding to regions of extensive neuroepithelial infoldings into the lumen of the neural tube were noted. The inpocketing of the neuroepithelium removed it from the vascularized mesenchyme, and led ultimately to necrosis of the cells, resulting in open lesions. Bergquist (1959) induced overgrowth in the brains of chick embryos, by exposure to low oxygen tension, to uncover its possible origin. Evidence of damage to the chordamesoderm tissue layer led to the theory

that the chordamesoderm must control not only the initial induction of the neural plate, but morphogenesis of the early neural tube as well. Further histological studies of chick development (Burda, 1968) indicated that it is a lack of contact between the underlying notochord and cells of the neural tube that induces overgrowth. Recent studies (Freeman, 1975) have determined that the process of overgrowth involves a significant increase in mitotic activity of the neuroepithelial cells during neural tube formation.

A second possible mechanism to account for the failure of the neural tube to close is severe spinaflexion (Kvist, 1975). Administration of vitamin A to developing chick embryos resulted in severe retroflexion, with associated somite disorganization. The subsequent abnormal twisting of the embryo prevents the neural folds from coming into contact and fusing. This situation had been previously noted with the induction of exencephaly in mice treated with trypan blue on day 8 gestation (Hamburgh, 1954). The developing neural folds became wavy, with irregular twists and bleb formation. Also there was increased growth of the neural tissue, further blocking the fusion of the folds along the midline.

The third mechanism put forth to explain the formation of exencephaly is that of insufficient amounts of neural tissue due to extensive cell death. The neural folds do not meet because there is not enough tissue to allow

contact. This can be further subdivided into a lack of sufficient neuro-epithelium, a lack of sufficient mesoderm (the underlying supportive tissue), or both.

A decrease in mesoderm has been demonstrated in golden hamsters exhibiting exencephaly after treatment with vitamin A (Marin-Padilla and Fern, 1965; Marin-Padilla, 1966). In the cephalic region of the neural folds, the cells of the mesoderm show severe shrinkage of their cytoplasm, followed by a significant reduction in the mitotic rate of mesodermal cells. The changes result in the eventual death of the cell, indicated by pyknotic nuclei. The failure of the neural folds to meet and fuse is thus associated with a lack of sufficient mesoderm to push the folds together. Morriss and Steele (1977) have studied vitamin A-induced exencephaly in the rat, and have observed that the ultrastructure of the mesodermal cells demonstrates swelling of the endoplasmic reticulum and Golgi apparatus. Such changes are associated with cell death, the cause of decreased proliferative activity. This finding opposes the conclusions of a similar E/M study by Theodosis (1974), in which cell death was restricted to the neuroepithelium.

For chick, rat, and mouse embryos ultrastructural alterations resulting in cell necrosis have been limited to the neuroepithelium following the administration of cadmium (Yamamura et al, 1972), maternal malnutrition (Shimada et al, 1977), hydroxyurea (Sadler and Cardell, 1977), EDTA (Daniels and Moore, 1972) and FUDR (Cardell and Langman, 1977). Abundant cell death and severely decreased

mitotic activity in the cell population following these treatments is associated with a decreased amount of neuroepithelium that is capable of making contact, and thus the brain develops into an exencephalic form (Crowley et al, 1978).

Therefore some authors propose the primary defect to be localized in the mesoderm (Marín-Padilla and Fern, 1965), while others (cited above) postulate a loss of neuroepithelium. However, this conflict may be partly resolved by noting that whether the loss of cells is in the neuroepithelium or in the mesoderm could depend on the specific treatment. Different teratogens could interfere with the survival of cells in either of the two layers.

3. Spontaneous exencephaly in the mouse

The presence of inherited congenital malformations of the central nervous system is a common occurrence in certain strains of mice, but the underlying causes of the defects have seldom been conclusively established. Studies of the embryological development during the period of neural tube closure have often assumed associated effects of the abnormal development (i.e. wavy neural tube) to be the initial cause of the malformation. In fact, cellular changes occurring within the tissues of the neural folds could be the underlying factor accounting for the gross morphological abnormalities seen. Therefore, although the genetics of inherited exencephaly have been well-defined, the proposed causal mechanisms can be questioned.

In 1923, Little and Bagg irradiated a strain of mice, and noted the appearance of exencephalic-like mice in the fourth generation. The gene, my (myencephalic blebs), is recessive and therefore only homozygotes are affected. Cystic fluid filled vesicles erupt along the neural folds, preventing their complete closure in the mesencephalic region. This was demonstrated after an extensive histological examination of the affected embryos (Carter, 1959), and was in opposition to an earlier study by Bonnevie (1934), who felt the blebs were the result of increased cerebrospinal fluid reopening a closed neural tube. The latter study, however, lacked the strong morphological evidence found in Carter's work. Pseudencephaly (Bonnevie, 1936) was also found in a stock that carried the my gene, although its genetic disassociation from my was never firmly established. An exposed brain characteristic of exencephaly was present, and microscopic examination revealed the neural tissue to be histologically well differentiated, in spite of the spacial reorganization. The failure of the neural tube closure was associated with extreme irregularities and curvatures in the cervical region, and the resultant tension produced by this twisting was believed to be the mechanism causing nonclosure. However, any underlying cellular conditions stimulating the production of these flexures were not determined. Johnson (1967 a) reported a semi-dominant gene, Extra-toes (Xt), that acts as a lethal in its homozygous form, producing severe polydactyly frequently

accompanied by exencephaly. An allele of *Xt*, known as brachyphalangy (*Xt^{bph}*, Johnson, 1967 b), also produces digital defects and exencephaly. The embryological changes leading to the neural tube defect have not been investigated. Other reports of inherited exencephaly include the recessive genes open eyelid (*oel*, Brown and Hame, 1973) and exencephaly (*xn*, Wallace, 1976), the *tw⁸* allele of the Brachyury gene (Bruch, 1967), and the dominant gene Bent-tail (*Bn*, Butler and Lyon, 1967). All these genes express exencephaly regularly in a proportion of the homozygotes.

Exencephaly has also been reported in association with spina bifida (a lesion of the neural tube in the lumbosacrocaudal area) for other genes of the mouse. Splatch (*Sp*), an autosomal dominant, shows open neural folds of the head region in addition to myelocschisis of the hind area in some homozygotes (Auerbach, 1954). Extensive overgrowth is considered to be the causal force that prevents the folds from fusing. This theory is supported by studies measuring the mitotic index of affected neural tubes (Wilson, 1974) which showed a significant increase in cell proliferation in the regions of nonclosure. Chesley (1935) noted neural tube abnormalities in the development of the mutant Short-tail (*Sd*). In the homozygous form, this autosomal semi-dominant severely affects the axial skeleton. An embryological study (Gluecksohn-Schoenheimer, 1945) revealed severe degeneration of the tail due to notochord discontinuity. Blabs of surface ectoderm anterior to the sacral region of the neural tube resulted in nonclosure, producing both spina bifida and exencephaly.

Still another semi-dominant gene producing exencephaly in some homozygotes is Loop-tail (Lp, Strong and Hollander, 1949). The failure of the neural folds to fuse is extensive, extending past the cephalic region down the dorsal surface of the embryo. Recent electron microscopic examination of the tissue detected surface defects of the neuroepithelial cells, ultimately resulting in necrosis of this layer (Wilson and Michael, 1975).

The two mutant genes used in the present study also exhibit spontaneous exencephaly. Rib fusions (Rf) and Crooked-tail (Cd) are autosomal semidominant genes that cause lethal exencephaly in the homozygous form. The Crooked-tail gene, reported by Morgan (1954), produces a series of axial skeletal defects in both heterozygotes and homozygotes, with the latter exhibiting an increased frequency and severity of the malformations. The characteristic crooked tail arises from vertebral anomalies. The one consistent criterion to distinguish the gene-bearing mutants from the unaffected wildtype is the presence of abnormal caudal vertebrae. The vertebrae in this region may be small, misaligned and/or fused, with variation in the number affected. The homozygotes can be separated from the heterozygotes by possession of malformed vertebrae extending up into the thoracic region, and missing vertebrae in the lumbar and thoracic regions. Of the embryos examined on D₁₈ gestation 4% of the homozygotes are exencephalic, a malformation not seen in the heterozygous condition.

The Rf gene affects the formation of the ribs and spinal column in the developing embryo. Unlike the Crooked-tail mutant studies, embryological observations were made (Theller and Stevens, 1960) to determine the mode of action of the Rib fusion gene. Homozygotes can be identified by D 9 of gestation, when abnormalities in somite and neural tube formation are first detected. The neural folds are irregular and wavy in appearance, an effect that is thought to be associated with the observed presence of disorganized somites. By D 10, 15% of the homozygotes are exencephalic, and by D 12 additional abnormalities of the ribs appear. Heterozygotes never develop exencephaly, and are detected only by the presence of fused ribs by D 12.

The presence of spontaneous exencephaly in a proportion of the homozygous Cd and Rf mutants, and its absence in the heterozygous state, prompted the use of these two genes in the present study.

4. Induced exencephaly in the mouse

Teratogens affecting the central nervous system interfere with the normal pattern of neural tube development, however their underlying mechanism is not always well established. Some prevent neural tube closure and induce exencephaly. To be effective the teratogen must be administered during a specific time in gestation. This 'critical period', during which the organism is capable

of responding to the action of the teratogen, is dependent on the embryo's stage of development, the duration of the insult's effectiveness, and the mechanism by which the malformation is produced (Landauer, 1954).

Exencephaly has been induced in several species with a wide range of substances. It has been produced in rabbits treated with concanavalin A (Desesso, 1976), in cats with antifungal drugs (Scott et al, 1975), in frogs with trypan blue (Greenhouse and Hamburg, 1968), and in chicks with methylmercury (Gillani, 1974), histones (Horel et al, 1973), hypoxia (Jaffee, 1974), inhibitors of DNA synthesis (Lee et al, 1976), antibiotics (Singh and Singh, 1974), and vitamin A (Kvist, 1975). Rat fetuses exhibit exencephaly after treatment with sodium arsenate (Beaudoin, 1974), diazo dyes (Beaudoin, 1969), procarbazine (Chaube and Murphy, 1969), glucose in culture (Cockcroft and Coppola, 1977), vitamin A (Kochhar, 1968), hyperthermia (Edwards, 1968), diphenylhydantoin (Mercier-Parot and Tuchmann-Duplessis, 1974), maternal zinc deficiency (Warkany and Petering, 1971), and salicylate poisoning (Warkany and Takacs, 1959). Administration of sodium arsenate (Carpenter and Fern, 1977), cadmium (Fern, 1971), trypan blue (Fern, 1958), retinoic acid (Shenefelt, 1972), 6-aminocaproic acid (Turbow et al, 1971) and hyperthermia (Kilham and Fern, 1976) each yield exencephaly in the golden hamster.

Though some substances are teratogenic in several different species it cannot be assumed that a single mode of action is equally effective in all organisms exposed to them. Therefore there are limitations in applying experimental animal data to humans and only guarded extrapolations should be made. Though the morphological changes are well characterized, the underlying mechanisms to explain such alterations remain obscure. Exceptions to this are the studies on the effects of trypan blue (Dencker, 1977), excess vitamin A (Marín-Padilla, 1966), EDTA (Daniels and Moore, 1973), and hydroxyurea (Sadler and Cardell, 1977), in which histological examination of the affected neural tissue has isolated cellular abnormalities responsible for the malformation.

Exencephaly can be induced in the mouse with many substances, including mycotoxins (Hayes et al, 1974), kidney antisera (McCallion, 1972), nitroguanidine (Inoue, 1975), methamphetamines (Kasirsky and Tansy, 1971), polybrominated biphenyls (Corbett et al, 1975), phenobarbital (Gibson and Becker, 1969), cytochalasin D (Shepard and Greenaway, 1977), inhibitors of DNA synthesis (Skalko, 1971), trypan blue (Hamburgh, 1952), cadmium (Pierro and Haines, 1977), maternal fasting (Miller, 1962), and stress (Hamburgh et al, 1974).

The administration of insulin has also been demonstrated to induce exencephaly (Smithberg et al, 1956; Smithberg and Runner, 1963). Several inbred strains of pregnant mice were injected with 4-5 units/kg. of protamine zinc insulin

on D 8 of gestation, and their offspring showed significant increases in the frequency of exencephaly. Vertebral and rib defects were also noted. Vertebral abnormalities have also been found in the fetuses of rats treated with insulin throughout pregnancy (Lichtenstein et al, 1951). Many of the vertebral centra lacked complete ossification, as did the carpals and phalanges of the limbs. Pregnant rats treated with insulin on D 7-9 of gestation produced offspring with fused or duplicated centra. When the rats were subjected to a 48 hour fast prior to the treatment additional ossification defects of the axial skeleton were encountered (Hannah and Moore, 1971). This is in opposition to a similar study by Ream and his coworkers (1970) in which administration of massive doses of insulin to pregnant rats on D 7-9 gestation failed to produce skeletal defects.

Previous work had indicated the teratogenicity of insulin in chick development. Duraiswami (1950) observed a poorly ossified skeleton and shortened beak and limbs after insulin treatment of chick embryos on D 0-6 of incubation. Landauer (1946, 1962) injected insulin into the yolk sac of developing chick embryos and induced several types of malformations. Rumplessness, a partial or complete lack of tail structures, was induced after injection of insulin on the first day of incubation (24 hour stage), while micromelia and malformed beaks were produced after treatment on day 4 (96 hours). Examination of cells of the brain and trunk regions of chick embryos affected by insulin treatment have

demonstrated ultrastructural changes that include a severe decrease in the accumulation of RNA and protein (Hickey and Klein, 1971).

The evidence for the action of insulin as a teratogen of neural tube and skeletal development prompted its use in the present study.

5. Anencephaly

The human counterpart to mouse exencephaly is known as anencephaly. In affected human fetuses due to the long gestational period, the exposed mass of neural tissue degenerates, leading to the absence of not only the cranial vault, but also the overlying tissue as well. The severity of the defect is dependent upon the extent of cranioschisis. The shortened, thick neck, protruding tongue and flattened nose characteristic of many anencephalics are strikingly similar to animal exencephalics. The embryological origin of anencephaly is generally accepted to be an initial formation of exencephaly due to a failure of neural tube closure (Recklinghausen, 1886; Marin-Padilla, 1970), followed by subsequent necrosis of the rudimentary brain. Some, however, argue that the cause is the reopening of a closed neural tube (Gardner, 1977; Chaurasia et al, 1976). In human development the anterior portion of the neural tube closes between days 24-26, while the posterior neuropore closes by day 35 (reviewed by Patten, 1968). Failure of closure of the latter results in the condition known

as spina bifida. The similar etiology of both malformations has led to the proposal that both are due to identical forms of defective closure occurring in isolated regions of the neural tube (Leck, 1972). The frequency of both defects occurring simultaneously is 10% (Warkany, 1971). Neural tube defects may occur alone or associated with other malformations (David and Nixon, 1976).

Anencephaly is a relatively common malformation. The incidence averages 1/1000, but many geographical areas show a significant increase in this figure. Variations in rates range from 5.9 (per 1000 births) in Ireland (Coffey, 1957) and 4.5 in South Wales (Carter et al, 1967) to .7 in Australia (Collman et al, 1968) and .8 in Japan (Neel, 1958). In Canada the average incidence is 1.6 (Elwood, 1974), with the rate in the province of Quebec being 1.4 (Herowitz and McDonald, 1969).

Epidemiological studies of neural tube defects have uncovered variations in pattern that suggest a multifactorial and complex causation. The prevalence of anencephaly has been related to geographic and ethnic differences. Variations with place can be seen within Canada, with regional differences extending from 2.1 in Prince Edward Island to .6 in British Columbia (Elwood, 1974; Trimble and Baird, 1978), and a gradient in prevalence extending from London (1.4) to Belfast (4.2) within the United Kingdom. (Elwood and Nevin, 1973). Ethnic differences have been demonstrated in a study where families

of French and English origin living in Quebec were shown to have a similar occurrence of neural tube defects (3.4 and 3.2, respectively), while the Jewish population had a much lower rate of .7 (Horowitz and McDonald, 1969).

Variations with time have also been observed in many studies of neural tube defects. The first is a long-term trend shown by an extended study (1950 - 65) in England in which a gradual, significant increase in the rate of neural tube defects followed by a return to the original level was noted (Leck, 1966). Seasonal fluctuations were also observed, with the rate of anencephaly in England and Wales increasing threefold among children conceived in the spring versus the fall, during the 1940's and 50's (Elwood and Nevin, 1973). Spina bifida has also been seen to follow this pattern, even in the absence of fluctuating seasonal rates for anencephaly (Carter and Evans, 1973).

Associations of maternal age and parity with the prevalence of neural tube defects have also been uncovered. The general trend is an increase in incidence near the end of reproduction (Leck, 1974), and in first births (Carter and Evans, 1973). The rate declines in second births, then increases again with successive births (Naggan, 1971). The effect of socioeconomic conditions has been extensively studied in England, where the rate of anencephaly has been found to be as much as fourtimes greater in the lower classes, although

this trend has been absent in many other studies, including one of the Jewish population in Boston (Naggon and MacMahon, 1967).

To avoid ambiguities in sex identification of early fetuses, chromosomal studies of phenotypically female anencephalics have been performed (Nakano, 1973). The variation of the sex ratio is wide, but overall indicates a preponderance of females. Pedigree studies to determine familial occurrence have demonstrated increased risks for sibs of affected children (Carter and Evans, 1973). However, concordance rates for twins, whether monozygotic or dizygotic, are lower than the frequency of recurrence in sibships (Yen and MacMahon, 1968). Since this indicates an environmental effect, Knox (1970) has explained discordance in twins by postulating the elimination of one twin, in cases of both affected, by some mechanism of 'fetus-fetus interaction'.

Environmental factors affecting the incidence of anencephaly and other neural tube defects have been inferred from pedigree studies. Attempts to identify these influences have correlated the prevalence of anencephaly to intake of tea (Fedrick, 1974), canned meats (Knox, 1974), and soft water (Elwood, 1977). Exposure to herpes virus has also been implicated in the increase of neural tube defects (McDonald et al, 1974). One of the more popular hypotheses to explain the rate of neural tube defects in Great Britain was the ingestion of blighted potatoes (Renwick, 1973). Spiers (1974) conducted an American study and could

not find such a correlation. The administration of the glycoalkaloid compounds found in blight to rats (Swinyard and Chaube, 1973; Ruddick, 1974), mice (Pierro, 1977) and rhesus monkeys (Allen et al, 1977) yielded negative results, although there is some indication of teratogenicity in chick embryos (Jelinek et al, 1976).

A study in which 13/14 diabetic women had children with neural tube deformities indicated an increased antagonism of the fetal plasma albumin to insulin (Wilson and Vallance-Owen, 1966). However, although cases of insulin administration during pregnancy have been reported to be associated with anencephalic births (White, 1949), neural tube defects are not considered a frequent congenital malformation in the infants of diabetic women (Pederson et al, 1964).

At present the only successful prevention of neural tube defects is early intra-uterine detection and abortion of affected fetuses. Between 13-16 weeks of gestation, the alpha-fetoprotein levels in the amniotic fluid rise sharply, indicating an open lesion (Brock and Sutcliffe, 1972). Recently, the amniotic alpha-fetoprotein levels have been tested in rats (Smith and Kellsher, 1977), and mice (Adinolfi et al, 1976) and a trend similar to the situation in human fetuses has been found. Therefore, in view of the severity and preponderance of anencephaly as a congenital malformation, the necessity of unravelling possible causes remains essential, despite the complexity

of the issue. The exencephalic condition in laboratory mammals may closely resemble the embryopathy and morphology of the early stages in human anencephaly. If similar patterns in tests of detection may be considered to be a mutual expression of the defect, then the mouse may yet serve as a valid model for studies of the etiology of anencephaly.

6. Gene-teratogen Interaction

Goldschmidt (1935) first used the term phenocopy to describe non-hereditary modifications in phenotype due to treatment with some environmental agent. In his experiments (1917, 1935), Drosophila flies exposed in the prepupal stages to increased temperatures deviated from normal morphological development. The malformations included eye, wing, bristle, body shape, and colour variations, and resembled the phenotypes of well known mutant genes. Thus, after an increase in temperature from 25° C to 31° C during the larval period, stubby, forked, extra and missing bristles, vestigial and spread wings, rough eyes, and dark coloured bodies were found instead of the wild-type characters. Other studies (Plough, 1933; Plough and Ives, 1935; Grossman and Smith, 1933) involving hundreds of thousands of flies and employing heat shock as the environmental insult also yielded a significant increase in the frequency of somatic variations. All flies were from the Florida wild stock, yet exhibited such phenotypes as crossveinless, sepia, sooty, and

truncate wing, normally restricted to mutant genotypes. Other studies using different environmental stimuli, such as neutron bombardment (Enzmann and Haskins, 1939) and x-rays (Blanc and Villée, 1942), produced individuals resembling genotypes other than the ones used. Additionally, Goldschmidt found the time at which certain phenocopies can be induced is highly specific. He had shown (1935) eye shape to be thermally sensitive during most of the third larval instar period, while wing effects such as truncate (Blanc and Child, 1940) and vestigial (Hersh and Ward, 1932) could be induced only at pupation.

Based on these studies Goldschmidt (1945) proposed a hypothesis of relative reaction velocities to account for the time-specific induction of phenocopies. He considered the role of a gene as controller of the cellular activities initiated during the process of development and subsequent differentiation. The normal action of the gene would be to trigger the production of those determining substances (hormones, catalysts, precursors) needed for the maintenance and specialized functions of a mature cell. Mutant genes interfere with these processes, possibly by disrupting these necessary chemical reactions, leading to a significant change in their reaction velocities. Environmental agents (i.e. heat shock) also interfere with the metabolic processes of the cell. Should these processes be the same as the ones acted on by mutant genes, then a phenocopy will occur. The final morphological entity is a total of all functioning developmental processes, and therefore any substance, be it

mutant gene or external effect, that can successfully interfere with these functions will yield some variations of the normal phenotype.

A consequence of Goldschmidt's theory was the prediction that organisms possessing a mutant gene known to effect some developmental event would respond more readily and more frequently upon exposure to an environmental agent associated with the production of a phenocopy of that mutant. This was demonstrated for bristle development in drosophila by both Plunkett (1926) and Ives (1939). The former used heterozygotes for the recessive genes dichaete and hairless, the latter used heterozygotes for the recessive gene scute. In both studies the exposure of the heterozygotes during the larval period to increased temperatures yielded a significantly higher frequency of phenocopies than among the treated wild-types. The same trend was established for mutant gene vestigial wing heterozygotes (Hersh and Ward, 1932; Stanley, 1935). This expressivity of a recessive gene in a single dose after exposure to a teratogen was designated as 'reversal of dominance' (Child et al, 1940). In all of the above studies the authors attributed the increased phenocopy frequency found among the treated heterozygotes to the dual presence of mutant gene and environmental insult, both acting on the same metabolic processes. Hersh and Ward found that the affected developmental event could be expressed as an exponential function of temperature. By plotting the phenocopy frequency (dependent variable) against the logarithm of the temperature (independent variable)

the slope of the line indicated the change in the reaction rate. The magnitude of this change in reaction velocity for the developmental process of wing formation was not the same for the treated heterozygotes and wild-type. The interaction of the gene with the teratogen had resulted in a new reaction velocity (slope of the line) that represented a unique underlying mode of action.

The work on phenocopies was further elucidated by Landauer using chick embryos. The administration of nicotine to chick embryos at 72 to 96 hours of incubation resulted in a shortening and twisting of the neck due to malformations of the cervical vertebrae (Landauer, 1960). Higher doses produced dwarfing, shortened beak, and hypoplasia of the muscles. These features paralleled those observed in the recessive 'crooked-neck dwarf' mutation. Treatment of phenotypically normal heterozygotes with nicotine gave a higher frequency of response to the teratogenic effects of nicotine than the wild-types. Another teratogen, insulin, whose phenotypic effects differed from those of the recessive mutant, failed to induce a higher frequency of response in the heterozygotes. This suggested that nicotine, but not insulin, interacted with the recessive gene by acting on the same metabolic pathway (s).

Treatment of chick embryos with 6-aminonicotinamide (6-AN) produced a syndrome of micromelia and beak defects (Landauer, 1957). In another set of experiments the interaction of 6-AN with several types of recessively inherited micromelia was studied (Landauer, 1965). The heterozygous embryos of the mm^A gene were more susceptible to 6-AN-induced micromelia than the normal

genotype. Heterozygotes of the mm^H and ch mutants, however, did not show this increased frequency in response. The conclusion was the mm^A gene and 6-AN exerted their effects on the same metabolic processes, while the mm^H and ch mutants had routes of action independent of 6-AN's. Landauer stressed that conclusive evidence for a gene-teratogen interaction would lie in the delineation of the underlying mechanism disrupting the cell processes.

Studies on the interaction of mutant genes with teratogens have also been performed in mice. The administration of trypan blue to mice heterozygous for the recessive gene eyelessness yielded a higher frequency of anophthalmia in these offspring than those of the treated normal strain (Barber, 1957; Beck, 1963). However later work indicated subline differences, in susceptibility to trypan blue, between the normal and gene-carrying populations (Beck, 1964). Therefore the differences in response could be quite unrelated to a gene-teratogen interaction. Heterozygotes for the recessive gene microphthalmia showed an increased frequency of affected embryos compared to the normal group after treatment with trypan blue (Hoshino et al, 1972). The effect of trypan blue on two autosomal dominant genes has also been examined. After treatment of pregnant females offspring homozygous for the Extra-toes gene demonstrated a higher frequency of exencephaly than the corresponding wild-type (Johnson, 1970). If an interaction was present one would expect the penetrance of the gene to be increased in the heterozygous offspring after treatment also. However, the frequency of exencephaly in the

heterozygotes did not differ significantly from that of the wild-type. Therefore Johnson concluded the pathways of action of the gene and teratogen to be different from one another, though no evidence was offered to support such a statement.

The administration of trypan blue to pregnant females also produced taillessness in the offspring heterozygous for the Brachyury gene, with the wild-type remaining unaffected (Hamburgh et al, 1970). Since this condition occurs spontaneously only in the homozygous mutant form, it was felt the treatment increased the penetrance of the gene. This could be accomplished by the action of gene and teratogen on the same metabolic pathway, but no evidence defining such an underlying mechanism was presented.

The mutant gene *lid gap*, which causes failure of eyelid fusion, fails to penetrate in 30 per cent of the mice who possess it. In an attempt to increase its penetrance pregnant females were treated with cortisone, but the offspring, all *lid gap* homozygotes, instead demonstrated a significant decrease in expressivity of the mutant phenotype (Watney and Miller, 1964). To hypothesize some mechanism by which the cortisone interfered with the action of the gene would have been mere speculation, a point well emphasized by the authors. Dagg (1967) studied the effect of fluorouracil (5-FU) and two mutant genes on limb development. High doses of 5-FU caused preaxial hyperphalangy and tibial hemimelia in the mouse. The mutants, *luxoid* and *luxate*, were two autosomal dominant genes that caused

polydactyly in heterozygotes, and tibial hemimelia in homozygotes. A low, non-teratogenic dose of 5-FU was administered to pregnant females and produced tibial hemimelia in the heterozygous offspring, a condition not found in the homozygous normal sibs. Still, Dagg stressed that the action of the gene and teratogen could not be surmised to act on the same biochemical processes. Similar results have been obtained from studies with 5-FU and the mutant Strong's luxoid (Forsthoefel, 1972; Forsthoefel and Williams, 1975), and 5-fluorodeoxycytidine and the limb deformity gene (Degenhardt et al, 1968). In these studies the heterozygous offspring, after treatment, phenotypically resembled the mutant homozygote.

Actinomycin D, an inhibitor of RNA synthesis, was administered to pregnant females in an attempt to analyze its potentiating effect on the Brachyury gene, T (Winfield and Bennett, 1971). As a heterozygote the T gene produces short tails, as a homozygote it is lethal. The recessive alleles (t) can all interact with the T gene to produce taillessness and deformities of the central nervous system, leading to early developmental arrest. After treatment heterozygous (T/+) females produced abnormal embryos at a frequency of 50%. The malformed embryos, presumed to be T/+, were phenotypically similar to those of T homozygotes and the lethal t allele. The authors suggested the actinomycin D must interact with the T gene in changing the heterozygotes into phenocopies of the T/T and t allele homozygotes. They felt the increase in expressivity of

the T gene by actinomycin was due to similar routes of action, but admitted the causative biochemical mechanism remained undefined. Tallness was also produced in heterozygous offspring after the pregnant females were exposed to T-2 toxin (Lary, 1977). Again, some underlying effect on a common metabolic route was postulated but not conclusively established.

Thus, many studies have described environmental-based changes in phenotype that mimic some variant known to be due to a change in genotype. The underlying mechanism in the production of these phenocopies is assumed to be a disruptive effect of both the mutant gene and the teratogen on the same developmental process, i.e. by acting on the same metabolic pathways. However, in many of these studies presented here, this underlying mechanism is not or cannot be brought to light. Thus there remained a need to establish some method by which a gene-teratogen interaction could be truly indicated. The term 'gene-teratogen interaction' could be considered to imply that these two factors join together to form a unique relationship, and in doing so, change the response of the organism. In a true interaction, the quality as well as the quantity of the response changes. What becomes important is not that the frequency of the malformation is increased, but that in some way the gene and teratogen act together to produce this response in a new and specialized manner.

Lewontin (1974) has used the term 'norm of reaction' to refer to the relationship of genotype and environment to phenotype. Given any two

genotypes, should one somehow interact with the environment in a way different from the other, the increments of change in the environment will not yield the same unit change in the two phenotypes. In a graph of genotype vs environment, the phenotypes could be represented as intersecting lines, their norms of reaction being truly different. Referring back to the work on drosophila, it was seen that a gene-teratogen interaction could be defined as some change in the reaction rate of a developmental process, and that this new reaction velocity could be characterized graphically as some differential change in slope. Therefore it became plausible to think of an interaction as a unified force leading to a unique change in the rate of a developmental process, represented by a change in the slope of the response curve.

This approach has been used in the study of genotype-teratogen interactions for cortisone-induced cleft palate (Biddle and Fraser, 1976; Biddle, 1977). Increasing response frequency was plotted against increasing dose of teratogen. The statistical transformation of the data to a set of straight lines was achieved by the use of probit analysis, to be discussed in detail later. The series of parallel dose-response curves obtained in these studies indicated the underlying mechanism for the production of cortisone-induced cleft palate to be the same for the strains tested. Intersecting lines, had nonparallelism been demonstrated, would have reflected a differential change in the mode of response, a reaction velocity change in the developmental event due to some gene-teratogen interaction.

The difficulties encountered in previous studies when attempting to discern the existence of an interaction have rested on the necessity of locating and defining the underlying mechanism. An increase in the frequency of response after treatment is not in itself conclusive evidence for a similar route of action of gene and teratogen. Probit analysis and the study of dose response curves can thus represent a statistical tool with which interactions may be established. Once an interaction has been shown to exist on a mathematical basis, then the search for the underlying biological mechanism that defines this new type of response may proceed.

8. Materials and Methods

1. General

All mice used in this study were kept in the animal quarters of the Department of Biology, McGill University. They were housed, five or less, in plastic cages with wood chip bedding, and fed Purina Lab Chow and tap water ad libitum. They were maintained on a cycle of 16 hours light and 8 hours darkness.

The Rib fusions (Rf), Crooked-tail (Cd), and SWV mice were all provided from colonies kept at McGill. All are inbred strains and are maintained as such by brother-sister mating. The preferred breeding design was to mate heterozygotes to wild-types, as this not only produced the heterozygous and wild-type males to be used as sires in the experiments, but also avoided the production of homozygotes, which do not survive to birth. Both Rib fusions and Crooked-tail heterozygotes possess vertebral malformations of the tail that give it a kinked and knotted appearance. Wild-type males (denoted in this study as $+/+Cd$ and $+/+Rf$) were separated from heterozygotes on this basis and further checked for trueness of genotype by a mating with a wild-type female. The litter produced was examined, and the presence of any abnormal tailed offspring eliminated the male from the study. Fifteen males were used in each cross, i.e. 15 $Cd/+$ ♂♂'s, 15 $+/+Cd$ ♂♂'s, 15 $Rf/+$ ♂♂'s, etc., and the same males were used for mating with both the A/J and SWV dams. Each male was housed separately.

Virgin A/J (A) females were obtained from the Jackson Laboratory, Bar Harbour, Maine. They were 6 to 8 weeks old when received, and maintained in isolation for at least two weeks before use. The SWV females, also nulliparous, were 6 weeks of age when mated. Females were placed with males on a one-to-one basis and were not removed until mating had occurred. Females were checked each morning and, if a vaginal plug was present, they were removed to a new cage in groups of up to five. By convention, the time of conception was considered to be 2 a.m. on day 0, the day a vaginal plug was detected (Snell et al, 1940).

2. The dose-response experiments

1) A/J dams

For the dose-response work the crosses were established as follows (by convention, the female genotype is listed first): A x CdA, A x +/+^{Cd}, A x Rf/+, A x +/+^{Rf}, and A x A. Ten untreated litters were collected from each cross to serve as controls. For the A x CdA, A x +/+^{Cd}, and A x +/+^{Rf} crosses the doses of insulin administered were 6.25, 7.5, 10.0, 12.5, and 13.75 i.u./kg. The A x A cross received only 4 doses: 6.25, 7.5, 10.0, and 12.5 i.u./kg. At least 10 litters were collected at each dose, and this number was exceeded at some of the doses.

Protamine zinc Insulin was purchased from a local pharmacy in a concentration of 100 i.u./cc, which was diluted with sterile distilled water. The insulin was injected intraperitoneally, in an amount proportional to the weight of the female on the day the vaginal plug was found. The time of administration was D8/12, suggested by Smithberg and Runner (1963), and verified as the time of maximal response in this study by a preliminary time-response experiment. A dose of 10.0 i.u./kg. of insulin was administered to the females at one of the following times: D7/18, D8/6, D8/12, D8/18, and D9/6. Three litters were collected at each time for each cross, and scored for the frequency of exencephaly. The results, found in Table B1 and Figure B1, indicated the maximum response was obtained with treatment on D8/12.

Food and water was removed from the cages for six hours following treatment. The treated females were sacrificed by cervical fracture and the embryos collected on D13 or D14. Resorptions were noted, and the remaining embryos were scored for exencephaly and other malformations, and stored in 95% alcohol. In an attempt to identify Cd/+ and Rf/+ embryos, the embryos were cleared and the skeletons were stained with methylene blue using one of two procedures (Gruneberg, 1953; Inouye and Mineru, 1976), but sufficient delineation of the cartilaginous skeleton could not be obtained.

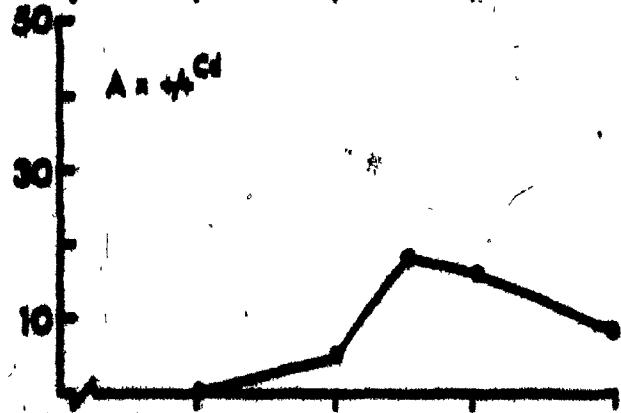
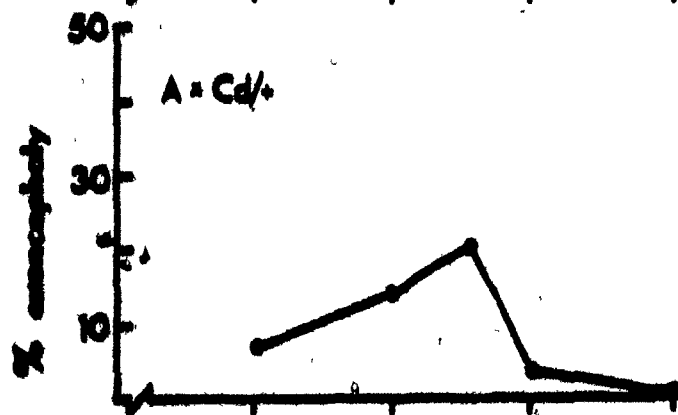
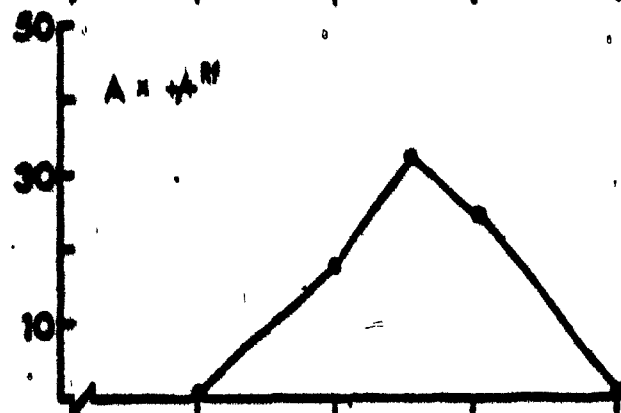
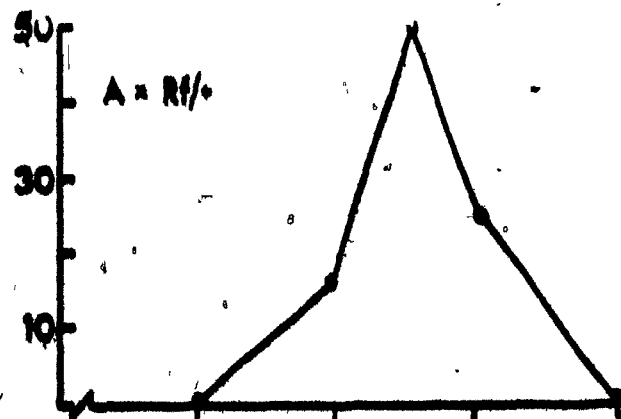
TABLE 81

Insulin time response data; A/J dams (10 i.u./kg)

gestational time (day/hour)	no. of litters	no. of live embryos	no. of exencephalics	% exencephaly
<u>Cd/4 sire</u>				
7/18	3	14	1	7.1
8/6	3	15	2	13.3
8/12	3	14	3	21.4
8/18	3	13	1	7.7
9/6	3	13	0	0.0
<u>+/+Cd sire</u>				
7/18	3	15	0	0.0
8/6	3	17	1	5.9
8/12	3	15	3	20.0
8/18	3	14	2	14.3
9/6	3	15	1	6.7
<u>Rf/+sire</u>				
7/18	3	15	0	0.0
8/6	3	13	2	15.4
8/12	3	16	8	50.0
8/18	3	13	3	23.1
9/6	3	13	0	0.0
<u>+A/Rf sire</u>				
7/18	3	14	0	0.0
8/6	3	14	2	14.3
8/12	3	13	4	30.8
8/18	3	14	3	21.4
9/6	3	16	0	0.0
<u>A/J sire</u>				
7/18	3	14	1	7.1
8/6	3	15	1	6.7
8/12	3	16	2	12.5
8/18	3	12	1	8.3
9/6	3	13	0	0.0

Figure 21.

The figure shows a series of small, dark, irregularly shaped objects, possibly cells or microorganisms, arranged in a horizontal line. The objects are set against a light, grainy background. The overall appearance is that of a microscopic view or a high-magnification photograph of a sample.



II) SWV dams

For the dose-response work with the SWV inbred females, the crosses used were SWV x Cd/+, SWV x +/A^{Cd}, SWV x Rf/A, SWV x +/A^{Rf}, and SWV x SWV. The time-response study, involving three litters at each of the times used in the A/J study, also indicated the time of maximum response to be D8/12 for each of the crosses (Table B2, Figure B2). Insulin was administered in the same manner as it was to the A/J dams; the doses used were 10.0, 20.0, 25.0, 30.0, and 40.0 I.u./kg. The higher doses were used in this study as the SWV were not as susceptible to the lethal effects of insulin as were the A/J females. Ten untreated litters from each cross were collected as controls. Due to the larger litter sizes of the SWV mice, as few as six litters were collected at each dose for the treated crosses.

The females were sacrificed by cervical fracture and the embryos collected on D18. Examination of the embryos at a later gestational time than in the A/J study was done to improve the possibility of satisfactorily staining the skeletons. As in the A/J study, the litters were scored for resorptions and malformations, and stored in 95% alcohol. The ossified skeletons were cleared and stained with alizarin red S. The skeletons were then examined for vertebral and rib malformations. The dose-response (in the present study this term will be used to refer to the data for induced exencephaly) and resorption data from the experiments using both the A/J and SWV dams were analyzed by probit analysis.

TABLE 82

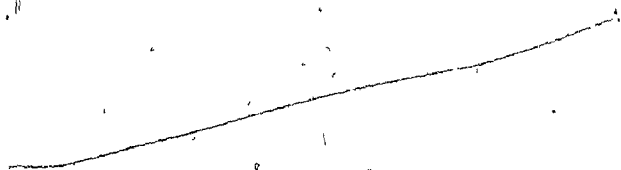
Insulin time response data; SWV dams

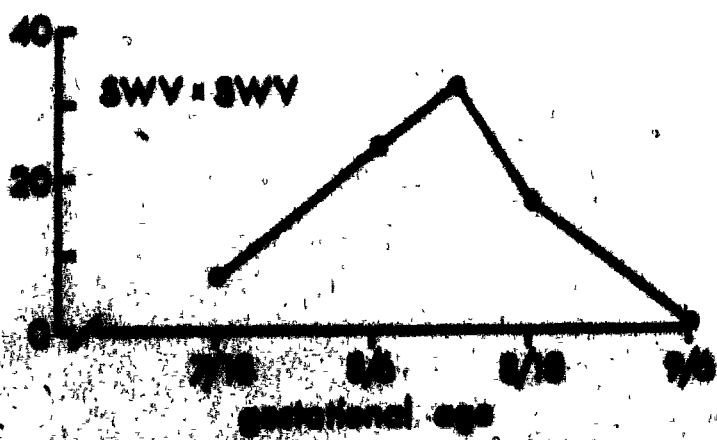
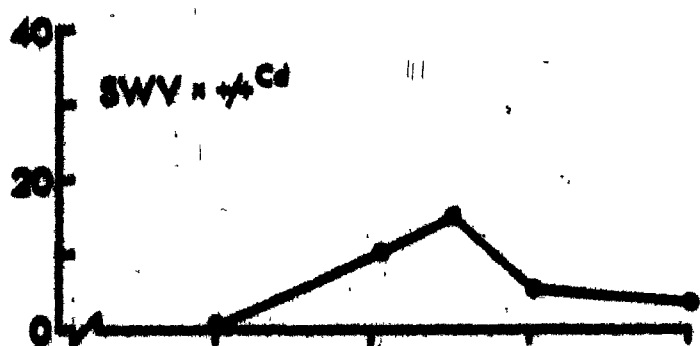
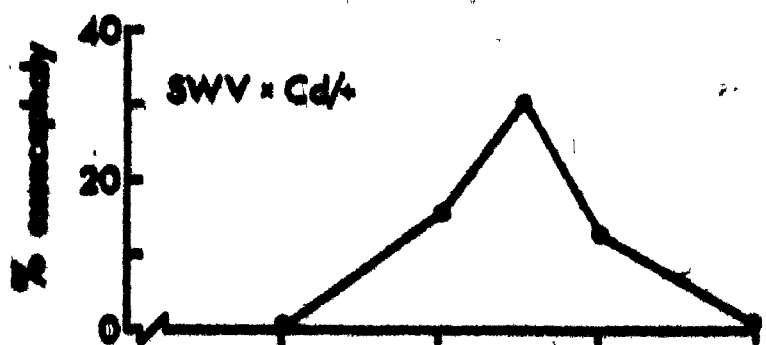
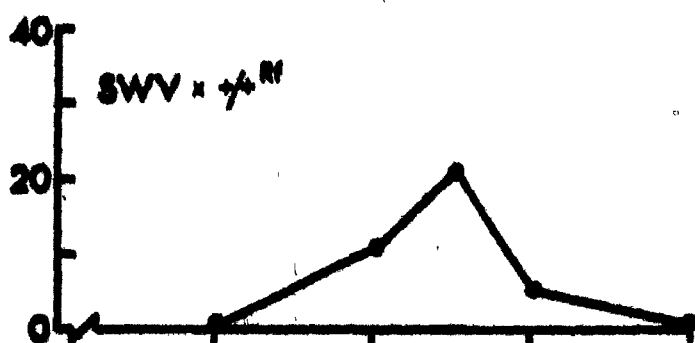
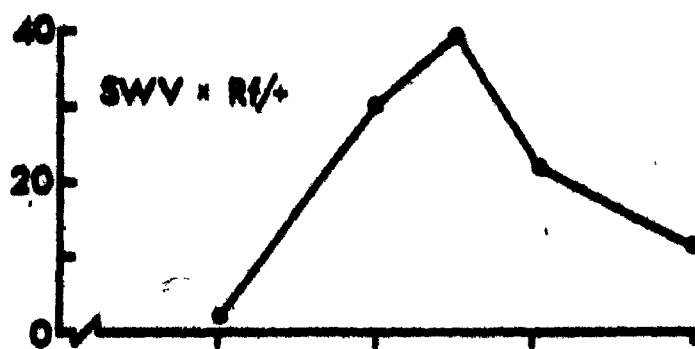
gestational time (day / hour)	no. of litters	no. of live embryos	no. of exencephalics	% exencephaly
<u>Cd/+ sire</u>				
7/18	3	25	0	0.0
8/6	3	26	4	15.4
8/12	3	24	7	29.2
8/18	3	26	3	12.8
9/6	3	25	0	0.0
<u>+/-Cd sire</u>				
7/18	3	27	0	0.0
8/6	3	28	3	10.7
8/12	3	27	4	14.8
8/18	3	30	2	6.7
9/6	3	28	1	3.6
<u>R/+ sire</u>				
7/18	3	28	0	0.0
8/6	3	21	6	28.6
8/12	3	26	10	38.5
8/18	3	27	6	22.2
9/6	3	28	3	10.7
<u>+/-R sire</u>				
7/18	3	24	0	0.0
8/6	3	27	3	11.1
8/12	3	26	5	19.2
8/18	3	27	1	3.7
9/6	3	29	0	0.0
<u>SWV sire</u>				
7/18	3	28	2	7.1
8/6	3	28	8	28.6
8/12	3	28	8	34.8
8/18	3	29	5	17.2
9/6	3	26	0	0.0

4-



0





3. Probit analysis

The recent impressive treatment of dose-response data by probit analysis in the investigation of genotype-teratogen interactions (Biddle, 1977; Biddle and Fraser, 1976; 1977; Jurilloff, 1978) prompted its use in the present study. It was felt that the rigorous statistical procedures of probit analysis represented the best and most complete approach to use in the study of gene-teratogen interactions.

Probit analysis (Finney, 1971) is similar to linear regression analysis, but is used when quantal responses of a binomial population are to be examined. That is to say the range of responses the subject can offer is not normally distributed, but falls into one of two mutually exclusive categories, i.e. normal vs exencephalic brain. The response itself, in addition to being binomially distributed, is quantal because the subject either responds totally, or remains totally unresponsive. Therefore at any given dose, the effectiveness of that treatment is expressed as the percentage of subjects responding. As the dosage is increased, an ever increasing percentage of the subjects respond, until finally some dose is reached that yields 100% response.

The administration of a range of doses, with each sample from the population receiving one of several doses, and the resultant response frequencies are used to estimate the cumulative frequency distribution of the response sensitivity to the treatment for the given population. Any trend to be observed from the

Increasing response frequency with increasing dose is only accurately established when the response at several different dose levels is examined. Thus in these experiments 5 doses were administered to all the crosses except the A x A cross, which was treated with 4 doses. The dose-response curve may thus be considered to represent the cumulative frequency distribution of that population, normalized by the mathematical transformations applied to the raw response data, and valid only over the range of doses employed. An underlying continuum of response to the treatment, with higher doses yielding a higher frequency of affected fetuses, allows the raw data to be transformed into a continuous distribution, with any graphical representation of this response pattern confined to the limits of the dose range.

If one plots these increasing response rates against the logarithms of the doses used, a symmetrical sigmoid curve is obtained, whose midregion is roughly linear. The dosage which elicits a response among 50% of the subjects is known as the median effective dose, the "ED₅₀". As the sigmoid curve is most linear in this region, responses near the ED₅₀ are considered the most reliable. The large deviations from linearity seen at very low and very high frequencies are eliminated by changing the response frequencies into probit values. A probit value is a measure of the response increment caused by changing the log dose by one standard deviation. It is therefore a representation of the deviation of any given response from the midrange response value, the ED₅₀. A plot of the probit values against the log dose values yields the linear dose-response curve.

The methods of probit analysis specialize in the handling of quantal response data; other forms of linear regression do not. As the response in every dosage group is based on a sample, assumed representative of the population, sampling variances will differ from dose to dose. In order to estimate the best possible regression line, each response must be weighted to reflect its relative reliability, and the weight given will be directly proportional to the number of subjects tested at that dose. Also, since the graph of the cumulative frequency distribution showed the greatest deviations from linearity at the extreme frequencies, i.e. furthest from the ED_{50} , the values are also weighted to decrease their contribution to the final regression line as they deviate more widely from the ED_{50} . In these experiments a larger number of litters was collected at the low and high response frequencies to give further reliability to the response estimates at these doses. The best representation of the regression line is obtained by successive iterations, until the probit values for the given doses change by less than 0.1 from the previous round of calculations.

The ED_{50} , as the dose required to obtain a response in half of the population, represents the relative sensitivity of the subject to the treatment. Therefore a comparison of the ED_{50} 's for all the crosses tested in this study will yield differences in reactivity to the treatment. The slope of the dose-response curve reflects the variance, or range, of the response data, with smaller changes in frequency from dosage group to dosage group yielding a smaller value for the variance, which in turn is represented as a steeper curve. The slope is thus a

measure of the change in rate of some developmental process as a function of the log dose. Interactions may be identified as nonparallel lines. Intersecting dose-response curves are due to a significant difference in slope values, which is indicative of different rate changes per unit dose increment.

Thus probit analysis was applied to both the dose-response and the resorption data for all crosses used in this study, to determine if interactions, represented as nonparallel regression lines, existed. For the dose-response data the frequency of exencephaly was scored as the number of exencephalics per total number of live implants. For the resorption data the frequency of resorptions was determined as the number of resorptions per total number of implants. The regression lines for the resorption data were corrected for the spontaneous frequency, as only insulin-induced resorptions were of interest in this study. It was not necessary to correct the insulin-induced exencephaly dose-response curves for spontaneous occurrence of the malformation.

Systematic deviations of the data from the calculated regression line indicate that the attempt to fit the data to a straight line is inappropriate, and a nonlinear curve would better suit the data. Should such deviations exist they are detected by a significant value for a goodness-of-fit χ^2 test, performed on the final equation of the line.

The standard errors of the slopes, and the fiducial limits of the ED₅₀ values were also calculated.

To test for parallelism regression lines of appropriate subgroups of the crosses tested were subsequently fitted to a common slope. Differences in the χ^2 values between the summed values for the independently fitted regression lines and that of the common line were used to determine significant deviations from parallelism. Lines which did not fit a common slope were considered as nonparallel, and the presence of an interaction was indicated.

In the probit analysis, as with all other statistics employed in this study, the level of significance was taken to be 5%.

4. Morphological rating

To elucidate the underlying biological mechanism(s) responsible for the formation of an exencephalic embryo, embryos were examined during the period of neural tube closure and scored for several morphological variables. Three untreated litters from each of the crosses were collected at each of the following gestational times: 8/12, 8/18, 9/6, 9/12, 9/18, and 10/6. The same design was employed to collect three treated litters from each of the crosses, with the $A \times CdA$, $A \times \sqrt{+Cd}$, and $A \times A^{Rf}$ crosses receiving 13.75 I.U./kg insulin and the $A \times RfA$ and $A \times A$ crosses receiving 12.5 I.U./kg. The SWV dams from all the crosses were given 40.0 I.U./kg. These were the doses that would yield the highest percentage of affected embryos, insuring that a sufficient number of exencephalics would be examined. In all, 2837 embryos were collected.

The uteri were fixed in Bouin's for 24 hours, after which the embryos were removed and examined under a dissecting microscope before being placed in 70% alcohol. Resorptions were noted, and the embryos were scored for somite number, stage of neural tube closure, and stage of turning. The system used as a guideline for normal embryological development is listed in Table B3. As was mentioned previously, the somite number is considered to be a reliable index of the gestational development of the embryo, and the assignment of somite number to gestational age was based on the comprehensive study of mouse development by Theller (1972) and the examination of control litters in this study. The examination of the control litters also aided in establishing the stages of neural tube closure (Table B4), modified slightly from the system used by Rajchgot (1971), and the stages of turning (Table B5), as the embryo moves from a lordotic to kyphotic position during the period of neural tube closure. Other morphological traits, such as development of the otic and optic vesicles, were eliminated as variables to be used because their period of active morphological development did not span the entire time period examined in this experiment.

After being morphologically rated, representative embryos were photographed with a Wild photographic system.

TABLE 83

System used for morphological ratings of D8-10 embryos

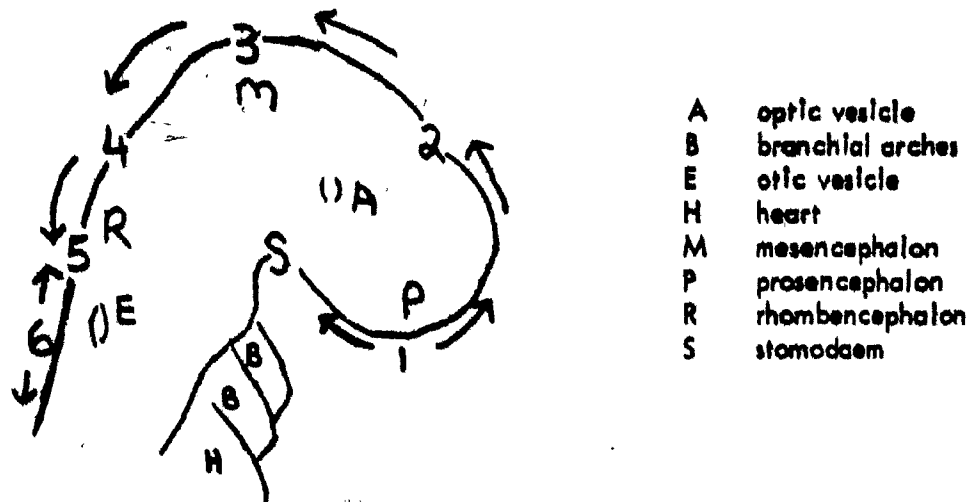
gestational age (day / hour)	no. of somite pairs**	stage of closure of neural tube*	stage of turning of embryo*
8/12	8 - 12	0 - I	0 - 1
8/18	12 - 15	II	1 - 2
9/6	13 - 20	III - IV	3 - 4
9/12	21 - 29	V	4
9/18	28 - 32	VI	4
10/6	30 - 36	VII	4

* see tables for description of stages

** modified from Thelier (1972)

TABLE B4

Stages of neural tube closure*



STAGE 0. The Neural tube is completely open. Fig. C11

I Closure occurs at the middle of the prosencephalon (1). Fig. C12. It then proceeds towards the stomodaeum (S) and the mesencephalon. Closure also occurs at the level of the fifth somite (6), in the region of the otic vesicle (E), and proceeds caudally towards the posterior neuropore, and in a cephalic direction as far as the caudal end of the rhombencephalon (5).

II The Neural tube is completely closed over the prosencephalon (2).

III Closure to the middle of the mesencephalon (3) results in the formation of the anterior neuropore. Fig. C14, C15.

IV Closure to the caudal end of the mesencephalon (4) closes the anterior neuropore.

V The roof of the rhombencephalon remains thinly covered, making closure over the rhombencephalon incomplete. Fig. C16, C17.


VI With the thickening of the rhombencephalic roof epithelium, the neural tube closes completely in the head region. Fig. C18, C19.

VII With closure of the posterior neuropore, neural tube closure is complete over the tail.

* modified from Rajahget, 1971

TABLE B5

Stages of turning of the embryo

- 0 Not yet starting to turn, the embryo possesses an S-shaped body configuration with a concave curvature. The hindbody lies in the same plane as the head. Fig. C11.
1.  The embryo begins to turn its head in a clockwise direction, with the cranial axis slightly out of line with the caudal part of the axis. Fig. C12.
2. The axis anterior to the mid-trunk region begins to follow the rotation of the head, until the cranial axis is at a right angle to the hindbody. Fig. C13.
3. The caudal part of the axis, which begins to twist slightly before the cranial region has completed its 90° rotation, continues to turn in a clockwise direction. It will complete its turn later than that of the cranial region.
4. The caudal portion of the axis completes its 90° turn, so that the embryo now possesses a C-shaped configuration, with a convex curvature. The interior of the curvature is the ventral surface of the embryo, the exterior the dorsal surface. The tail bud continues to grow and in doing so comes to rest on the right side of the head and anterior axis. Fig. C14, C15, C16.

5. Log-linear Analysis

The morphological data obtained was statistically examined using a BMD computer program for log-linear analysis. The program places the data, categorized by several variables, into a multiway frequency table. The analysis fits a model to the observed cell frequencies. The final model, describing the relationships among the variables, is obtained after all the variables are tested and ordered for significant interactions. Each variable is known as a main effect, and the different interactions are formed by consecutively setting these effects equal to zero, and noting subsequent changes in probabilities. The model is known as a hierarchical one because any higher order effect is present only if the composite lower order and main effects are included in the model as well. To illustrate this concept suppose, in the study of the possible interactions among 5 variables listed A, B, C, D, and E, a third order model, ABC, is found to be a significant interaction. This implies, due to the hierarchical nature of the analysis design, that all the second order effects (AB, BC, and AC) and the main effects (A, B, and C) which are subsets of the third order model are immediately included as significant contributing factors. Thus, among all possible interactions of the 5 variables, one third order interaction (ABC), 3 second order interactions (AB, BC, and AC), and 3 main effects (A, B, and C) are found to be of significance and would be ordered for their relative importance. The cell frequencies are analyzed by either a goodness-of-fit or a likelihood ratio

chi-square test. The likelihood ratio χ^2 is used for nested models, as the partitioned effects are not additive under such conditions using the goodness-of-fit χ^2 .

To screen for significant interactions with which to build a final model, tests of partial and marginal association are used. The partial association tests the effect of setting an interaction to zero on the full model. For example, a full third order model ABC is fitted, and then the same model is fitted again with one of the interactions, i.e. AB, set to zero. The difference in the tests of fit determines the relative contribution of AB.

Marginal associations are determined by setting up frequency tables for the lower order interactions of a higher order model. Again, in a third order model ABC, each of the two-factor interactions (i.e. AB, BC, and AC) is separately analyzed by a two-way table and the relative importance of each interaction is determined. The tests of marginal association are equal to those of the partial association for the main effects and the highest order interaction. Significance for both the test of marginal association and the test of partial association is the criterion used to determine the significant interactions involved in establishing a model.

The final model is the combination of all significant interactions needed to sufficiently explain the data. For example, if the model chosen is

(AC, BC, D), then AC and BC are two significant two-factor interactions, and D is a significant main effect not included in the given second order interactions, remembering that the main effects A, B, and C are also included as significant factors in the above model. The model is then tested to insure that the combination of interactions is indicative of a good representation, again using the two chi-square tests.

6. Histology

After rating the embryos, they were prepared for examination with the light microscope. Due to the large number of embryos collected, only a representative sample could be sectioned. After a 24 hour fixation in Bouin's, the D8, D9, and D10 embryos were transferred to 70% alcohol for at least one week prior to being embedded in paraffin. Serial transverse and frontal sections were cut at 7 μ , dehydrated, and stained with Erlich's Haematoxylin and Eosin Y. Eight embryos from both the mutant and the nonmutant crosses, treated and control, were examined at each of the six gestational ages observed. Although all the crosses were examined, it was not possible to study all the gestational ages for each cross. To avoid biasing the data, the identity of the histological material was not known at the time of examination. Mitotic indices were calculated for the cephalic region of the neural tube, with the index determined as the number of mitoses per one hundred cells. Mitoses were scored using metaphases, anaphases, and telophases,

but not the prophase stage, which can be difficult to identify. The area covered was bounded by a one square centimeter grid, placed in the eyepiece of the light microscope, and examined at 1,000 X magnification. Every fourth section of the cephalic (brain) region was counted, and the mean mitotic index was defined as $100 \times$ the ratio of the mean number of mitoses / grid (cm^2) to the mean number of cells / grid (cm^2). The mean mitotic indices for the neuroectoderm and the underlying mesoderm were calculated separately.

7. Protection with glucose

One effect of insulin is to increase the storage of glucose, as glycogen, in the liver of the treated female. The decrease in the blood glucose concentrations results in hypoglycemia, a transitory condition from which the animal spontaneously recovers by six hours after the insulin treatment. The lowered glucose concentration decreases the amount of substrate available for breakdown by the tricarboxylic acid cycle and electron transport system of oxidative phosphorylation. The lack of glucose, by disrupting carbohydrate metabolism, could be the active teratogenic agent acting on the developing tissues.

To test this, 5 litters were collected from each of the A and SWV crosses to CdA, +A^{Cd}, RfA, and +A^{Rf} males. The A crosses were treated with 13.75 I.U./kg, except the A x Rf/+ cross, which received 12.5 I.U./kg of insulin. The SWV crosses received 40.0 I.U./kg. All were treated on D8/12 in the same manner as for the dose-response work. One hour after the insulin treatment the females received an

Intraperitoneal injection of 30% glucose dissolved in distilled water. The volume administered was based on the body weight of the mouse. The females were sacrificed on D18, and the litters were examined for resorptions and malformations. The frequency of exencephaly was scored as the number of exencephalic embryos per live embryos, as done in the dose-response work.

Glucose concentrations in the blood were determined by a Beckwith Autoanalyzer micromethod assay. Forty μ l. of blood, drawn from the orbital sinus, was a sufficient quantity with which to perform the analysis. The blood glucose level does not vary significantly among members of an inbred strain of mice (Smithberg and Runner, 1963). The maternal genotype of all the crosses tested was either A/J or SWV, both inbred strains. Therefore, it was not necessary to collect many blood samples, and so the blood of four pregnant females from each strain was analyzed for the concentrations of glucose in the blood. Two of the A/J and the SWV females received insulin without any supplement of glucose. The other two A/J and SWV females received an injection of glucose one hour after the insulin treatment. Blood samples were collected two hours before and two hours after the insulin treatment. In case the blood collection procedure had been unduly stressful, the data collected from these mice was not used in the main analysis.

C. Results

1. Induced exencephaly; A/J dams

For the crosses involving the A/J females, the frequencies of insulin-induced exencephaly for the various doses administered are shown in Table C1. A frequency of 0% was obtained at the lowest dose in all the crosses, with the highest frequency of response varying from 14% for the AxA cross to 58% for the AxRf/+ cross. The calculated line of best fit for each of the crosses is shown in Figures C1 and C2. No corrections for a spontaneous occurrence of the malformation were necessary. None of the data points deviated systematically from the regression lines, and therefore the dosage-dependent frequencies for insulin-induced exencephaly can be correctly expressed as a linear function. The five probit regression lines are shown together in Figure C3. It can be seen that these regression lines may be subdivided, based on apparent slope differences, with the lines for the AxRf/+ and AxCd/+ crosses (slope values of 5.17 and 5.44, respectively) in one group, and the lines for the A x A, Ax+/+Cd, and Ax +/+Rf crosses (slope values = 3.13, 3.28, and 3.44) in the other. A test of parallelism was performed on these five crosses and the significant χ^2 value obtained ($\chi^2 = 13.552$, $df = 4$) indicated the probit regression lines did not fit a common slope. A test of parallelism on the regression lines of the mutant (AxRf/+, AxCd/+) crosses indicated these lines could be fitted to a common slope ($\chi^2 = 0.061$, $df = 1$; ns). A common slope was also obtained for the regression lines of the

TABLE C1

Insulin dosage response data; A/J dams

Dose (I.U./kg)	no. of litters	total implants	% resorbed	number embryos	% exencephaly
<u>CdA sire</u>					
13.75	7	51	59	21	43
12.50	14	98	46	53	34
10.00	10	74	30	52	21
7.50	14	96	22	75	9
6.25	14	96	19	78	0
<u>+/+Cd sire</u>					
13.75	7	48	37	30	20
12.50	15	108	30	76	13
10.00	14	97	22	76	9
7.50	13	89	16	75	7
6.25	13	89	13	77	0
<u>Rf/+ sire</u>					
12.50	21	146	66	50	58
10.00	14	92	43	52	44
7.50	15	100	26	74	27
6.25	14	93	16	78	14
5.00	13	87	11	77	0
<u>+/+Rf sire</u>					
13.75	8	48	27	30	30
12.50	12	80	31	55	22
10.00	15	103	24	78	18
7.50	15	100	20	80	14
6.25	13	90	15	76	0
<u>A/J sire</u>					
12.50	11	78	36	50	14
10.00	10	66	30	46	11
7.50	13	94	26	69	7
6.25	10	67	24	51	0

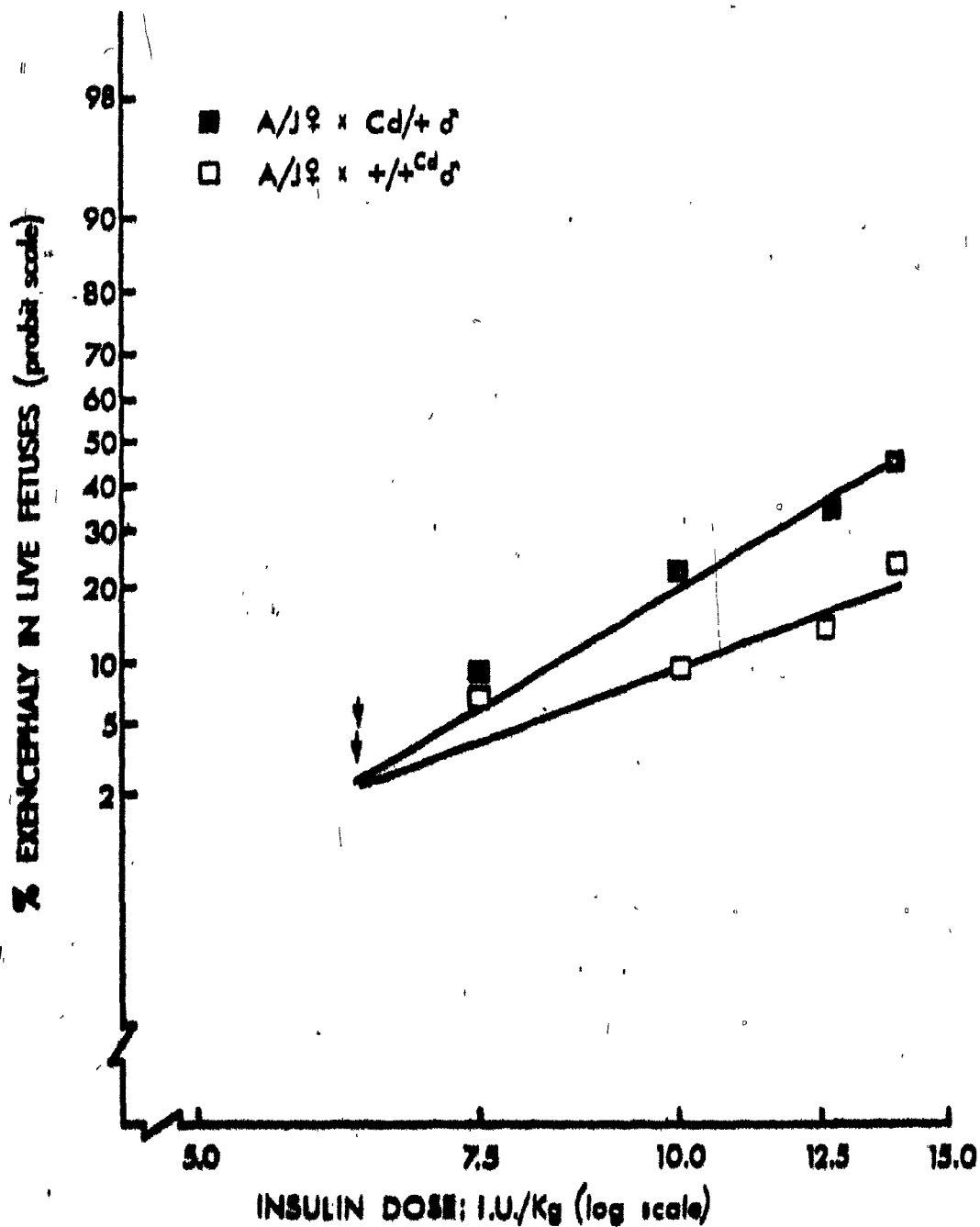


Figure C1. Independently fitted probit dose-responses of insulin-induced exencephaly for the A x Cd/+ and A x +/-Cd crosses. Arrows indicate 0% response.

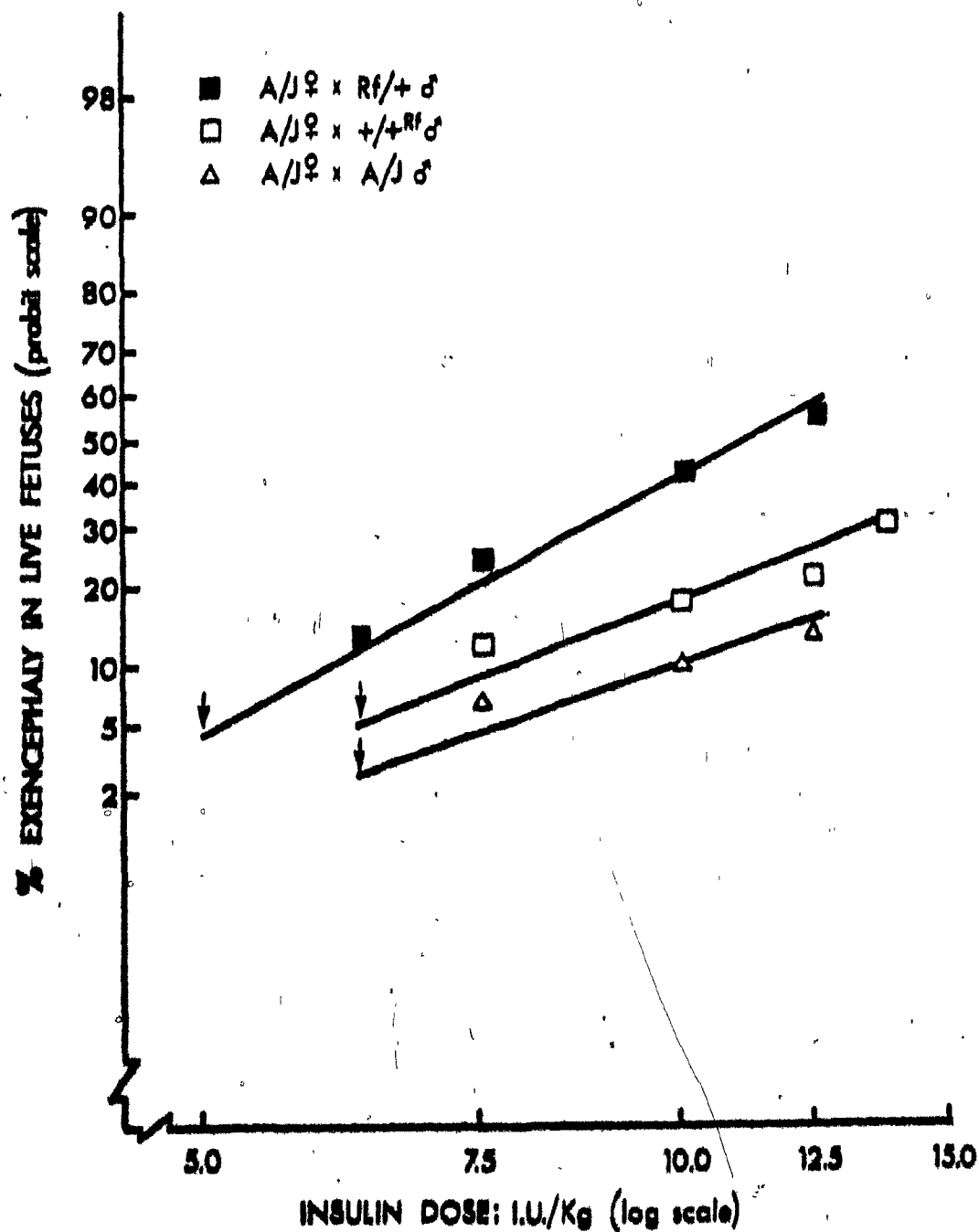


Figure C2. Independently fitted probit dose-responses of insulin-induced exencephaly for the A x Rf/+, A x +/-Rf, and A x A crosses. Arrows indicate 0% response.

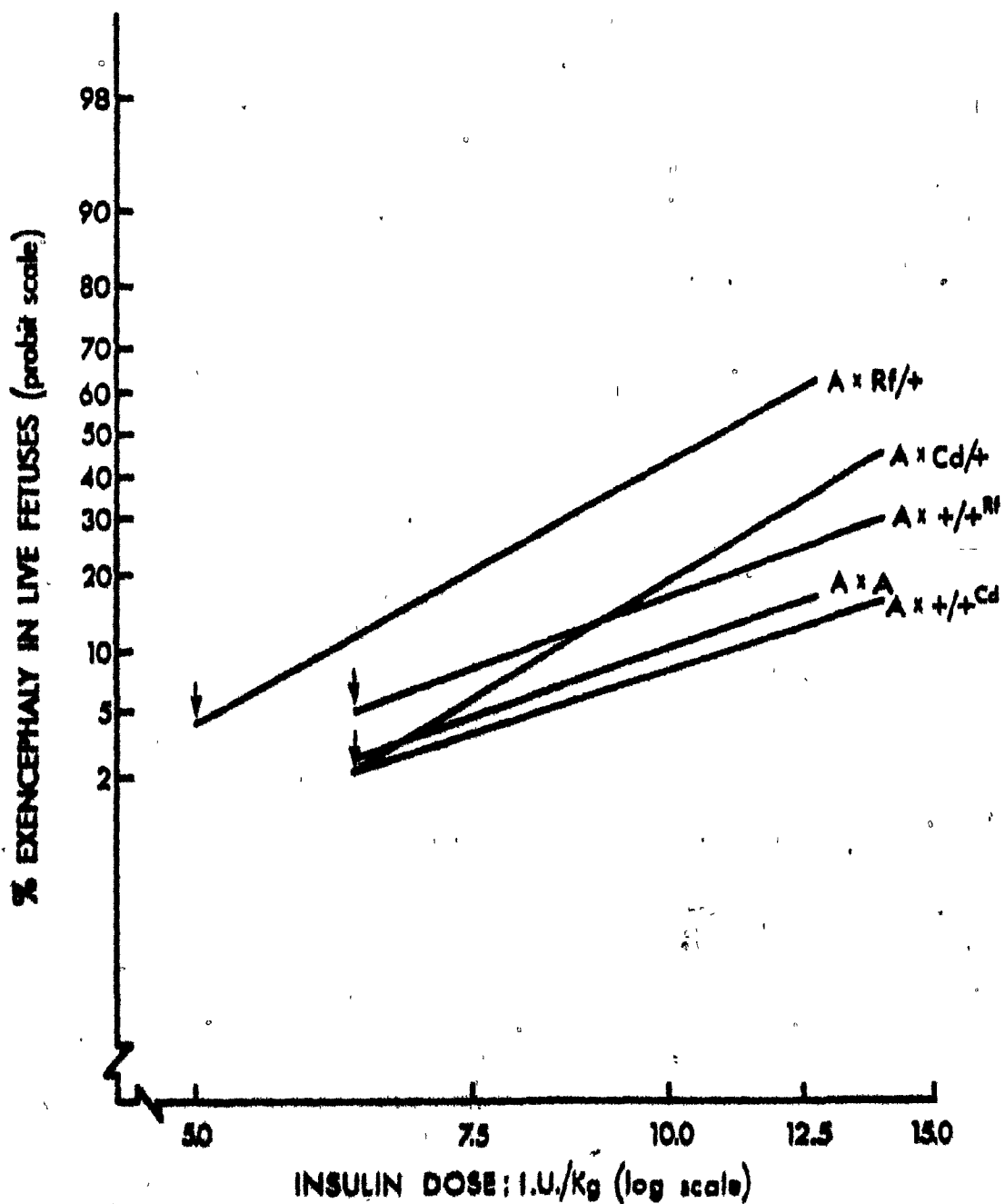


Figure C3. Independently fitted probit dose-responses of insulin-induced exencephaly for the crosses with the A/J dams. Arrows indicate 0% response.

nonmutant ($A \times A$, $A \times +/+^{Rf}$, $A \times +/+^{Cd}$) crosses again determined by a test of parallelism ($\chi^2 = 2.296$, $df = 2$; ns). The common slope value for the regressions of the mutant crosses was 5.261, and 3.324 for those of the nonmutant crosses. A summary of the common and independently fitted slopes for these probit regressions is found in Table C2, and the tests of parallelism are seen in Table C3.

The probit regression lines for insulin-induced exencephaly in the A/J crosses indicated an interaction. Significant slope differences were detected between the mutant and nonmutant crosses, with a common slope fitted to the regression lines within each of these two groups.

The ED_{50} 's were calculated, and are also shown in Table C2. As all the lines are not parallel, the ED_{50} 's can be compared only within the subgroups, which do fit a common slope. The $A \times Rf/+$ cross exhibited an ED_{50} of 10.724 I.U./kg, making it more sensitive to treatment than the $A \times Cd/+$ cross ($ED_{50} = 14.497$). Among the nonmutant crosses $A \times +/+^{Rf}$, with an ED_{50} of 18.733 I.U./kg, appeared more susceptible to insulin than either $A \times A$ ($ED_{50} = 25.145$) or $A \times +/+^{Cd}$ ($ED_{50} = 25.882$). The differences were small, however, suggesting a similar sensitivity to treatment.

2. Induced exencephaly; SWV dams

For the crosses using SWV females the dosage-dependent frequencies for insulin-induced exencephaly are shown in Table C4. Although 0% frequency

TABLE C2

ED₅₀'s and Common & Independently fitted slopes of probit regressions for lead-in-induced encephaly in A/J and SWV crosses

Cross	constrained to parallelism		independently fitted		ED ₅₀ (I.U./kg)	95% Fiducial limits
	Y intercept	slope	Y intercept	slope \pm S. E.		
AxCdA	-1.139	5.261	-1.319	5.440 \pm 0.156	14.477	12.941 to 17.623
Ax $\frac{1}{2}$ Cd	0.317	3.324	0.359	3.284 \pm 0.410	25.882	18.416 to 29.253
AxRfA	-0.409	5.261	-0.326	5.170 \pm 0.095	10.724	9.886 to 11.990
Ax $\frac{1}{2}$ Rf	0.737	3.324	0.623	3.440 \pm 0.254	18.733	15.001 to 32.687
AxA	0.379	3.324	0.570	3.129 \pm 0.546	25.145	16.142 to 54.246
SWV x CdA	-2.650	5.122	-3.153	5.475 \pm 0.154	30.843	28.692 to 33.725
SWV x $\frac{1}{2}$ Cd	0.182	2.769	0.034	2.875 \pm 0.274	53.387	42.614 to 89.127
SWV x RfA	-2.347	5.122	-2.030	4.898 \pm 0.162	27.841	27.246 to 32.354
SWV x $\frac{1}{2}$ Rf	0.237	2.769	0.096	2.869 \pm 0.224	51.237	30.294 to 62.979
SWV x SWV	0.511	2.769	0.708	2.630 \pm 0.164	42.821	11.193 to 47.645

TABLE C3

Tests of Parallelism; dose-response data

<u>Crosses</u>	<u>Source</u>	<u>df</u>	<u>SS</u>
<u>1. A/J dams</u>			
A/J ₁ mutant and nonmutant	parallelism	4	13.552*
	heterogeneity	14	17.676
	total	18	31.228*
A/J ₁ mutant	parallelism	1	0.061
	heterogeneity	6	9.664
	total	7	9.725
A/J ₁ nonmutant	parallelism	2	2.296
	heterogeneity	8	8.012
	total	10	10.308
<u>2. SWV dams</u>			
SWV ₁ mutant and nonmutant	parallelism	4	21.971*
	heterogeneity	15	9.829
	total	19	31.800*
SWV ₁ mutant	parallelism	1	0.471
	heterogeneity	6	2.521
	total	7	2.992
SWV ₁ nonmutant	parallelism	2	0.158
	heterogeneity	9	6.231
	total	11	6.389

* $P \leq .05$

was never obtained, the smallest dose given did yield low frequencies. The range extended as high as 84%, for the SWV x Rf/+ cross, while for the other crosses the highest frequencies were less. As with the A/J crosses, it was difficult to obtain very high frequencies ($> 80\%$) since increasing doses drastically increased the proportion of females succumbing to the lethal effects of the insulin treatment. Though the SWV were not quite as susceptible as the A/J females to mortality from treatment, the rate still approached 50% at the highest dose given (40.0 I.U./kg). In the A/J females the highest dose tested (13.75 I.U./kg) killed about 65-70% of the females treated. It should be noted that, while the frequencies at the highest dose given were the highest one could reasonably obtain, probit analysis works best when the response frequencies are evenly distributed around the midpoint (50%). The large fiducial limits for the calculated ED₅₀'s for both the A/J and SWV crosses further reflect the violation of this design. It was felt that, although one of the conditions of the analysis was not properly met, unless systematic deviations of the data points from linearity occurred, there was enough flexibility in the analysis to warrant its use. It has been noted previously (section 8.3) that the response frequencies are weighted in proportion to the sample size at that frequency. Therefore, to overcome the limitation of a narrow frequency range, larger numbers of embryos were collected at those dosages inducing very low ($\leq 20\%$) or very high ($\geq 80\%$) frequencies, adding further weight to these frequency values.

TABLE C4

Insulin dosage response data; SWV dams

Dose (I.U./kg)	no. of litters	total implants	% resorbed	number of embryos	% exencephaly
<u>Cd4 sire</u>					
40.00	9	101	48	56	73
30.00	8	88	41	51	53
25.00	7	80	30	54	36
20.00	10	115	22	90	7
10.00	9	100	15	85	3
<u>1/4 Cd sire</u>					
40.00	7	78	33	52	35
30.00	6	73	26	54	22
25.00	9	98	23	76	17
20.00	8	89	18	73	14
10.00	9	98	13	85	1
<u>Rf/4 sire</u>					
40.00	12	132	42	76	84
30.00	8	88	34	54	61
25.00	7	72	28	52	40
20.00	8	83	18	78	15
10.00	9	96	12	84	5
<u>1/4 Rf sire</u>					
40.00	9	96	35	62	39
30.00	10	106	25	79	27
25.00	10	103	21	81	17
20.00	9	89	15	76	10
10.00	8	83	8	74	3
<u>SWV sire</u>					
40.00	9	96	35	62	47
30.00	10	111	29	79	39
25.00	10	107	24	81	27
20.00	8	91	16	76	12
10.00	7	88	11	74	7

The calculated probit regression lines for the crosses with the SWV females are shown in Figures C4 and C5. Correction for a spontaneous frequency was not needed and systematic deviations from linearity were not detected. The five regression lines are shown together in Figure C6. Again the regression lines for the mutant crosses (SWV x Cd/+ and SWV x Rf/+) seemed to have a different slope than those for the nonmutant crosses (SWV x +/+^{Cd}, SWV x +/+^{Rf}, and SWV x SWV). A test of parallelism on the five lines indicated that it was not possible to fit them to a common slope ($\chi^2 = 21.971$, $df = 4$). The regression lines of the mutant crosses did fit a common slope of 5.122 ($\chi^2 = 0.471$, $df = 1$, ns), and those of the nonmutant crosses were fitted to a common slope of 2.769 ($\chi^2 = 0.158$, $df = 2$, ns). The common and independently fitted slopes and the associated tests of parallelism for these crosses are found in Tables C2 and C3.

Again, an interaction was implied from the nonparallel lines for the dose-response curves of insulin-induced exencephaly. The probit regression lines for the mutant crosses fitted a common slope that was significantly different from the common slope for the probit regression lines for the nonmutant crosses. As the lines do not all possess the same slope, the ED₅₀'s may be compared only within each of the two subgroups. The SWV x Rf/+ cross had an ED₅₀ of 27.841 I.U./kg; the ED₅₀ of the SWV x Cd/+ cross was 30.843. Among the nonmutant crosses, the ED₅₀'s were 42.821 (SWV x SWV), 51.237 (SWV x +/+^{Rf}), and

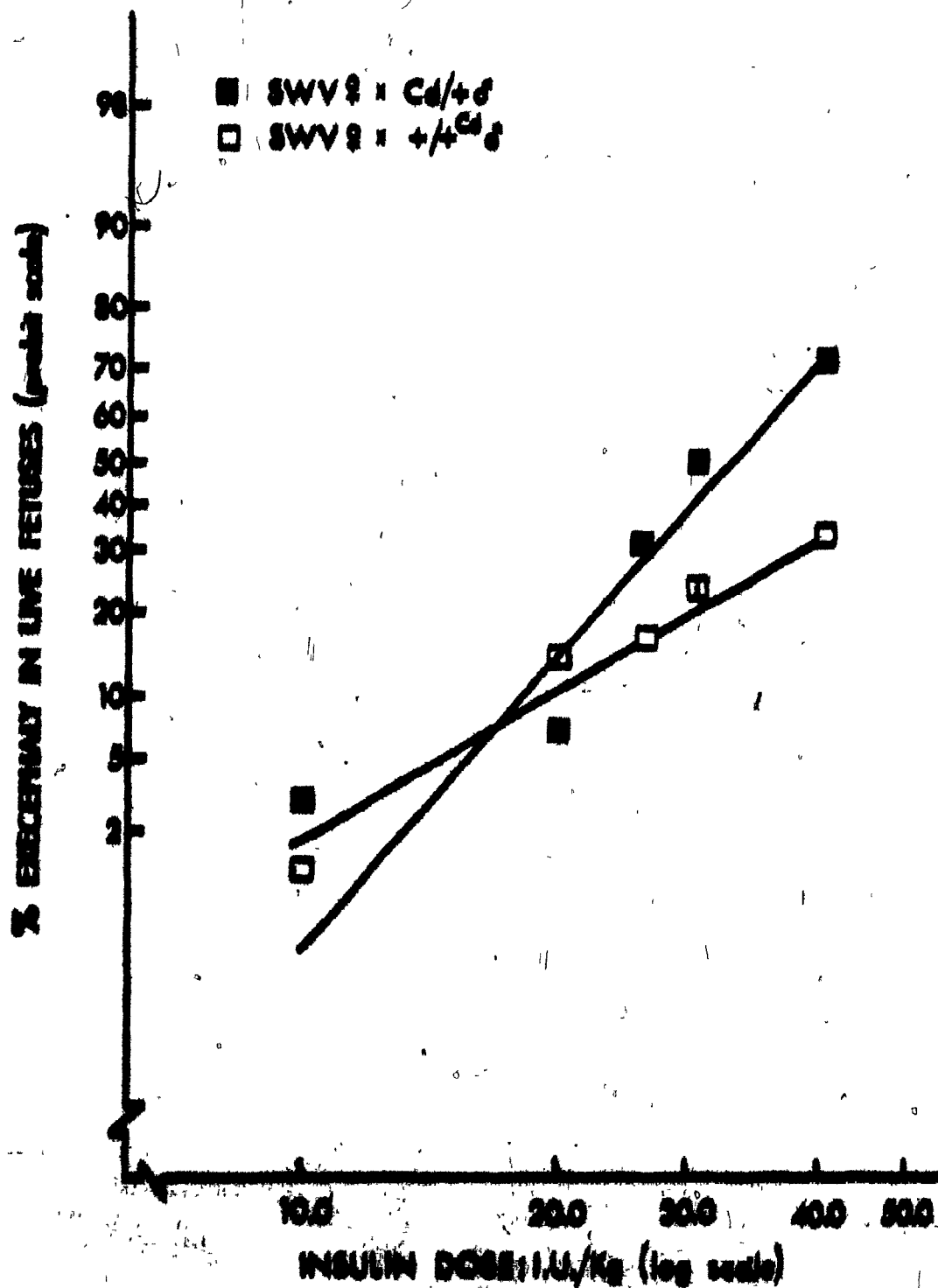


Figure C4.

Independently fitted sigmoid dose-responses of insulin-induced

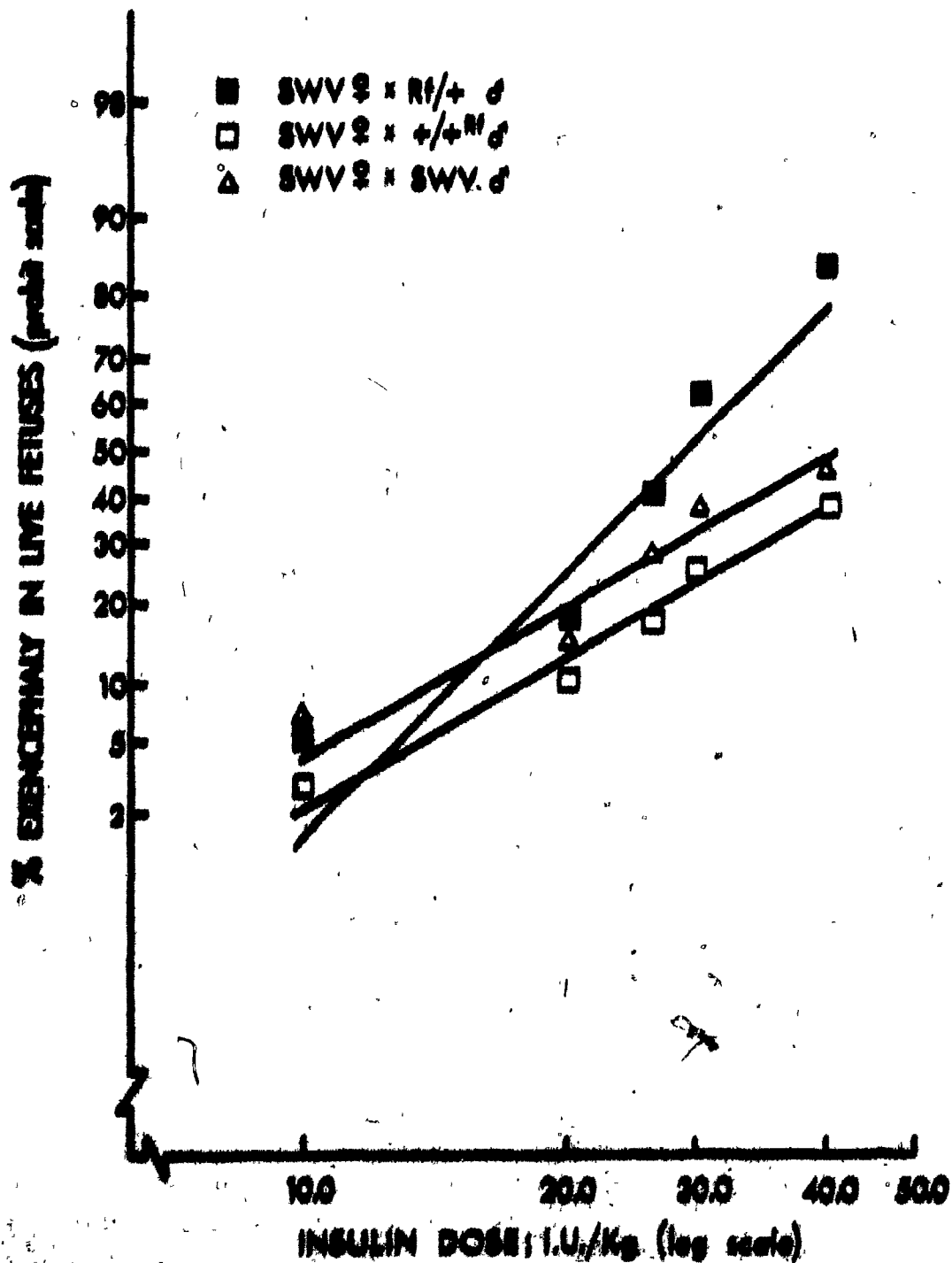


Figure C1. Independently fitted probit dose-response of insulin-induced embryonicity for the SWV x Rf/+, SWV x +/-M, and SWV x SWV groups.

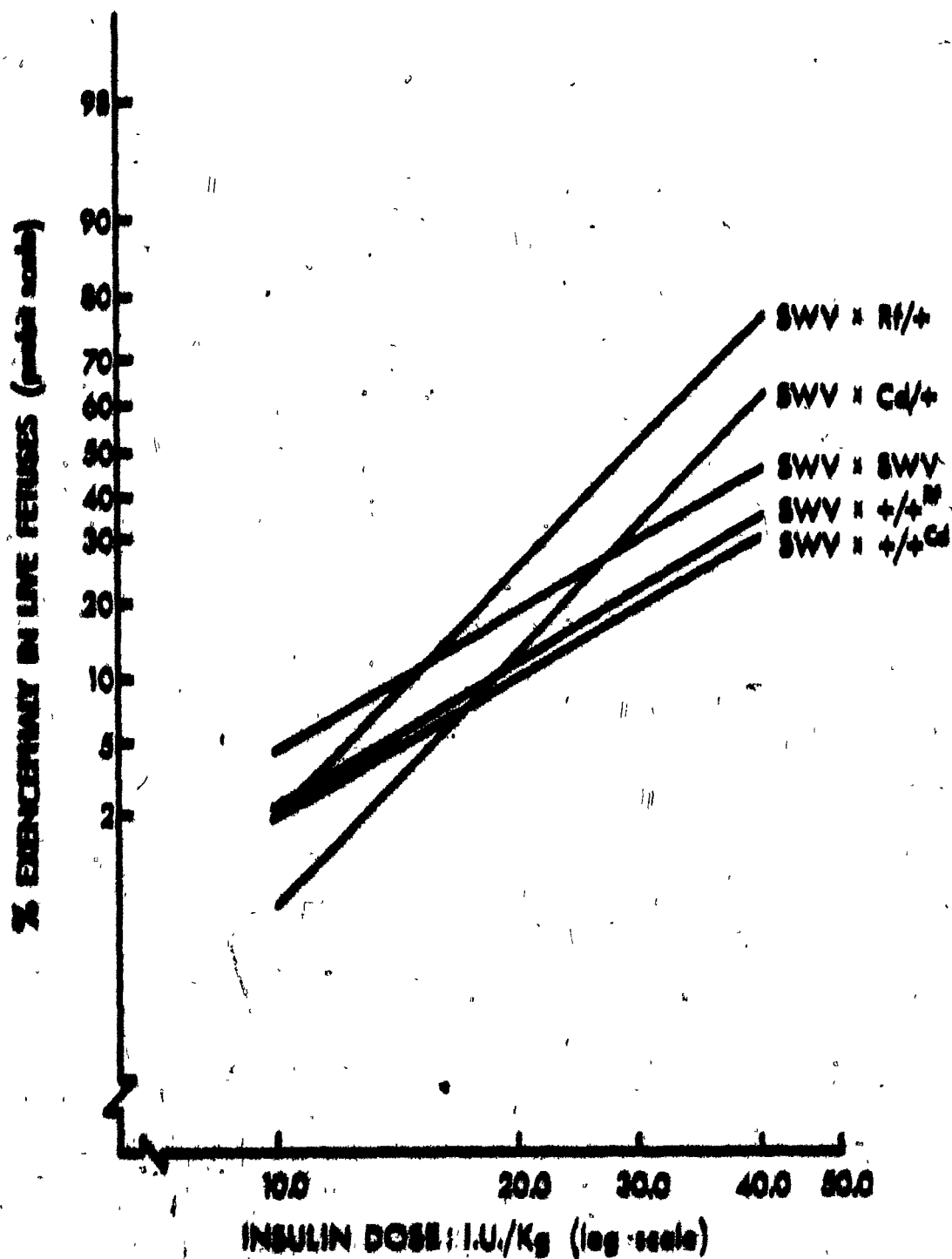


Figure C6.

Independently fitted probit dose-responses of insulin-induced exencephaly for the crosses with the SWV dams.

53.387 (SWV \times $+/4^{Cd}$). As differences in the ED₅₀ values within each group were small, and the large fiducial limits decrease the reliability of these estimates, it can only be stated that the relative reactivities were very similar for all the crosses within each group.

3. Analysis of the stained skeletons

The embryos from the SWV crosses were collected on D18 to allow for clearing and staining of the ossified skeletons with alizarin red S. Staining of the cartilaginous skeletons of the embryos from the A/J females (collected on D14) had been unsuccessful. It has been mentioned earlier (section A.3) that embryos heterozygous for the mutant genes Cd or Rf will exhibit vertebral or rib anomalies, respectively. Furthermore it was known that insulin induces fused ribs in mice (Smithberg and Runner, 1963). In the crosses of these experiments heterozygous males were outcrossed to inbred females to study the possible interaction of a single gene dose and a teratogen in producing a phenotype of the homozygous mutant state. Litters collected from the mutant crosses will consist of 50% heterozygous and 50% wild-type embryos. If there is to be an interaction between the gene and the teratogen one would expect many of the exencephalic embryos from the mutant crosses to also carry the mutant gene, and therefore display a vertebral or rib malformation. As the insulin treatment never produced 100% response frequency, there will be some mutant carrying embryos

that are not exencephalic. Also, since the treatment did induce exencephaly in the nonmutant crosses, there will be exencephalic embryos that are free of rib or vertebral malformations. Overall, however there should be a greater proportion of exencephalics with skeletal malformations in the mutant crosses if one is to postulate a relationship between gene and teratogen.

The control litters were examined for skeletal abnormalities.

The results are presented in Table C5. No abnormalities were detected in the embryos from the nonmutant crosses. 30.7% (23/75) of the embryos from the SWV x Cd/+ cross had malformed vertebrae. These varied from small to fused or missing centra, and occurred in the lumbosacral and caudal regions of the vertebral column. 35.8% (29/81) of the embryos from the SWV x Rf/+ cross exhibited missing or fused ribs. No other malformations were noted in these crosses, and the malformations seen expressed themselves in the same manner as within the mutant inbred strains. Since one would have expected 50% of the embryos from each of these mutant crosses to possess skeletal malformations, the lower frequencies obtained could be due to incomplete expression of the genes, although the potential of the stain to elucidate skeletal structure must also be questioned.

Next the D18 embryos from the dose-response study were examined for skeletal malformations. The results are seen in Table C6. Vertebral malformations, composed of small, irregular shaped, fused or missing sacral and caudal centra, were found only in embryos from the SWV x Cd/+ cross. Fused or missing ribs were seen

TABLE C5

frequency of vertebral and rib malformations among D18 control embryos; SWV dams

cross	total live embryos	no. embryos with vertebral malformations ¹ (%)	no. embryos with rib malformations ² (%)
SWV x CdA	75	23 (30.7)	-
SWV x $\frac{1}{4}$ Cd	79	-	-
SWV x R/A	81	-	29 (35.8)
SWV x $\frac{1}{4}$ R	85	-	-
SWV x SWV	84	-	-

1 small, fused, abnormally shaped, and missing centra

2 fused and missing ribs

TABLE C6

Frequency of vertebral and rib malformations among D18 embryos from the dose-response study; SWV data

	total live cross embryos	total normal	total craniofacial malformations	%	no. embryos with vertebral malformations ¹ (%)		no. embryos with rib malformations ² (%)	
SWV x CD4/5	338	242	96	28.4	40 (14.5)	50 (61.4)	8 (3.3)	2 (2.1)
SWV x 1/4 ¹ CD ⁶	340	206	54	15.9	-	-	8 (2.9)	1 (1.9)
SWV x RE/± ⁵	346	211	135	39.0	-	-	42 (19.9)	86 (83.7)
SWV x 1/4 ¹ CD ⁶	372	303	69	18.5	-	-	11 (3.9)	2 (2.9)
SWV x SWV ⁶	372	276	96	25.8	-	-	10 (3.9)	3 (3.1)

- * p ≤ .05
- 1 small, fused, abnormally shaped, and missing centra
 - 2 fused and missing ribs
 - 3 % = no. normal with malformation/total no. normal
 - 4 % = no. craniofacial with malformation/total no. craniofacial
 - 5 analyzed by χ^2 test
 - 6 analyzed by two-tailed Fisher's exact test

In all five crosses, with a much higher frequency in the SWV x Rf/+ cross. The ratio of exencephalia/normal embryos without the specific malformation was compared to the ratio of exencephalia/normal embryos with the skeletal malformation for each cross to determine if a preponderance of exencephalias with rib or vertebral abnormalities existed. Two-way tables were constructed and analyzed by a χ^2 test of independence or by a two-tailed Fisher's exact test. (Sokal and Rohlf, pp. 585). Only the SWV x Cd/t cross ($\chi^2 = 65.66$, $df = 1$) and the SWV x Rf/t cross ($\chi^2 = 67.50$, $df = 1$) yielded a significantly higher frequency of malformations among the exencephalic embryos. The SWV x Cd/+ exencephalic embryos had a high frequency (61.4%) of small, missing, fused or abnormally shaped centra, and the SWV x Rf/+ exencephalic embryos a high frequency (63.7%) of fused and missing ribs. Overall, in the SWV x Cd/+ cross 29.2% (99/338) of the embryos had vertebral malformations, a frequency which did not differ significantly from that found in the control embryos ($\chi^2 = 0.077$, $df = 1$). The SWV x Rf/+ cross had 36.9% (128/346) of the embryos exhibiting rib malformations, again, a frequency not significantly different from that seen in the control litters ($\chi^2 = 0.063$, $df = 1$).

15.9% (54/340) of all the embryos collected from the SWV x +/+Cd cross were exencephalic. For the SWV x +/+Rf cross, the overall frequency of exencephaly was 18.5% (69/372). It was therefore considered that a certain proportion of the exencephalias from the mutant crosses were of the wild-type

genotype. The frequencies from the nonmutant crosses were used as the true percentage of wild-type exencephalics present in the mutant crosses. The tests of independence were subsequently recalculated for the mutant crosses, this time adjusting the value for the number of exencephalics without an associated malformation by subtracting these percentages. For example, in the two-way table for the SWV x Cd/+ cross, the number of normal embryos without vertebral malformations remains the same at 202 (242-40), but the number of exencephalics without vertebral malformations, previously 37 (96-59), now becomes 31 ($.159 \times 37 = 6$). For the SWV x Rf/+ cross the correction involved subtracting 9 ($.185 \times 49$) from the 49 (135 - 86) exencephalics that did not possess rib anomalies. For the SWV x Cd/+ cross the new χ^2 value was 70.74 (df = 1), and for the SWV x Rf/+ cross χ^2 was equal to 77.68 (df = 1), both highly significant at the 5% probability level.

In addition to the SWV x Rf/+ cross, rib malformations were detected at a low frequency (< 4%) in all the other crosses. Although none of the control litters exhibited rib anomalies, and insulin administration has been associated with the induction of rib malformations, two-tailed Fisher's exact tests indicated that the frequencies of this occurrence were not significantly different from the control values.

Therefore the examination of the skeletal structure of the treated embryos indicated that a significantly higher frequency of exencephalic embryos in the mutant crosses possessed rib and vertebral malformations, the expression of the mutant genes.

4. Resorption data; A/J dams

The frequencies of resorptions at the various doses of insulin administered to the A crosses were also fitted to straight lines by probit analysis. The probit regression lines, with the data points for the five crosses, are seen in Figure C7. The frequency of resorptions, taken as the number of resorptions per total implants, at any given dose is shown for the five crosses in Table C1. To obtain the insulin-induced frequencies for resorption, these values were corrected by removal of the spontaneous frequency (Finney, 1971, pp. 125) before the best fitting lines were calculated. The spontaneous resorption frequencies for the crosses were determined from the control litters collected, and are shown in Table C7.

The insulin-induced resorption regression lines, as seen in Figure C8, can be tentatively subdivided, based on slope differences, into the mutant and nonmutant crosses. The test of parallelism indicated that all five probit regression lines could not be fitted to a common slope ($\chi^2 = 28.196$, $df = 4$), but that the subgroups could. The probit curves of the mutant crosses (A x Rf/A and A x Cd/4) fitted a common slope of 5.725 ($\chi^2 = 0.035$, $df = 1$, ns), while those of the

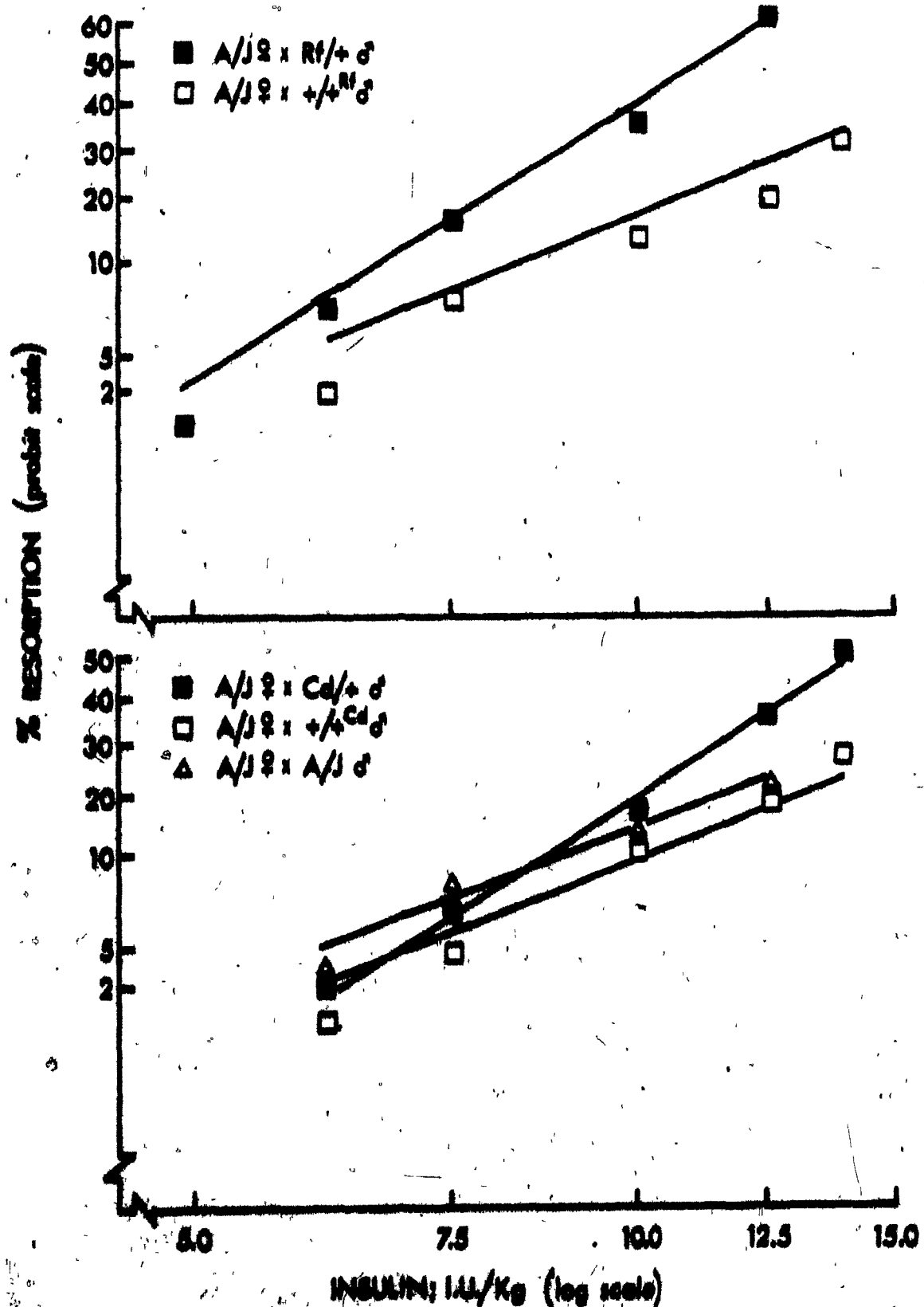


Figure C7. Independently fitted probit dose-responses of resorption for the crosses with the A/J dams (corrected for spontaneous resorption).

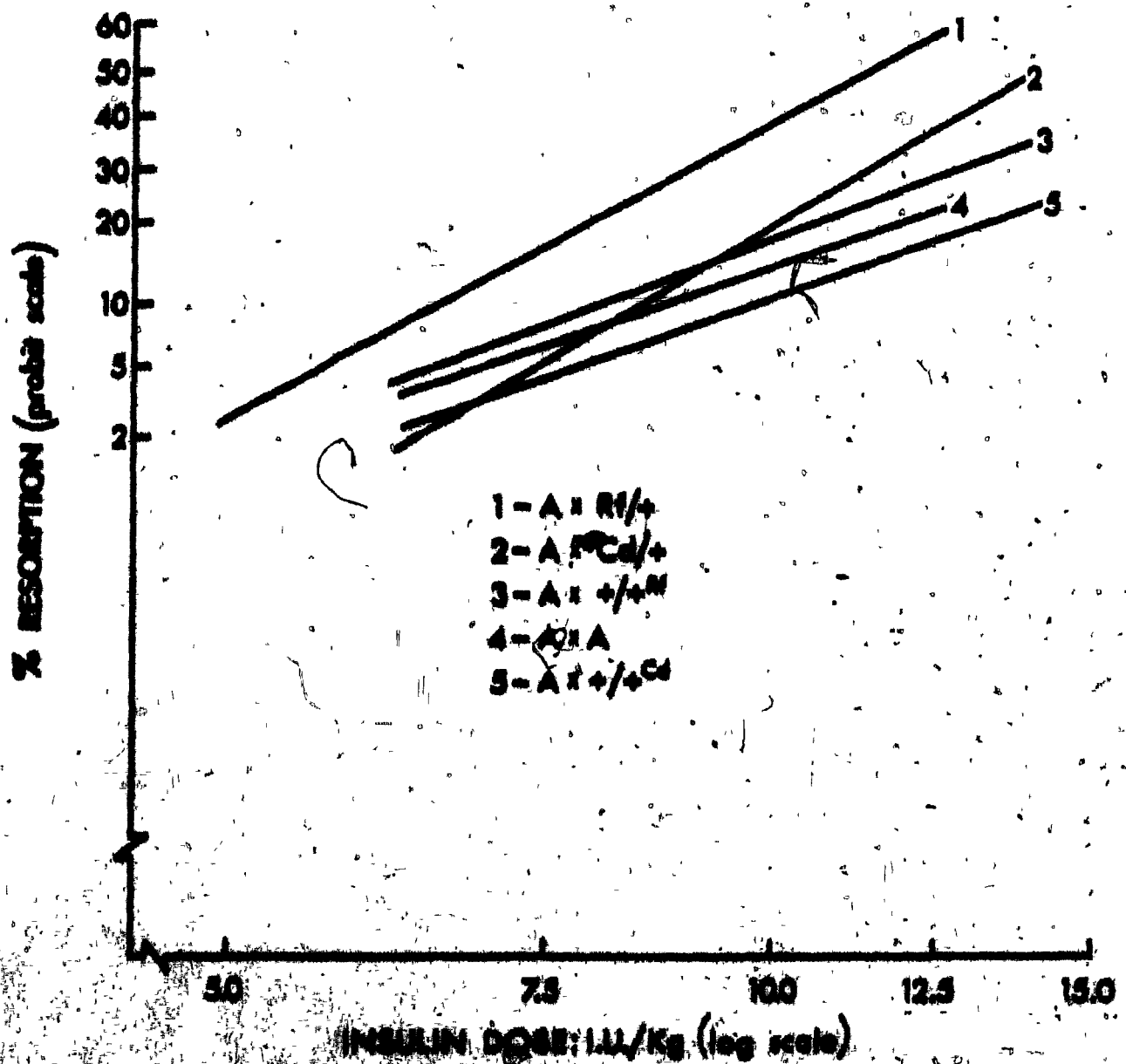


Figure C1. Independently fitted probit dose-response of resorption for the groups with the 1/2 dose (corrected for spontaneous resorption).

TABLE C7

spontaneous resorption data; A/J and SWV dams

cross	no. of litters	total implants	no. of resorptions	% resorptions
<u>1. A/J dams</u>				
A x Cd/+	10	62	11	17.4
A x +/-Cd	10	60	7	11.7
A x Rf/+	10	60	6	10.0
A x +/-Rf	10	63	9	14.3
A x A	10	59	13	22.0
<u>2. SWV dams</u>				
SWV x Cd/+	10	85	10	11.8
SWV x +/-Cd	10	90	11	12.0
SWV x Rf/+	10	90	9	10.0
SWV x +/-Rf	10	93	8	8.6
SWV x SWV	10	91	7	7.7

nonmutant crosses ($A \times A$, $A \times +/+^{Rf}$, and $A \times +/+^{Cd}$) fitted a common slope of 3.866 ($\chi^2 = 0.799$, $df = 2$; ns). The common and independently fitted slopes of these lines, and their corresponding tests of parallelism are found in Tables C8 and C9.

The ED_{50} 's within each group indicated only small differences in reactivity. The $A \times Rf/+$ cross, with an ED_{50} of 11.164 I.U./kg was slightly more sensitive than the $A \times Cd/+$ cross, whose ED_{50} was 14.462. In the nonmutant crosses the most sensitive cross was $A \times +/+^{Cd}$ (18.872 I.U./kg), followed by $A \times +/+^{Rf}$ (20.246 I.U./kg), and $A \times A$ (23.604 I.U./kg). Again, due to the slope differences, ED_{50} 's cannot be compared between the mutant and nonmutant crosses. The large fiducial limits again reflected the lack of data points above the 50% response point, a situation that was made worse as the spontaneous frequencies were removed from the observed frequencies, lowering the values for the induced response.

Thus, the significant change in slope value between the mutant and nonmutant crosses indicated an interaction, with the embryos from the mutant crosses interacting with the drug to resorb by a mechanism unique from that of the treated nonmutant crosses.

5. Resorption data; SWV data

The resorption frequencies at the given dates for the crosses using SWV data are shown in Table C4. The insulin-induced resorption frequencies were

TABLE C8

ED₅₀'s and common & independently fitted slopes of probit regressions for insulin-induced resorptions in A/J and SWV crosses¹

cross	constrained to parallelism		independently fitted		ED ₅₀ (I.U./kg)	95% fiducial limits
	Y intercept	slope	Y intercept	slope \pm S.E.		
A x Cd/+	- 1.699	5.725	- 1.807	5.867 \pm 0.098	14.462	9.237 to 28.655
A x +/+ ^{Cd}	- 0.072	3.866	- 0.697	4.466 \pm 0.198	18.872	7.288 to 26.091
A x Rf/+	- 0.995	5.725	- 0.929	5.657 \pm 0.145	11.164	9.322 to 17.561
A x +/+ ^{Rf}	- 0.032	3.866	0.234	3.801 \pm 0.247	20.246	11.192 to 32.667
A x A	- 0.083	3.866	0.598	3.279 \pm 0.140	23.604	11.479 to 27.618
SWV x Cd/+	0.524	2.621	0.546	2.605 \pm 0.196	51.237	42.946 to 69.785
SWV x +/+ ^{Cd}	0.118	2.621	0.124	2.616 \pm 0.359	63.0333	46.747 to 74.389
SWV x Rf/+	0.444	2.621	0.341	2.692 \pm 0.194	53.798	39.465 to 72.695
SWV x +/+ ^{Rf}	0.213	2.621	- 0.236	2.930 \pm 0.252	61.195	48.723 to 69.014
SWV x SWV	0.352	2.621	0.732	2.356 \pm 0.262	64.832	55.424 to 69.705

¹ corrected for spontaneous frequency

TABLE C9

Tests of Parallelism; resorption data

crosses	source	df	SS
<u>1. A/J dams</u>			
A/J: mutant and nonmutant	parallelism	4	28.196*
	heterogeneity	14	4.678
	total	18	32.874*
A/J: mutant	parallelism	1	0.035
	heterogeneity	6	2.157
	total	7	2.192
A/J: nonmutant	parallelism	2	0.799
	heterogeneity	8	2.521
	total	10	3.320
<u>2. SWV dams</u>			
SWV: mutant and nonmutant	parallelism	4	0.719
	heterogeneity	15	5.555
	total	19	6.274

* $P \leq .05$

calculated by removing the spontaneous frequencies, determined from the control litters and shown in Table C7. The insulin-induced resorption frequencies were subsequently fitted to probit regression lines, shown in Figure C9. No systematic deviations from linearity were indicated. In Figure C10 the five probit regression lines are seen together, and a test of parallelism fitted the five lines to a common slope of 2.621 ($\chi^2 = 6.274$, $df = 19$; ns), verifying the appearance of parallelism. As no interaction was indicated, the ED_{50} 's for the five crosses could be compared for their relative reactivities to the treatment. An ED_{50} value of 51.237 I.U./kg made the SWV x Cd/ cross the most sensitive, followed by SWV x Rf/ (53.798), SWV x +/-^{Rf} (61.195), SWV x +/-^{Cd} (63.033), and SWV x SWV (64.832), the most resistant of the crosses. However, the differences among the values were small, indicating a similar sensitivity to treatment. The large fiducial limits reflected the inability of the frequency range to extend above the 50% point.

6. Common slopes: A comparison of the calculated probit regressions

From the list of common and independently fitted slopes for the insulin-induced exencephaly and resorption probit curves it became of interest to determine which subgroups of curves could be fitted to a common slope. Comparisons were made only among crosses with the same female genotype, that is, the regression line for a cross with an SWV female was never tested for parallelism with the regression line for a cross with an A/J female. Different doses were administered

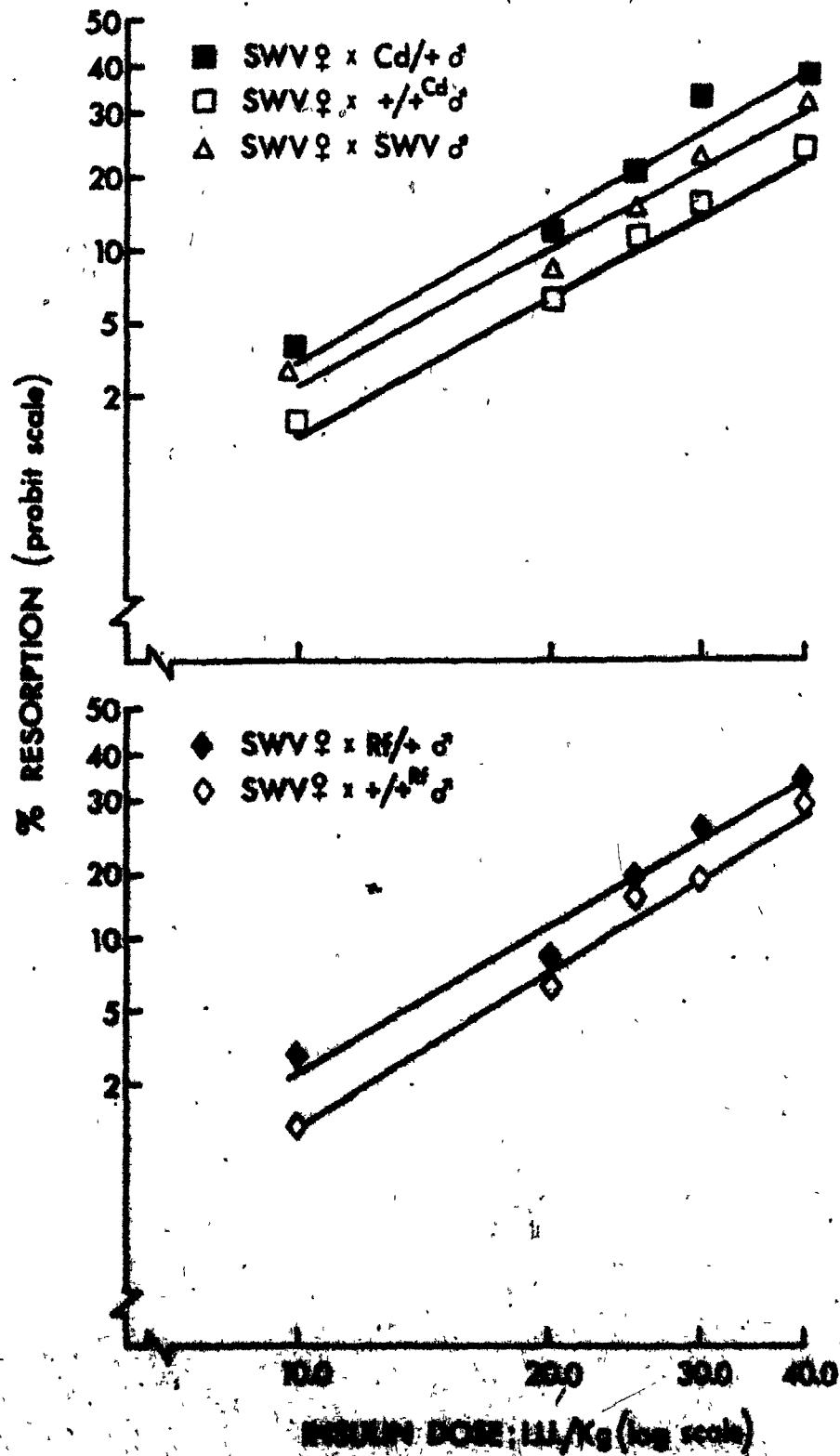


Figure 10. Independently fitted probit dose-response of resorption for the

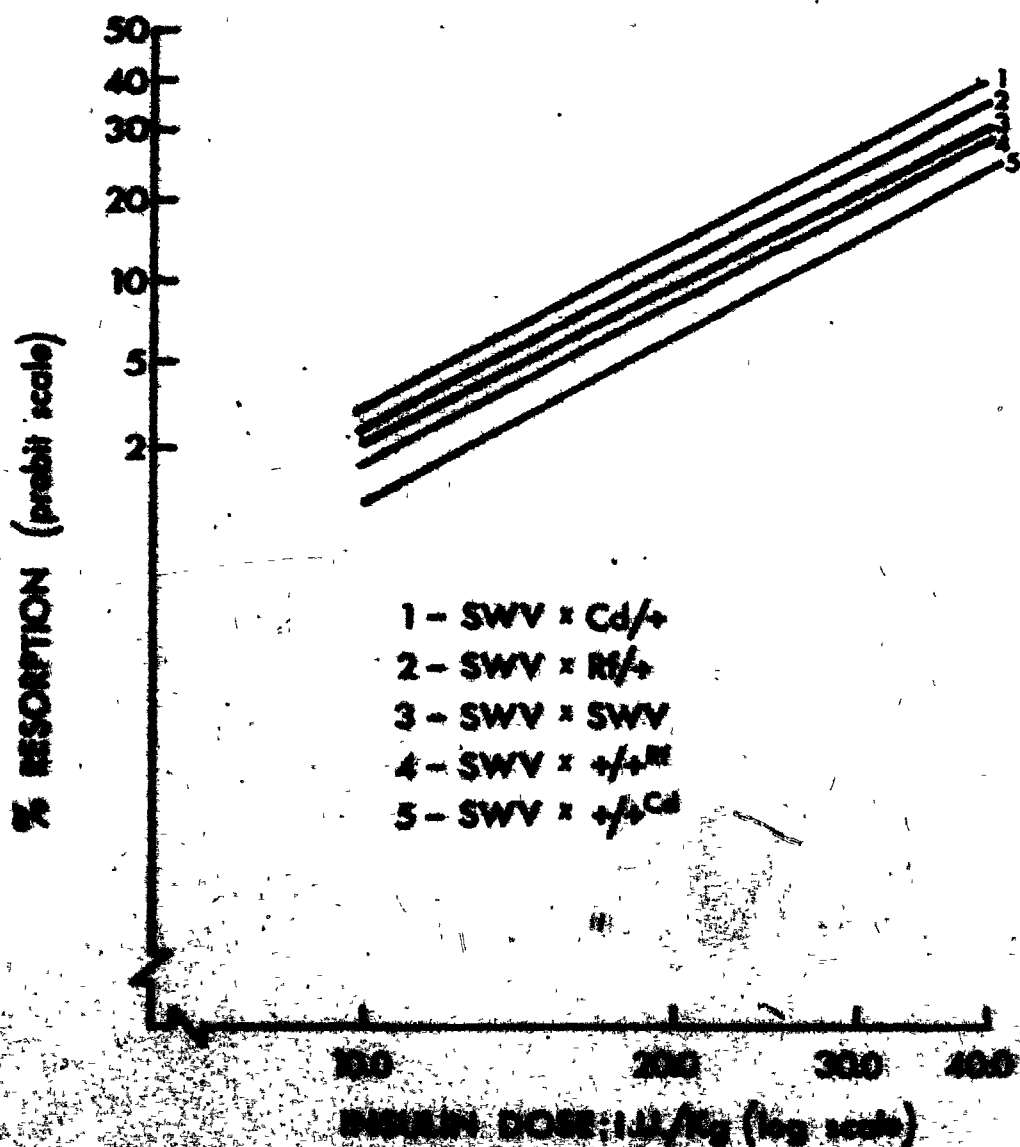


Figure 510. Independence of dose upon dose-response of resorption for the insecticide SWV dose (corrected for spontaneous resorption).

to each of these two groups of crosses, and the calculated regression lines hold true only over the given range of doses. As mentioned previously (section B.3), extrapolations of the probit curves assume that the condition of linearity prevails beyond the given dose range. As it could be possible for a nonlinear situation to arise over a different set of doses, extrapolations are an invalid procedure, violating one of the basic assumptions of the analysis. Therefore, as the crosses involving the A/J females were treated over a different dose range than that of the SWV crosses, any analysis for parallelism was restricted to within each of the two groups of crosses. The tests of parallelism are shown in Table C10 and are summarized as follows:

1. Crosses with A/J dams

The regression lines for the induced exencephaly data of the mutant crosses and the regression lines for the resorption data of the mutant crosses were fitted to a common slope ($\chi^2 = 0.546$, $df = 3$; ns). The regression lines for the nonmutant dose-response and resorption data was also fitted to a common slope ($\chi^2 = 10.639$, $df = 5$; ns), that was significantly different from that for the mutant crosses, as indicated by the inability to fit all the resorption and dose-response data to one common slope ($\chi^2 = 30.905$, $df = 9$).

2. Crosses with SWV dams

The regression lines for the resorption and dose-response data of the mutant and nonmutant crosses could not be fitted to a common slope ($\chi^2 = 40.669$, $df = 9$). The regression lines for the resorption data of the mutant and nonmutant

TABLE C10

tests of parallelism; analysis of the calculated common slopes for the induced exencephaly (dose-response) and resorption data.

Cross	source	df	SS
<u>1. A/J dams</u>			
mutant and nonmutant A/J dose-response data, mutant and nonmutant A/J resorption data	parallelism	9	30.905*
	heterogeneity	28	22.354
	total	37	53.259*
mutant A/J dose-response data, mutant A/J resorption data	parallelism	3	0.546
	heterogeneity	12	11.821
	total	15	12.367
nonmutant A/J dose-response data, nonmutant A/J resorption data	parallelism	5	10.639
	heterogeneity	16	10.533
	total	21	21.172
<u>2. SWV dams</u>			
mutant and nonmutant SWV dose-response data, mutant and nonmutant SWV resorption data	parallelism	9	40.669*
	heterogeneity	30	14.308
	total	39	54.977*
nonmutant SWV dose-response data, mutant and nonmutant resorption data	parallelism	7	1.043
	heterogeneity	24	11.787
	total	31	12.830
mutant SWV dose-response data (Table C3)	parallelism	1	0.471
	heterogeneity	6	2.521
	total	7	2.992

* $p \leq .05$

crosses, and for the dose-response data of the nonmutant crosses were parallel ($\chi^2 = 1.043$, $df = 7$; ns), and this common slope was significantly different from the one calculated for the regression lines for the dose-response data of the mutant crosses ($\chi^2 = 0.471$, $df = 1$; ns).

7. Analysis of the morphological data

Exencephalic embryos were not detected among the D8, D9, and D10 embryos obtained from the control crosses. Upon collecting the D8, D9, and D10 embryos from treated females for morphological examination it was noticed that, for the A/J crosses, the frequencies of exencephaly were higher among these embryos than among the D14 embryos collected at the same dose for the dose-response study. This situation did not exist among the SWV crosses. The frequencies of exencephaly among the morphologically rated embryos from the SWV crosses were very similar to those obtained from the dose-response work (collected on D18). The frequencies of exencephaly for the morphological and dose-response data for the crosses are shown in Table C11. For the morphological data, the frequency of exencephaly was determined as the percentage of affected embryos per total implants. Total implants were the sum of the number of maturing embryos and the number of resorptions. Resorptions were represented by mushy, transparent and necrotic embryonic tissue or, in advanced cases, the remains of a placenta. Exencephalic embryos were scored at collection times D9/12, D9/18, and D10/6 but not at the earlier times (D8/12, D8/18, and D9/6), as it was felt the malformation could be unequivocally detected only by D9/12.

TABLE C11

Fisher's exact test; A/J and SWV dams, a comparison of the frequency of exencephaly for the dose-response (collected on D14 and D18) and the morphological data (collected on D9/12, D9/18, and D10/6).

cross	% exencephaly		two-tailed probability
	dose-response data ¹ (exencephalics/live embryos)	morphological data (exencephalics/total implants)	
A x Cd/+	33.9 (18/53)	57.7 (30/52)	0.019*
A x +/- ^{Cd}	13.1 (10/76)	35.2 (19/54)	0.005*
A x Rf/+	58.0 (29/50)	76.4 (42/55)	0.060
A x +/- ^{Rf}	2.18 (12/55)	52.5 (31/59)	0.001*
A x A	14.0 (7/50)	46.7 (28/60)	0.0004*
SWV x Cd/+	73.2 (41/56)	73.8 (62/84)	1.000
SWV x +/- ^{Cd}	34.6 (18/52)	40.7 (35/86)	0.588
SWV x Rf/+	84.2 (64/76)	86.7 (78/90)	0.665
SWV x +/- ^{Rf}	38.7 (24/62)	31.9 (29/91)	0.393
SWV x SWV	46.8 (29/62)	51.8 (43/83)	1.000

* $p \leq .05$

¹ from Tables C1 and C4

Therefore, the numbers shown were the totals obtained by combining the data from D9/12, D9/18, and D10/6.

Using a two-tailed Fisher's exact test it was shown that for the A/J crosses, the frequencies of induced exencephaly from the morphological data were significantly higher than the frequencies obtained at the same dose from the dose-response data. This significant difference was found in four of the crosses, and the fifth cross, A x Rf/A, tended towards a significant increase in frequency ($P \leq .1$).

Two-tailed Fisher's tests did not reveal significant differences in the frequencies of induced exencephaly between the morphological and dose-response data for the SWV crosses. The results of the Fisher's tests are also seen in Table C11.

In addition to the discrepancy in the frequency of exencephaly between the morphological and the dose-response data, other points of interest were noticed while scoring the morphological development of the treated and untreated embryos during the period of neural tube closure. Many of the D9/12, D9/18 and D10/6 embryos, easily distinguished as normal or exencephalic, exhibited unusual behavior in their turning pattern. The embryo normally moves from an S to a C-shaped configuration on days 8 and 9. Some of the embryos

demonstrated delayed turning in that the turning process was still not completed by D9/12, although most embryos have completed turning by D9/6. However, the actual configuration of the body shape was not contorted. Other embryos did possess an abnormal body shape. The turning process, difficult to assess as incomplete or complete due to the unusual body configuration, had resulted in a twisted or kinked appearance below the area of the heart and forelimb buds (referred to in this study as the hindbody area). The kinked appearance sometimes extended to the tip of the tail bud, and was highly variable in expression. The abnormal hindbody shape was always found in those embryos that were exencephalic. Furthermore, these exencephalic embryos with the twisted turning were from the treated mutant crosses. This condition was not seen in the embryos collected from the untreated mutant and nonmutant crosses, nor was it seen in the exencephalic embryos from the treated nonmutant crosses. The embryos from the treated mutant and nonmutant crosses that did not develop exencephalic brains also did not possess the abnormal body shape.

Among the D9/12, D9/18 and D10/6 embryos delayed turning was also seen only in association with exencephaly. Unlike the abnormal body shape, it was observed among exencephalic embryos from both the treated mutant and nonmutant crosses. Delayed turning, however, was not seen among the embryos from the control crosses. It should be mentioned that, although the

stage of turning was scored for all the embryos collected at the specified times, delayed and abnormal turning were classifications used only when scoring the D9/12, D9/18 and D10/6 embryos. The embryo is only beginning to turn at D8/12 and D8/18. Therefore, the lack of extensive movement at the earlier times made any judgement of delay or abnormality much more arbitrary. Also, the main aim of the morphological study was to detect differences that could be associated with the occurrence of exencephaly. Since the brain malformation could only be clearly identified by mid D9, the most important factor to note was other deviations from normal development also appearing at that time.

The breakdown for the combined total of exencephalics from D9/12, D9/18 and D10/6 for each of the treated crosses, into normal, delayed, or abnormal turning is shown in Table C12. The exencephalic embryos from the nonmutant crosses, as mentioned before, did not demonstrate an abnormal body shape. Also, the frequency of delayed turning was considerably less among these embryos than among those from the mutant crosses. About one-third of the exencephalic embryos from each of the mutant crosses possessed an abnormal body shape, while another one-third showed a delay in the turning process.

TABLE C12

Analysis of the morphological data from the treated mutant and nonmutant crosses into normal, delayed, or abnormal turning classifications.

cross	total no. of exencephalic embryos	no. of embryos with normal turning (%)	no. of embryos with delayed turning (%)	no. of embryos with abnormal turning
A x Cd/+	30	9 (30.0)	11 (36.7)	10 (33.3)
A x Rf/+	42	14 (33.3)	13 (30.9)	15 (35.7)
A x $\frac{1}{4}$ + ^{Cd}	19	15 (79.0)	4 (21.0)	0 (0%)
A x $\frac{1}{4}$ + ^{Rf}	31	25 (80.7)	6 (19.3)	0 (0%)
A x A	28	24 (85.7)	4 (14.3)	0 (0%)
SWV x Cd/+	62	20 (33.3)	18 (29.0)	22 (35.5)
SWV x Rf/+	78	29 (37.2)	25 (32.0)	24 (30.7)
SWV x $\frac{1}{4}$ + ^{Cd}	35	30 (85.7)	5 (14.3)	0 (0%)
SWV x $\frac{1}{4}$ + ^{Rf}	29	22 (75.9)	7 (24.1)	0 (0%)
SWV x SWV	43	33 (76.8)	10 (23.2)	0 (0%)

0 Both normal and abnormal development during the process of neural tube closure can be seen in the following set of photographs. The pictures, at a 6 X magnification, represented the appearance of the treated and untreated embryos at various times in development.

Figures C11-C19 represent the normal pattern of development, as seen in the control specimens. Figures C11 and C12 show two D8/12 untreated embryos, each with 8 pairs of somites. The embryo in Figure C11 has a completely open neural tube (stage 0), and has not yet started to move out of its S-shaped configuration (stage 0). In Figure C12 the neural folds have fused in the area of the prosencephalon (stage 1), and the cranial axis of the embryo is slightly out of line with the caudal axis, indicating the initial movements of turning (stage 1). The neural folds of the D8/18 untreated embryo shown in Figure C13 still have not completely fused over the entire prosencephalon, but do indicate initial fusion (stage 1). Turning has progressed further, however, so that the cranial axis is now at a right angle to the hindbody, with the entire area anterior to the mid-trunk region having rotated (stage 2).

Figures C14 and C15 show front and back views of a normal D9/6 embryo. The neural folds in the region of the anterior neuropore (arrow, Figure C15) have yet to fuse, but closure has occurred over the entire

prosencephalic area to the middle of the mesencephalon (stage III, Figure C14). The embryo has essentially completed its turning, and now maintains a C-shaped configuration with the neural tube forming the exterior of the curvature (stage 4). The hindbody will, however, come to rest closer to the head region. Figures C16 and C17 show front and back views of an untreated D9/12 embryo. Turning is completed (stage 4), and the neural tube is now closed over the anterior neuropore region. Further to this, the roof of the rhombencephalon is covered with a thin epithelium (stage V). Upon thickening of this epithelium, the neural tube is completely closed in the cephalic region, as seen in the untreated D10/6 embryo (Figures C18 and C19). The posterior neuropore has also closed, making the process of neural tube closure complete (stage VII). The embryo now begins to show large increases in size.

The embryos from the treated crosses that showed normal brain development followed the pattern of development seen above. Of the D9/12, D9/18 and D10/6 embryos that were anencephalic, some developed the brain malformation in the absence of any associated turning defect, as seen in Figures C20 and C21. This is a D9/12 embryo from a treated A x +/+Cd cross. When compared to the D9/12 embryo seen in Figures C16 and C17, one

Immediately notes that the neural tube is open over the entire prosencephalic and mesencephalic area. The neural folds are growing in an everted manner, which will cause the underlying brain tissue to exude out of the open surface. The turning procedure is normal. The embryo has turned, and now all that remains is for the hindbody region to move up and come to rest next to the head region (stage 4). Though the turning of this embryo is not as fully complete as the normal D9/12 control embryo described earlier, this amount of variation in the process was considered normal.

Examples of exencephaly accompanied by delayed turning are seen in Figures C22 and C23. Figure C22 is a D9/12 exencephalic embryo from a treated SWV $x \pm / 4^{Rf}$ cross. The embryo is at the stage of turning (stage 2) normally seen in the D8/18 embryo (Figure C13). The brain, which should be entirely closed to the prosencephalic and mesencephalic area (Figures C16 and C17), has remained open, with the neural folds growing in an everted manner. The D9/18 exencephalic embryo from a treated SWV x CdA cross (Figure C23) shows severe delays in the turning process. Its cranial axis has only started to move out of the S-shaped configuration (stage 1, note Figure C12), although the process should have been completed by this time. The open mesencephalic area of the brain clearly denotes the embryo as exencephalic. The exencephalic embryos from the treated mutant crosses that demonstrated

an abnormal hindbody shape are seen in the following figures. Figure C24 is a side view of a D9/18 exencephalic embryo from a treated A x Cd/+ cross. The neural folds have failed to fuse, exposing the inner brain mass and, below the heart region, one can see a slightly kinked body shape. The somites (arrow) are not as regular in appearance as in a normal embryo. Figure C25 is a dorsal view of a D9/18 exencephalic embryo from a treated SWV x Rf/+ cross. Not visible here is the open mesencephalic area of the brain, although everted neural folds can be distinguished. The embryo possesses an extensive twisting and kinking of the hindbody region (arrows). Figure C26 is that of a resorbing D9/12 exencephalic embryo from a treated SWV x Cd/+ cross. The extensive somite disorganization could not be shown in photographic detail due to the transparency of the dying tissue. One can maintain, however, that the body shape is distinct from the normal pattern. The embryo shows only a mild form of exencephaly, with the entire neural tube closed except for a triangular area of the mesencephalon. Figure C27 is a D9/12 exencephalic embryo from a treated SWV x Rf/+ cross. The hindbody has twisted into a totally misaligned shape. The prosencephalon and mesencephalon have remained open. The D9/12 exencephalic embryo shown in Figure C28 is from a treated SWV x Cd/+ cross. This side view does not clearly demonstrate the open neural tube, but does readily show the twisted abnormal hindbody shape.

To further determine if these exencephalic embryos from the insulin treated mutant crosses were phenocopies of the mutant genes in their homozygous condition, several $Rf/+ \times Rf/+$ and $Cd/+ \times Cd/+$ matings were set up and the litters examined at D9/12 and D9/18 to see if similar abnormalities were present. It was known that the affected homozygous embryos would start to resorb on D9 (Theller and Stevens, 1960; Morgan, 1954) and also that only the homozygotes would show spontaneous exencephaly, so it was felt the affected homozygotes could be isolated with a high degree of certainty. Figure C29 is a D9/12 exencephalic embryo from a $Rf/+ \times Rf/+$ cross. The brain is open in the mesencephalic area, and the hindbody shows areas of twisting and kinking (arrows) similar to that seen in the exencephalic embryos from the treated mutant crosses. Figure C30 is a D9/18 exencephalic embryo from a $Cd/+ \times Cd/+$ cross which is showing early signs of resorption. The hindbody of this embryo also shows some twisting. Figure C31 is a D9/12 embryo from a $Rf/+ \times Rf/+$ cross. It has been resorbed quite extensively, and the area where the neural tube failed to close is only faintly visible (arrow). However, the body shape is abnormal, and bears striking resemblance to the D9/12 exencephalic embryo from the treated mutant cross that was also undergoing resorption (Figure C26).

The last three photographs are of D10/6 exencephalic embryos.

Figure C32 is a D10/6 exencephalic embryo from a treated A x CdA cross.

The body shape shows a definite twist about the central axis. Figure C33

is a D10/6 exencephalic embryo from a treated SWV x RfA cross. The

hindbody is tucked under, instead of resting next to, the head region. The

exencephalic brain has a large cyst growing out of one side, a condition often

seen in the severe exencephalic forms. Figure C34 is a D10/6 exencephalic

embryo from a treated A x +/Rf cross showing a much smaller cyst on one side

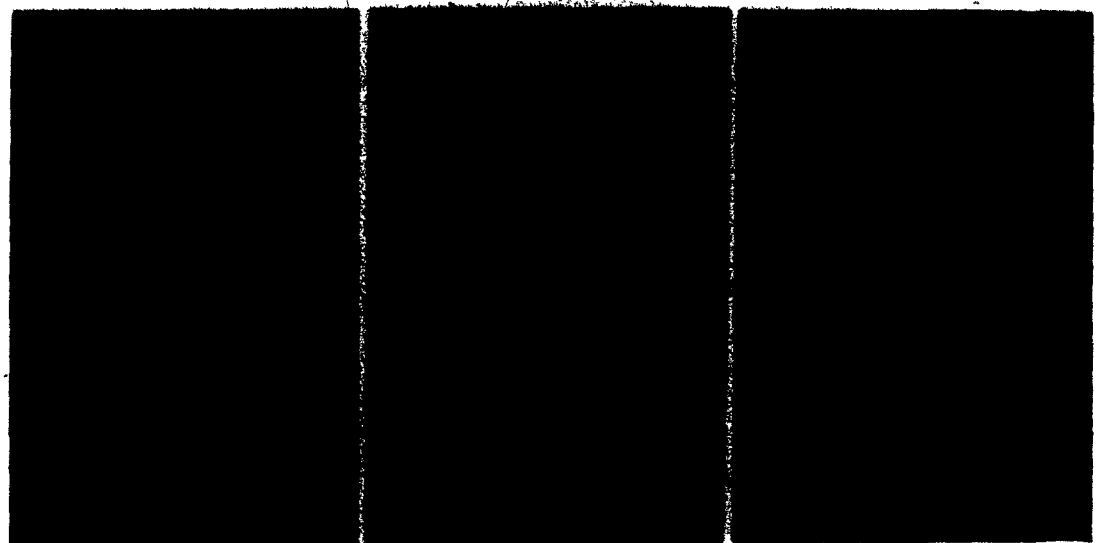
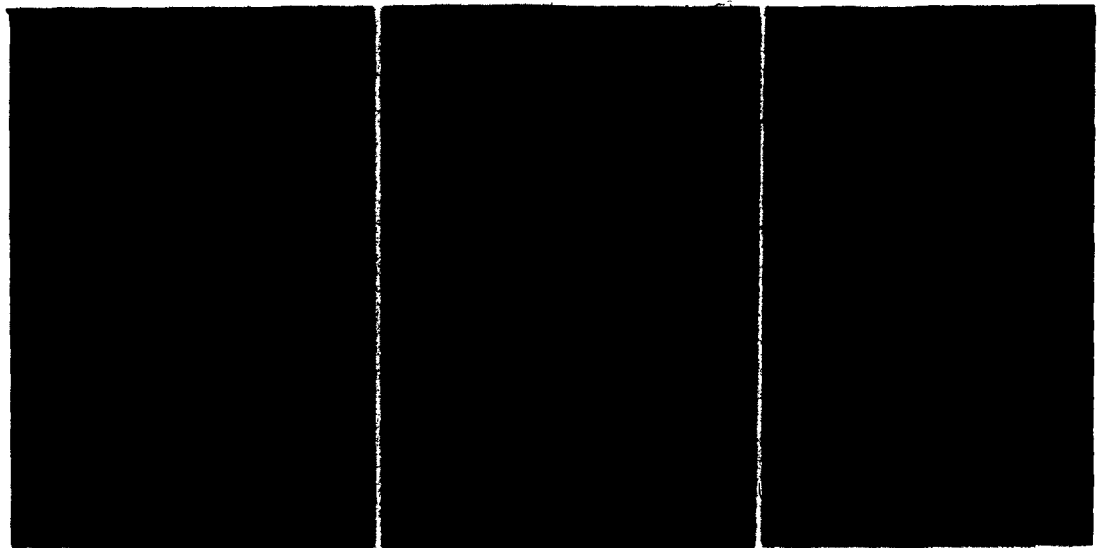
of the open brain, and a normal body shape.

After examining many embryos, similar to those shown in the photographs, it was felt that no obvious differences existed within the group of mutant crosses and the group of nonmutant crosses in the expression of the brain and, in the case of the mutant group, the turning malformations. This was an important factor to establish as time allowed only a limited number of embryos from any one cross to be sectioned for histological examination. It was therefore decided that, when selecting the embryos for sectioning, each would simply represent a mutant or nonmutant cross. Furthermore, initially the only exencephalic embryos from the mutant crosses to be examined histologically, would be those with an abnormal body shape. This was an occurrence unique to the mutant crosses, and therefore could be a part of the distinguishing feature that would delineate the underlying mechanism of the interaction.

- Figure C11 Photograph of a D8/12 untreated embryo with 8 pairs of somites. The neural tube is completely open (stage 0), and turning has not yet started (stage 0). nf, neural folds; p, prosencephalon. X 6
- Figure C12 Photograph of a D8/12 untreated embryo with 8 pairs of somites (S). The neural folds have fused in the area of the prosencephalon (arrow, stage 1), and the embryo has turned slightly (stage 1). X 6
- Figure C13 Photograph of a D8/18 untreated embryo. There is initial fusion of the neural folds (nf) in the region of the prosencephalon (arrow, stage 1). The cranial axis has now rotated so that it is perpendicular to the hindbody (stage 2). X 6
- Figure C14 Photograph of a normal D9/6 embryo. The embryo has completed turning, and the body now possesses a C-shaped configuration (stage 4). The hindbody will come to rest closer to the head region. Closure of the neural tube is complete over the entire prosencephalon (stage III). p, prosencephalon. X 6
- Figure C15 Photograph showing the dorsal view of this D9/6 embryo. Closure of the neural tube has progressed to the middle of the mesencephalon, known as the anterior neuropore (arrow). X 6
- Figure C16 Photograph of a normal D9/12 embryo. Turning has been completed (stage 4), and the neural folds have fused over the entire fore and midbrain. p, prosencephalon. X 6

x

C



Q

Figure C17

Photograph showing the dorsal view of this D9/12 embryo. Fusion of the neural folds is complete over the anterior neuropore region (arrow). The roof of the rhombencephalon is covered by a thin epithelium (stage V), whose transparency makes it impossible to be seen in the photograph. r, rhombencephalon. X 6

Figure C18

Photograph of an untreated D10/6 embryo. Turning and fusion of the neural folds over the prosencephalic (p) and mesencephalic (m) areas of the brain are both completed. X 6

Figure C19

Photograph of the dorsal view of this D10/6 embryo. The epithelium covering the roof of the rhombencephalon (r) has thickened, indicating that the process of neural tube closure in the cephalic region has been completed (stage VI). X 6

Figure C20

Photograph of a D9/12 embryo from a treated A x +/-^{Cd} cross. The neural tube is completely open over the prosencephalic (p) and mesencephalic (m) areas, with the neural folds growing in an everted manner, characteristic of exencephaly. The turning procedure, however, is within the normal range for this gestational age. X 6

Figure C21

Photograph of the dorsal view of this D9/12 exencephalic embryo. Again, one can see the open neural tube (arrow), and the everted neural folds (nf). X 6

Figure C22

Photograph of a D9/12 exencephalic embryo from a SWV x +/-^{Rf} cross. The embryo is at the stage of turning (stage 2) normally seen in the D8/18 embryo (Figure C13). The neural tube has remained open in the prosencephalic (p) and mesencephalic (m) areas. X 6

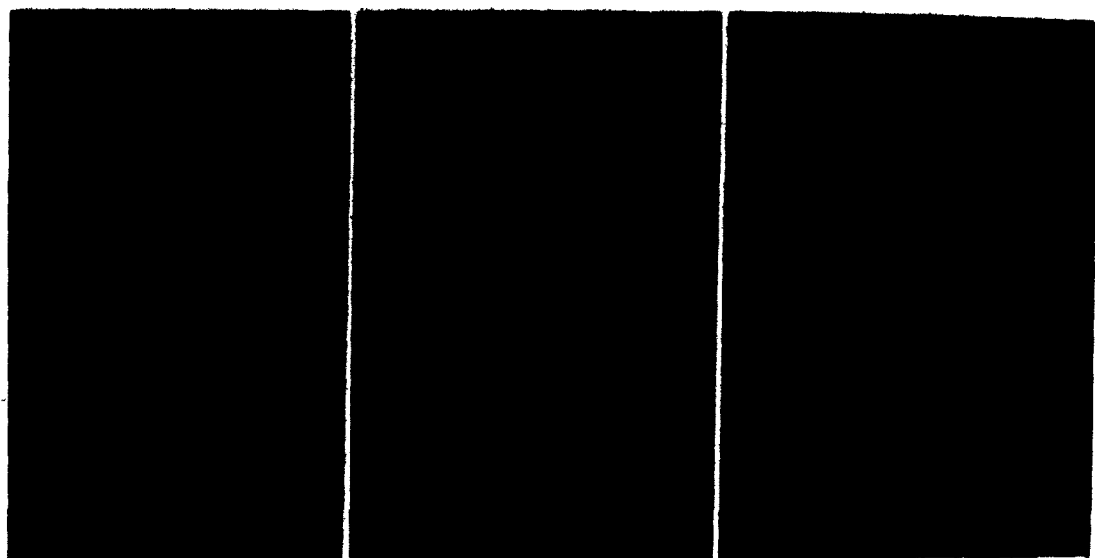
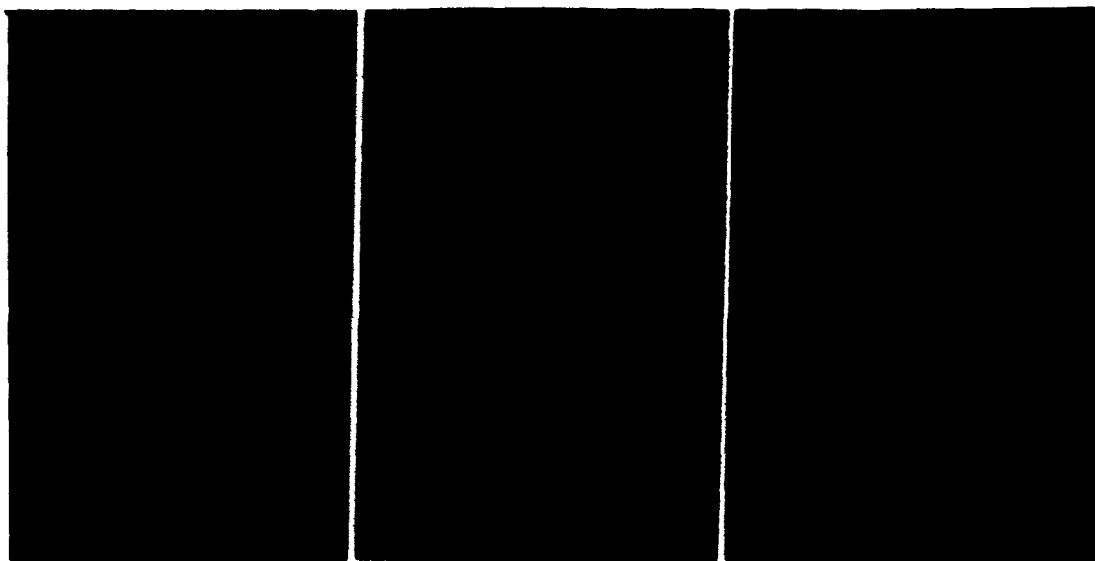


Figure C23

Photograph of a D9/18 exencephalic embryo from a treated SWV x Cd/+ cross. It shows a severe delay in the turning process, having only started to move out of an S-shaped configuration (stage 1). The neural tube is open in the fore and midbrain regions.

X 6

Figure C24

Photograph showing a side view of a D9/18 exencephalic embryo from a treated A x Cd/+ cross. The neural folds (nf) have failed to fuse, and the body has a kinked appearance below the region of the heart (h). The somites have an irregular appearance (arrow).

X 6

Figure C25

Photograph of a dorsal view of a D9/18 exencephalic embryo from a treated SWV x Rf/+ cross. The neural folds are growing in an everted manner, and there is extensive twisting of the hindbody (arrows).

X 6

Figure C26

Photograph of a D9/12 exencephalic embryo from a treated SWV x Cd/+ cross. The transparency of the tissue is a sign of resorption. The body shape has deviated from the normal pattern. The neural tube is open in the mesencephalon (m).

X 6

Figure C27

Photograph of a D9/12 exencephalic embryo from a treated SWV x Rf/+ cross. The prosencephalon and mesencephalon have remained open, and the hindbody possesses an abnormal shape.

X 6

Figure C28

Photograph of a side view of a D9/12 exencephalic embryo from a treated SWV x Cd/+ cross. The neural tube is open (arrow), and the hindbody has twisted into an abnormal shape.

X 6

X

B

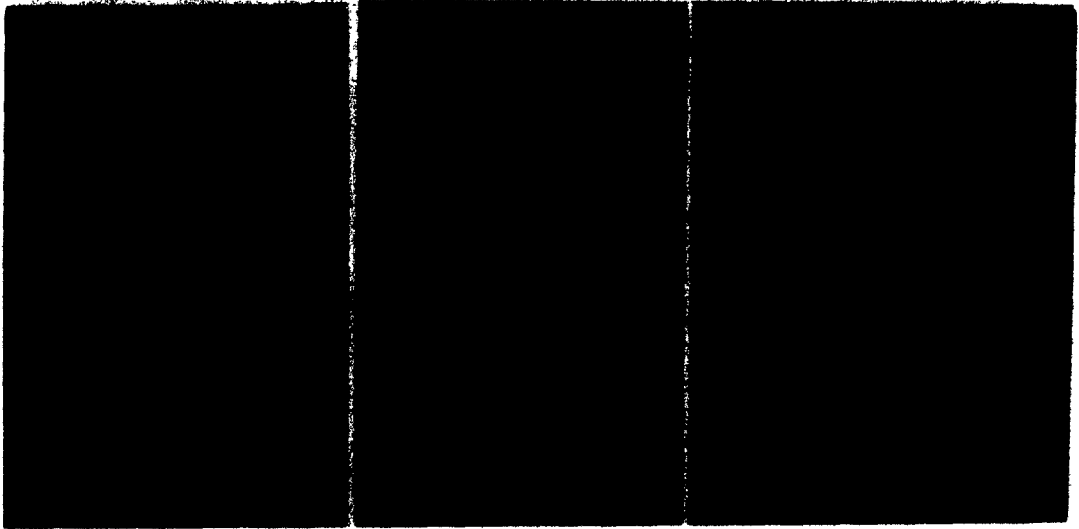
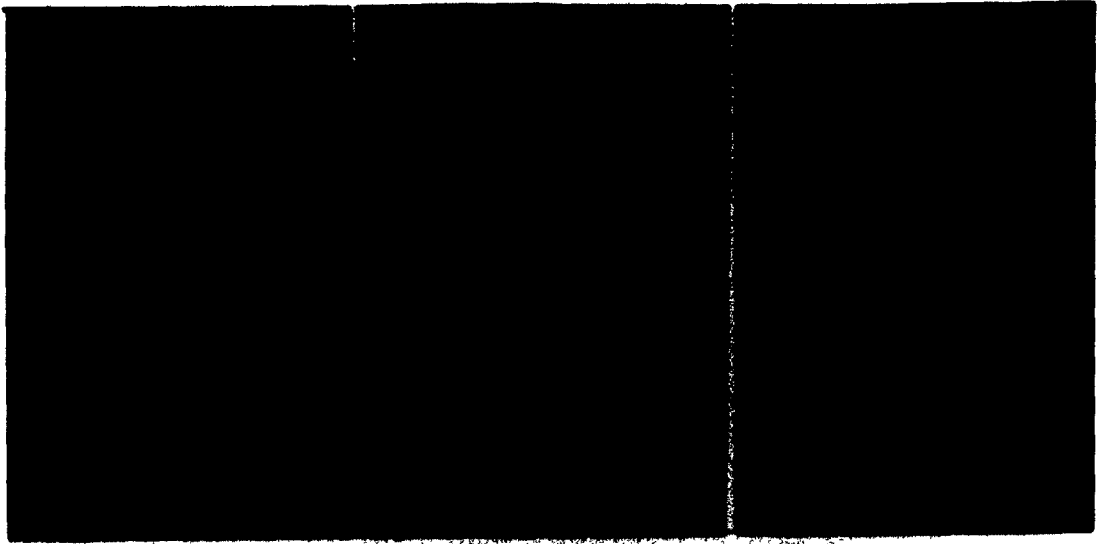


Figure C29

Photograph of a D9/12 exencephalic embryo from a $Rf/+ \times Rf/+$ cross. The brain is open in the mesencephalic region (m), and the hindbody shows areas of twisting and kinking (arrows).

X 6

Figure C30.

Photograph of a D9/18 exencephalic embryo from a $Cd/+ \times Cd/+$ cross, showing signs of resorption. The tissue is slightly transparent, and some degeneration has occurred (arrow). The hindbody is somewhat twisted, yielding an abnormal body shape.

X 6

Figure C31

Photograph of a D9/12 embryo from a $Rf/+ \times Rf/+$ cross. It has undergone extensive resorption. The area where the neural tube failed to close is slightly visible (arrow). The body shape is abnormal, and is strikingly similar to the D9/12 exencephalic embryo from the treated mutant cross that was also undergoing resorption (Figure C26).

X 6

Figure C32

Photograph of a D10/6 exencephalic embryo from a treated $A \times Cd/+$ cross. The body shape is twisted about the central axis. The brain is clearly exencephalic. m, mesencephalon; p, prosencephalon. X 6

Figure C33

Photograph of a D10/6 exencephalic embryo from a treated $SNV \times Rf/+$ cross. The hindbody has come to rest under the head region. There is a large cyst (c) present on one side of the exencephalic brain. m, mesencephalon; p, prosencephalon.

X 6

Figure C34

Photograph of a D10/6 exencephalic embryo from a treated $A \times +/+^{Rf}$ cross. The body shape is normal, and there is a cyst (c) on one side of the open brain. m, mesencephalon; p, prosencephalon.

X 6



Log-linear analysis was used to analyze the morphological data. Each embryo was scored on seven variables, which were its cross (C), its gestational age (A), whether the embryo was from a control or treated cross (T), its somite number (S), its stage of neural tube closure (B), its stage of turning (M), and whether the brain was exencephalic or normal (R). The analysis could only be performed on four variables at a time, so the four dependent variables (somite number, neural tube closure, turning, and response) were consecutively analyzed with the three independent variables (cross, age, and treatment). As the analysis could not be done on all the variables at once, the significant interactions detected could not be ordered for importance.

The results are shown in Table C13. As previously stated (section B.5) the tests of partial and marginal association together determine the significance of any interaction. Any significant higher order effect immediately implies that the lower order components of that effect make a significant contribution as well. Thus, the first analysis tested for any association among cross, age, treatment, and somite number variables. It can be seen that the CATS effect was not significant, nor were there significant interactions among the third order effects CAT, ATS, CTS, and CAS, second order effects CA, AS, TS, AT, and CS, and main effects A and S. Therefore

TABLE C13

Tests of partial and marginal associations for the variables of the morphological analysis

group of variables tested ¹	effect	partial association probability	marginal association probability
CATS	CATS	1.0000	-
	CAT	0.9933	0.9982
	ATS	0.8745	0.8742
	CTS	0.9365	0.9371
	CAS	0.8962	0.8714
	CA	0.9423	0.9397
	AT	0.1042	0.1045
	CT	0.0092*	0.0097*
	AS	0.8554	0.8562
	TS	0.7964	0.7899
	CS	0.7219	0.7263
	C	0.0025*	-
	A	0.0925	-
	T	0.0000*	-
	S	0.8932	-
CATB	CATB	0.8726	-
	CAB	0.9937	0.9966
	CTB	1.0000	0.9994
	ATB	0.0000*	0.0000*
	CT	0.0250*	0.0364*
	CB	0.0132*	0.0145*
	AB	0.0012*	0.0009*
	TB	0.0000*	0.0000*
	C	0.0045*	-
	A	0.0000*	-
	T	0.0000*	-
	B	0.0000*	-
CATM	CATM	1.0000	-
	CAM	1.0000	1.0000
	CTM	0.6217	0.2708
	ATM	0.0036*	0.0045*
	CT	0.0345*	0.0431*
	CM	0.0054*	0.0059*
	AM	0.0032*	0.0028*
	TM	0.0001*	0.0001*
	C	0.0010*	-
	A	0.0025*	-
	T	0.0000*	-
	M	0.0000*	-

Table C13 cont'd

.../2

CATR	CATR	1.0000	-
	CAR	0.9856	0.9963
	ATR	0.7523	0.8343
	CTR	0.0074*	0.0071*
	CT	0.0482*	0.0345*
	CR	0.0043*	0.0036*
	AR	0.1295	0.1342
	TR	0.0024*	0.0031*
	C	0.0019*	-
	A	0.0946	-
	T	0.0005*	-
	R	0.0012*	-
BMR	BMR	0.0016*	-
	BM	0.0023*	0.0020*
	MR	0.0012*	0.0017*
	BR	0.0000*	0.0000*
	B	0.0000*	-
	M	0.0000*	-
	R	0.0000*	-

*p ≤ .05
variable

C=cross
A= gestational age
T=treated or control
S=somite number
B=stage of neural tube closure
M=stage and type of turning
R=response (exencephalic or normal)

there was no association of somite number to cross or gestational age, nor did the insulin treatment affect the somite number of the embryos, a good indication that general development remained unimpeded by the treatment. There was a significant relationship of cross to treatment (CT), and interaction that was found to be significant when testing the other groups of variables (CATB, CATM, and CATR) as well. That is to say the effectiveness of the treatment in producing the malformation was partly dependent on the genetic background of the embryo. The interactions CAT, AT, and CA were also found to be highly nonsignificant ($P > .8$) when analyzing the CATB, CATM, and CATR groups of variables. Therefore the marginal and partial association probabilities for these effects were not listed for the other groups tested.

Analysis of the cross, age, treatment, and stage of neural tube closure set of variables (CATB) showed the ATB interaction to be significant. The age, the effect of the insulin treatment, and the stage of neural tube closure of the embryo were variables that interacted to form a significant relationship. Due to the design of the analysis, all the second order and main effects of the ATB interaction were also significant.

The next set of variables studied was the cross, age, treatment, and turning of the embryo. The CATM effect was not significant, but the ATM third order effect was. The age of the embryo, whether or not it came from a treated litter, and its turning process were all seen to be related to one

another. Following this all the second order and main effects composing the ATM effect also made significant contributions to the interaction. Analysis of the CATR set of variables indicated the interaction of cross, treatment, and subsequent response (CTR) to be highly significant. When the dependent variables neural tube closure, turning, and response were analyzed as a group (BMR), a significant interaction among the three was found. Again, the subset of lower order and main effects composing these interactions were significant as well.

In summary, the ATB, ATM, CTR, and BMR effects were all found to be significant interactions. Insulin treatment had significantly altered the pattern of turning and neural tube closure, two processes to which the age of the embryo was also significantly related. The response of the embryo to the treatment was highly dependent on the cross from which the embryo had come. Finally, the response of the embryo to the treatment was closely linked to the neural tube closure and turning processes. These significant interactions determined by log-linear analysis were in good agreement with the information collected by gross morphological examination of the embryos. Exencephalic embryos had been recovered after treatment, some of which exhibited delayed or abnormal turning in addition to the brain malformation. These responses of the embryos to the treatment had depended on the type of cross from which the embryos had come. Exencephalic embryos were found in much higher frequencies among the treated mutant crosses, those with the

associated abnormal turning being derived exclusively from the treated mutant crosses.

8. Analysis of the histology

As mentioned in section B.6 96 control and 144 treated embryos were serially cross or frontal sectioned to examine the tissue of the neural tube and to calculate mean mitotic indices. Eight embryos were examined at each of the gestational ages. Groups of both normal and exencephalic embryos from the treated crosses were examined at the D9/12, D9/18, and D10/6 collection times. Every fourth section of the cephalic region of the neural tube was studied. The slides were coded to prevent the origin of the material examined from being identified, allowing for a more objective histological analysis.

The results for the embryos of the mutant crosses were grouped together, as were those of the nonmutant crosses. It was necessary to combine the data in some manner as not all the gestational times were examined for any one cross. The classification into mutant and nonmutant crosses followed from the results of the dose-response work, with the two groups possessing significantly different slopes for the probit regression lines. It did not seem unreasonable to consider the underlying biological mechanism of the interaction as expressing itself as some unique effect on the developing brain tissue of the embryos from the mutant crosses. (See Appendix 1 listing genotypes of embryos.)

It has been stated previously (section A.2) that some teratogens primarily affect the neuroectoderm of the neural tissue , others only the mesoderm. With this in mind the mean mitotic indices were determined separately for the neuroectoderm and the mesoderm , as these tissues could show different responses to the insulin treatment.

The mean mitotic indices for the neuroectoderm of the treated and control mutant and nonmutant crosses are shown in Tables C14 and C15. The mean mitotic indices for the neuroectoderm of the control data for both the mutant (Table C14) and nonmutant (Table C15) crosses showed an increase over time , with the rate of mitotic activity on D10/6 (12.49 ± 0.36 and 11.48 ± 0.88) being roughly equal to twice that of D8/12 (6.14 ± 0.23 and 5.86 ± 0.93). Normal embryos from the treated mutant and nonmutant crosses also reflected this trend , while the exencephalic embryos from the nonmutant crosses showed a decrease in mitotic activity , with the rate on D10/6 (3.26 ± 0.39 , Table C15) being half that of D8/12 (6.21 ± 0.72). This decrease in the rate of mitosis was not seen among the exencephalic embryos from the mutant crosses. Rather , the rate by D10/6 (7.91 ± 0.51 , Table C14) was somewhat greater than the D8/12 value (5.89 ± 0.15), though it still differed considerably from the D10/6 control value (12.49 ± 0.36).

The mean mitotic indices for the mesoderm of the control data from the mutant (Table C16) and nonmutant (Table C17) crosses showed a

TABLE C14

Mean mitotic indices for the neuroectoderm of the cephalic neural tube region of embryos from treated and control mutant crosses

gestational age (day/ hours)	treated group		control group	
	no. embryos	mean M.I. ¹ \pm S.E. ²	no. embryos	mean M.I. \pm S.E.
8/12	8	5.89 \pm 0.15	8	6.14 \pm 0.23
8/18	8	5.84 \pm 0.23	8	5.93 \pm 0.40
9/6	8	6.09 \pm 0.31	8	6.52 \pm 0.16

gestational age (day/ hours)	exencephalic (abnormal body)		normal		control group	
	no. embryos	mean M.I. \pm S.E.	no. embryos	mean M.I. \pm S.E.	no. embryos	mean M.I. \pm S.E.
9/12	8	6.42 \pm 0.24	8	8.15 \pm 0.63	8	7.92 \pm 0.25
9/18	8	6.84 \pm 0.72	8	9.89 \pm 0.11	8	10.13 \pm 0.42
10/6	8	7.91 \pm 0.51	8	12.13 \pm 0.43	8	12.47 \pm 0.36

¹ M.I. = mitotic index

² S.E. = standard error

TABLE C15

Mean mitotic indices for the neuroectoderm of the cephalic neural tube region of embryos from treated and control nonmutant crosses

gestational age (day/ hours)	treated group		control group	
	no. embryos	mean M.I. ¹ \pm S.E. ²	no. embryos	mean M.I. \pm S.E.
8/12	8	6.21 \pm 0.72	8	5.86 \pm 0.93
8/18	8	6.14 \pm 0.64	8	5.32 \pm 0.80
9/6	8	6.32 \pm 0.32	8	6.14 \pm 0.24

gestational age (day/ hours)	exencephalic (normal body)		normal		control group	
	no. embryos	mean M.I. \pm S.E.	no. embryos	mean M.I. \pm S.E.	no. embryos	mean M.I. \pm S.E.
9/12	8	5.72 \pm 0.35	8	7.97 \pm 0.43	8	7.32 \pm 0.72
9/18	8	5.09 \pm 0.42	8	9.15 \pm 0.62	8	9.75 \pm 0.54
10/6	8	3.26 \pm 0.39	8	11.67 \pm 0.47	8	11.48 \pm 0.88

¹ M.I. = mitotic index

² S.E. = standard error

decrease over time. By D10/6 the rate of mitosis (4.05 ± 0.20 and 3.84 ± 0.62) was half that of D8/12 (8.43 ± 0.46 and 7.87 ± 0.72). This trend was also seen for the mean mitotic indices of the treated embryos, both normal and exencephalic, from the mutant and nonmutant crosses.

The exencephalic embryos from the treated mutant crosses sectioned and examined in this study were the embryos from the D9/12, D9/18, and D10/6 collection times that had exhibited an abnormal hindbody shape in addition to the brain malformation. This morphological phenomenon (discussed in section C.7) had not been found among any of the exencephalic embryos from the nonmutant crosses and had been seen as a distinguishing characteristic in approximately one-third of the embryos, from the mutant crosses, affected by the treatment. The obvious morphological difference between these exencephalic embryos and the ones from the nonmutant crosses had further supported the idea that histological changes might be found between the affected embryos from these two groups, and thus the exencephalics with the abnormal body shape had been chosen to represent the affected group from the mutant crosses. Yet, exencephalic embryos with a normal body shape had also been collected from the treated mutant crosses and, to determine if differences existed between these and their littermates with the abnormal body shape, sections from these embryos were examined as well. Ten treated D9/18 and ten treated D10/6

TABLE C16

Mean mitotic indices for the mesoderm of the cephalic neural tube region of embryos from treated and control mutant crosses

gestational age (day / hours)	treated group		control group	
	no. embryos	mean M.I. ¹ \pm S.E. ²	no. embryos	mean M.I. \pm S.E.
8/12	8	8.74 \pm 0.74	8	8.43 \pm 0.46
8/18	8	8.46 \pm 0.63	8	8.29 \pm 0.38
9/6	8	6.28 \pm 0.52	8	6.07 \pm 0.52

gestational age (day / hours)	exencephalic (abnormal body)		normal		control group -	
	no. embryos	mean M.I. \pm S.E.	no. embryos	mean M.I. \pm S.E.	no. embryos	mean M.I. \pm S.E.
9/12	8	5.84 \pm 0.71	8	5.73 \pm 0.21	8	5.93 \pm 0.16
9/18	8	4.96 \pm 0.69	8	5.02 \pm 0.34	8	4.87 \pm 0.29
10/6	8	3.89 \pm 0.35	8	3.92 \pm 0.60	8	4.05 \pm 0.21

¹ M.I. = mitotic index

² S.E. = standard error

TABLE C17

Mean mitotic indices for the mesoderm of the cephalic neural tube region of embryos from treated and control nonmutant crosses

gestational age (day/ hours)	treated group		control group	
	no. embryos	mean M.I. ¹ \pm S.E. ²	no. embryos	mean M.I. \pm S.E.
8/12	8	8.07 \pm 0.71	8	7.87 \pm 0.72
8/18	8	7.72 \pm 0.67	8	7.95 \pm 0.43
9/6	8	6.73 \pm 0.43	8	6.84 \pm 0.39

gestational age (day/ hours)	exencephalic (normal body)		normal		control group	
	no. embryos	mean M.I. \pm S.E.	no. embryos	mean M.I. \pm S.E.	no. embryos	mean M.I. \pm S.E.
9/12	8	6.15 \pm 0.16	8	5.84 \pm 0.56	8	5.92 \pm 0.82
9/18	8	5.02 \pm 0.53	8	4.86 \pm 0.34	8	4.97 \pm 0.54
10/6	8	3.94 \pm 0.38	8	4.07 \pm 0.40	8	3.84 \pm 0.62

¹ M.I. = mitotic index

² S.E. = standard error

embryos were sectioned and the mean mitotic indices for the neuroectoderm and the mesoderm were determined. The results are seen in Table C18.

The values of the mean mitotic indices for the mesoderm at D9/18 (5.08 ± 0.72) and D10/6 (4.09 ± 0.66) were very similar to those for the exencephalic embryos from the treated nonmutant crosses (5.02 ± 0.53 and 3.94 ± 0.38 , Table C17), and for the exencephalic embryos with the abnormal body shape from the treated mutant crosses (4.96 ± 0.69 and 3.89 ± 0.35 , Table C16). The D9/18 and D10/6 mean mitotic indices for the neuroectoderm of the exencephalic embryos with the normal body shape from the treated mutant crosses (5.17 ± 0.54 and 3.49 ± 0.37 , Table C18) also were similar to the values for the exencephalic embryos from the treated nonmutant crosses (5.09 ± 0.42 and 3.26 ± 0.39 , Table C15). Two-tailed t-tests showed that the mitotic indices at these times did not differ significantly between the two groups (for D9/18, $P > .9$; for D10/6, $P = .7-.6$).

As mentioned earlier, the mean mitotic indices for the neuroectoderm of the exencephalic embryos with the abnormal body shape from the mutant crosses did not show a decrease over time after treatment. Therefore, when comparing the D9/18 and D10/6 values (6.84 ± 0.72 and 7.91 ± 0.51 , Table C14) to the values for the exencephalics with the normal body shape from the treated mutant crosses, a greater discrepancy was noted. In this

TABLE C18.

Mean mitotic indices for the neuroectoderm and mesoderm of the cephalic neural tube region of exencephalic embryos with a normal hindbody shape from treated mutant crosses.

A. mean mitotic indices for the neuroectoderm

gestational age (day/hours)	no. embryos	mean M.I. ¹ ± S.E. ²
9/18	10	5.17 ± 0.54
10/6	10	3.49 ± 0.37

B. mean mitotic indices for the mesoderm

9/18	10	5.08 ± 0.72
10/6	10	4.09 ± 0.66

¹ M.I. = mitotic index

² S.E. = standard error

situation the mitotic indices did differ significantly between the two groups (for D9/18, $P = .05-.02$; for D10/6, $P < .001$).

In summary, the normal pattern of mitosis in the cephalic neural tube tissue, based on the control data, was seen as an increase in the mitotic rate of the neuroectodermal tissue over the period of neural tube closure and early brain formation (days 8-10). During this same period of time the rate of mitosis in the mesoderm was seen to decline. Both increments of change, the increase in rate in one tissue and the decrease in the other, were of a twofold magnitude. Mitosis in the mesoderm of the embryos from the treated mutant and nonmutant crosses, both normal and exencephalic, appeared to be unaltered by the insulin treatment, since the pattern did not seem to differ from the normal one. The mean mitotic indices for the neuroectoderm of the normal embryos from the treated mutant and nonmutant crosses also followed the pattern found in the control data. The exencephalic embryos from the treated mutant and nonmutant crosses differed from the control neuroectoderm values in the rate of mitotic activity by D10/6. The exencephalic embryos from the treated nonmutant crosses showed a twofold decrease (from the D8/12 value) in the rate of mitosis by D10/6. The exencephalic embryos with the normal body shape from the mutant crosses also showed this trend, while the D10/6 exencephalic embryos with the abnormal body shape showed a slight

0
increase in rate from the D8/12 value, though it did not appear to be as large an increase as that seen in the control data. The pattern of mitotic activity in the neuroectoderm of the D10/6 exencephalic embryos with the abnormal body shape therefore did not seem to be like that seen in either the exencephalic embryos with the normal body shape from the mutant crosses or the exencephalic embryos from the nonmutant crosses.

Deviations from the normal patterns of mitosis in these embryos seemed to be related to the effects of treatment, type of brain and hindbody formation, gestational age, and tissue layer. To determine if these relationships were significant ones, the data was analyzed by log-linear analysis, described in section B.5. As with the morphological data, only four variables could be analyzed at any one time, so that while significant interactions could be detected, they could not be ranked for importance. Scores were obtained for the mean mitotic index of the histological material (M), the gestational age of the embryo (A), whether or not the embryo came from a treated litter (T), the type of cross (N), the tissue layer histologically examined (L), the type of embryonic brain (B), and the embryonic hindbody shape (S). As the calculated mean mitotic indices were low percentage values ($< 30\%$) an arcsine transformation was applied to this data. Following the standards

established for the morphological ratings, the younger embryonic (D8/12, D8/18, and D9/6) brain type was classed as undecided, the division into exencephalic or normal being done on post D9/6 embryos only. As the main purpose was to search for true interactions of the mean mitotic Index variable with any of the others listed above, two groups of four variables each, MTNL and MABS, were analyzed, so that the mean mitotic Index was paired with each of the remaining variables. A probability value of less than or equal to .05 for both the tests of partial and marginal association was the criterion for a significant contribution by any one or set of variables tested. The results are seen in Table C19. As mentioned before, marginal association probabilities are not given for the highest order effect (i.e. MTNL) or for any of the main effects (i.e. M, T, N and L).

For the first group of variables tested, MTNL, third order effects MTN and MTL were significant. This meant that second order effects MT, MN, ML, TN, and TL, and main effects M, T, N, and L all made significant contributions to the interactions of these variables. The observed values for the mean mitotic Index were significantly related to the effect of the treatment, the type of cross from which the embryo originated, and the tissue layer being examined. The second group of variables examined, MABS, also had significant third order effects. MBS and ABS were seen to be significant interactions, and thus second order effects MA, MB, MD, AB, AS,

TABLE C19

Tests of partial and marginal associations for the variables of the mitotic index analysis

group of variables tested	effect	partial association probability	marginal association probability
MTNL	MTNL	0.7040	-
	MTN	0.0000*	0.0000*
	MTL	0.0007*	0.0008*
	MNL	0.4624	0.4637
	TNL	0.5747	0.8995
	MT	0.0000*	0.0000*
	MN	0.0005*	0.0005*
	ML	0.0000*	0.0000*
	TN	0.0412*	0.0331*
	TL	0.0425*	0.0477*
	NL	0.6475	0.9761
	M	0.0000*	-
	T	0.0026*	-
	N	0.0492*	-
	L	0.0464*	-
MABS	MABS	1.0000	-
	MAB	0.5147	0.7199
	MAS	0.7918	0.8562
	MBS	0.0422*	0.0468*
	ABS	0.0166*	0.0000*
	MA	0.0000*	0.0000*
	MB	0.0000*	0.0000*
	MS	0.0003*	0.0082*
	AB	0.0000*	0.0000*
	AS	0.0265*	0.0389*
	BS	0.0000*	0.0000*
	M	0.0001*	-
	A	0.0001*	-
	B	0.0017*	-
	S	0.0000*	-

1 variable

M = mitotic index

A = gestational age

T = treated or control

N = cross (mutant or nonmutant)

L = neuromastoderm or mesoderm

B = brain formation (normal or abnormal)

S = body shape (normal or abnormal)

and BS were also significant relationships, with main effects M, A, B, and S each making significant contributions to these effects. The mean mitotic Index values were therefore also determined in part by the gestational age of the embryo, and by whether or not the brain and hindbody structure were normal. It is interesting to note that the hindbody configuration (normal or abnormal) was also significantly related to the age of the embryo and the type of brain development (normal or exencephalic), interactions found previously in the analysis of the morphological data.

Thus any given pattern of mitotic activity seen during the period of neural tube closure was dependent on the age of the embryo and the type of tissue being examined, with any value for the mean mitotic Index showing variation with time and given tissue type (i.e. neuroectoderm or mesoderm). The control data showed that the rate of mitosis increased with time in the neuroectoderm, and decreased with time in the mesoderm. Differences in mean mitotic index values were also related to the effect of treatment, as well as to the development of abnormal brain and hindbody configurations. After insulin treatment, it was noted that the mean mitotic index for the neuroectoderm of the exencephalics from the nonmutant crosses showed a decrease over time, with the D10/6 value falling below the D8/12 value. The value for the mean mitotic index by D10/6 for the exencephalics

with the abnormal hindbody from the treated mutant crosses did not show a similar decline below the D8/12 value, but also did not show an increase in mitotic rate on the order of that seen in the control data. The type of cross (mutant and nonmutant) from which the embryo had come, and the administration of insulin, with the subsequent development of exencephaly and, in some cases, an abnormal hindbody configuration, were all seen to be significantly related to a given value for the mean mitotic index. Thus the patterns of mitotic activity seen in the neuroectoderm and the mesoderm of both control and treated embryos during the period of neural tube closure were due to the significant effects of the variables discussed above.

In addition to determining the rate of mitosis, the general appearance of the neural tissue on these coded slides was noted. The neuroectodermal tissue of both control and treated embryos consisted of a pseudostratified epithelium. Most mitoses were observed in the layer of cells that lined the lumen. These cells were easily spotted due to the presence of large nuclei containing condensed chromosomes. Cellular necrosis, characterized by cytoplasmic shrinkage and the formation of dark, dense, small nuclear bodies, was not seen in the treated tissue beyond the small amount also found in the control tissue. Gross changes in amount of the tissue were not visible.

Exencephalic embryos exhibited an open neural tube and the subsequent folding of brain tissue was reflected in the irregularity of the neuroectodermal shape (Figure C35). However, histologically the neuroectoderm remained normal, showing no signs of necrosis.

Abnormalities of the mesoderm were not detected in the sectioned material from the untreated mutant and nonmutant crosses. The mesoderm of the embryos, both normal and exencephalic, from the treated nonmutant crosses also did not show signs of degeneration. There was neither cell necrosis nor changes in tissue bulk. From the treated mutant crosses the exencephalic embryos with the normal body shape and the unaffected embryos also exhibited histologically normal mesoderm. However, the exencephalic embryos with the abnormal body configuration showed areas of somite disorganization in the thoracic and lumbar regions of the axial mesoderm. The cells of the mesodermal tissue were not necrotic, and normal amounts of the tissue were present. The developing somites, though composed of healthy tissue, were misaligned along the upper regions of the neural tube (Series C1). This was seen, as early as D9/12, only in those embryos with the abnormal body shape. The somite abnormality did not extend below the lumbar spinal region, and was not seen in the cephalic region of the neural tube.

Figure C35. A transverse section through the diencephalic brain region of a D9/12 anencephalic embryo with a normal body shape from a treated Δx $+/+$ cross. The neuroectoderm (n), instead of possessing a tubular shape enclosing the luminal cavity, shows the irregular pattern and everted tissue growth (arrows) caused by the failure of the neural folds to fuse (haematoxylin and eosin). d, diencephalon; o, optic vesicles; n, neuroectoderm. $\times 13$



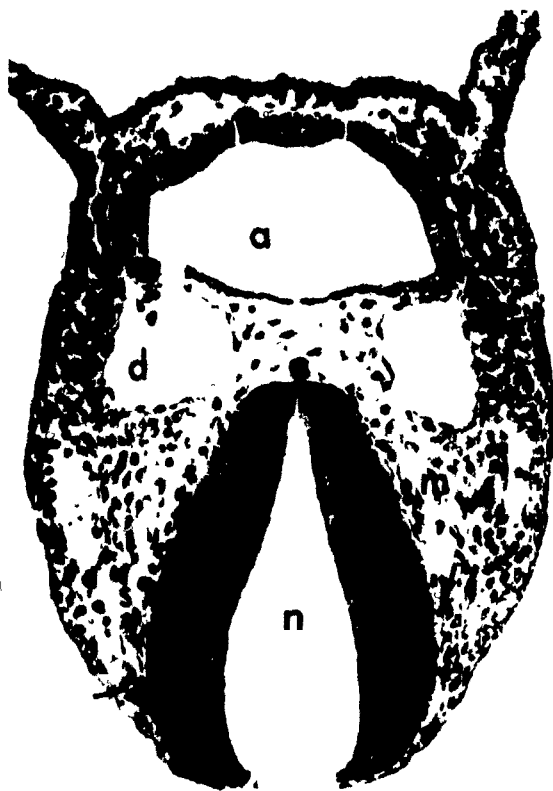
C35

Series C1. Histological sections of normal and abnormal neural and somite tissue.

- A. A transverse section through the thoracic region of a D9/l2 normal embryo from an untreated A x Cd/+ cross. Somite (s) development, proceeding normally, is readily visible (haematoxylin and eosin). sv, sinus venosus; n, neural tube; m, mesoderm. X 11
- B. A transverse section through the thoracic region of a D9/l2 exencephalic embryo with an abnormal hindbody shape from a treated A x Cd/+ cross. The somites (s) are poorly formed, with only rudimentary grouping of the tissue present (arrows) (haematoxylin and eosin). n, neural tube; d, dorsal aorta; a, atrium; mt, myocardial tissue; m, mesoderm. X 11
- C. A frontal section through the lower lumbar region of a D9/l2 normal embryo from an untreated SWV x Rf/+ cross. The developing somites (s) are properly aligned within the mesodermal tissue (haematoxylin and eosin). nc, neural tube. X 10
- D. A frontal section through the lower lumbar region of a D9/l2 exencephalic embryo with an abnormal body shape from a treated SWV x Rf/+ cross. The somites (s) are poorly formed, with large spaces (arrows) where they have failed to form. The tissue is highly disorganized. Due to the severe twisting of the hindbody the neural tube (nc) is not seen as an elongated canal structure, as shown in C (haematoxylin and eosin). X 10



A



B



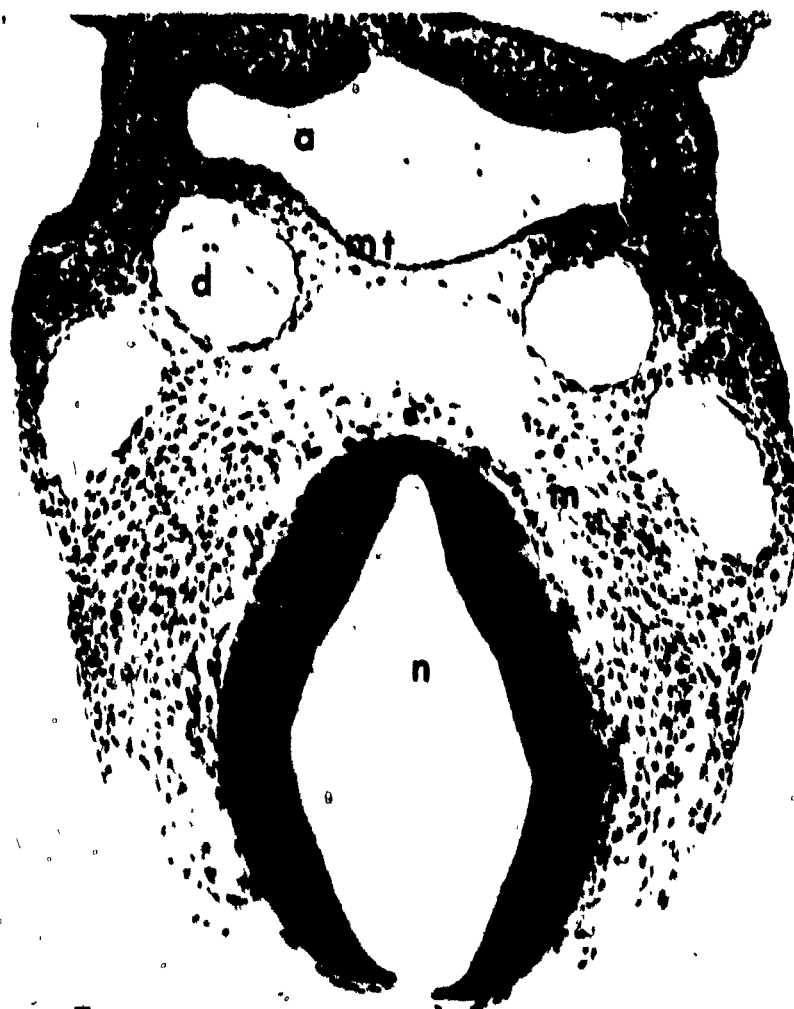
C



D

Series C1 (cont'd)

- E. A transverse section through the thoracic region of a D9/12 exencephalic embryo with an abnormal hindbody shape from a treated A x Rf/+ cross. There is a total lack of somite development, with large spaces (arrows) found in the mesodermal tissue (m), where somites are normally located (haematoxylin and eosin). a, atrium; n, neural tube; d, dorsal aorta; mt, myocardial tissue. X 12



E

Exencephalic embryos from $Rf/4 \times Rf/4$ and $Cd/4 \times Cd/+$ crosses were collected on D9 and embedded in an attempt to study sections of tissue for the abnormalities in the mesoderm described above. However, most of these embryos had already started to resorb, and the resultant extensive necroses prevented the necessary preservation of the tissue. Thus it was not possible to obtain satisfactory sections for study from these embryos.

9. Effectiveness of glucose supplements

The blood glucose values for each strain and for the given conditions were the average of two samples. Two hours prior to insulin treatment the blood glucose concentration was 170 mg per cent for the A/J strain, and 167 mg per cent for the SWV. Two hours after the injection of insulin, without a glucose supplement, the blood glucose level had decreased to 58 mg per cent for the A/J females, and 54 mg per cent for the SWV. Two hours after the insulin treatment, and one hour after the administration of a glucose supplement, the blood glucose level was 158 mg per cent for the A/J strain, and 149 for the SWV. Thus the addition of exogenous glucose prevented the severe drop in the blood glucose concentration normally seen after the administration of insulin. Table C20 shows the frequencies of exencephaly among the offspring of the crosses that received glucose supplements after the insulin treatment. The frequencies are

TABLE C20

Frequencies of exencephaly in the mutant and nonmutant crosses treated with insulin
or insulin + glucose.

cross	% exencephaly; insulin treatment (dose-response work)	% exencephaly; insulin + glucose treatment
A x Cd/+	43	37.5 (12/32)
A x $\frac{1}{4}$ Cd	20	23.3 (7/30)
A x Rf/+	58	52.9 (18/34)
A x $\frac{1}{4}$ Rf	30	35.7 (10/28)
SWV x Cd/+	73	73.7 (28/38)
SWV x $\frac{1}{4}$ Cd	35	36.1 (13/36)
SWV x Rf/+	84	80.0 (28/35)
SWV x $\frac{1}{4}$ Rf	39	41.2 (14/34)

compared to those obtained from the dose-response study, in which the effects of insulin alone were studied. The frequencies appeared to be unaltered by the addition of glucose after insulin treatment, and χ^2 tests of independence showed any differences to be nonsignificant. Therefore, although it did prevent hypoglycemia in the female, the glucose was ineffective in protecting the developing embryo from the effects of the insulin.

D. Discussion

1. Gene-teratogen interaction in insulin-induced exencephaly and resorption

The females from the crosses tested in this study were injected with one of several doses of insulin, and the dose-response curves for both insulin-induced exencephaly and resorption were determined. Probit analysis, specifically designed to deal with quantal responses, was employed to determine these regression lines. The slopes of the probit regression lines reflect the rate of the developmental process, being either the formation of exencephaly or the death of the embryo. Parallel lines indicate that the rate of a process is the same for the given groups of samples. If the regression lines are not parallel then the rate of the developmental process is different from one group to the next. The quality, as well as the quantity, of the response of the embryos within one group to the treatment is unique. Intersecting dose-response lines infer that the biological mechanisms at work in the formation of the malformation within one group are different from those acting upon the other group.

For insulin-induced exencephaly, in the crosses involving the A/J females, the probit regression lines for the mutant crosses ($A \times Cd/+$, $A \times Rf/+$) could be fitted to a common slope, indicating that the independently fitted slopes did not differ significantly from one another. The probit regression lines

for the nonmutant crosses ($A \times +/+^{Cd}$, $A \times +/+^{Rf}$, $A \times A$) could also be fitted to a common slope, one that was significantly different from that of the mutant crosses. These results were duplicated in the crosses involving the SWV females. The meaning of these differences in the slope values of the probit regressions may be better understood if one converts the frequency distributions of the response over the range of doses, seen in these crosses, to the distributions of tolerances that underlie the response. The tolerance of a subject is a measure of the tendency to respond. The underlying tolerance distributions of the response fit a normal distribution. As described earlier (section B.3), the observed frequencies of the response are converted to probit values, which represent set increments of deviation from the mean response. These probits may, in turn, be assigned ordinate values of the normal curve (page 157, Rohlf and Sokal, 1969). If these values are plotted against the logarithm of the dose, the normal distribution of the tolerance underlying the response is obtained. These are shown for the probit regression lines of the A crosses in Figure D1. One can see that the response of the embryos from the mutant crosses (1 and 2) extended over a much narrower range than the response of the embryos from the nonmutant crosses (3, 4, and 5). That is to say, the variances of the tolerance distributions for the mutant crosses were smaller than the variances for the nonmutant crosses. When

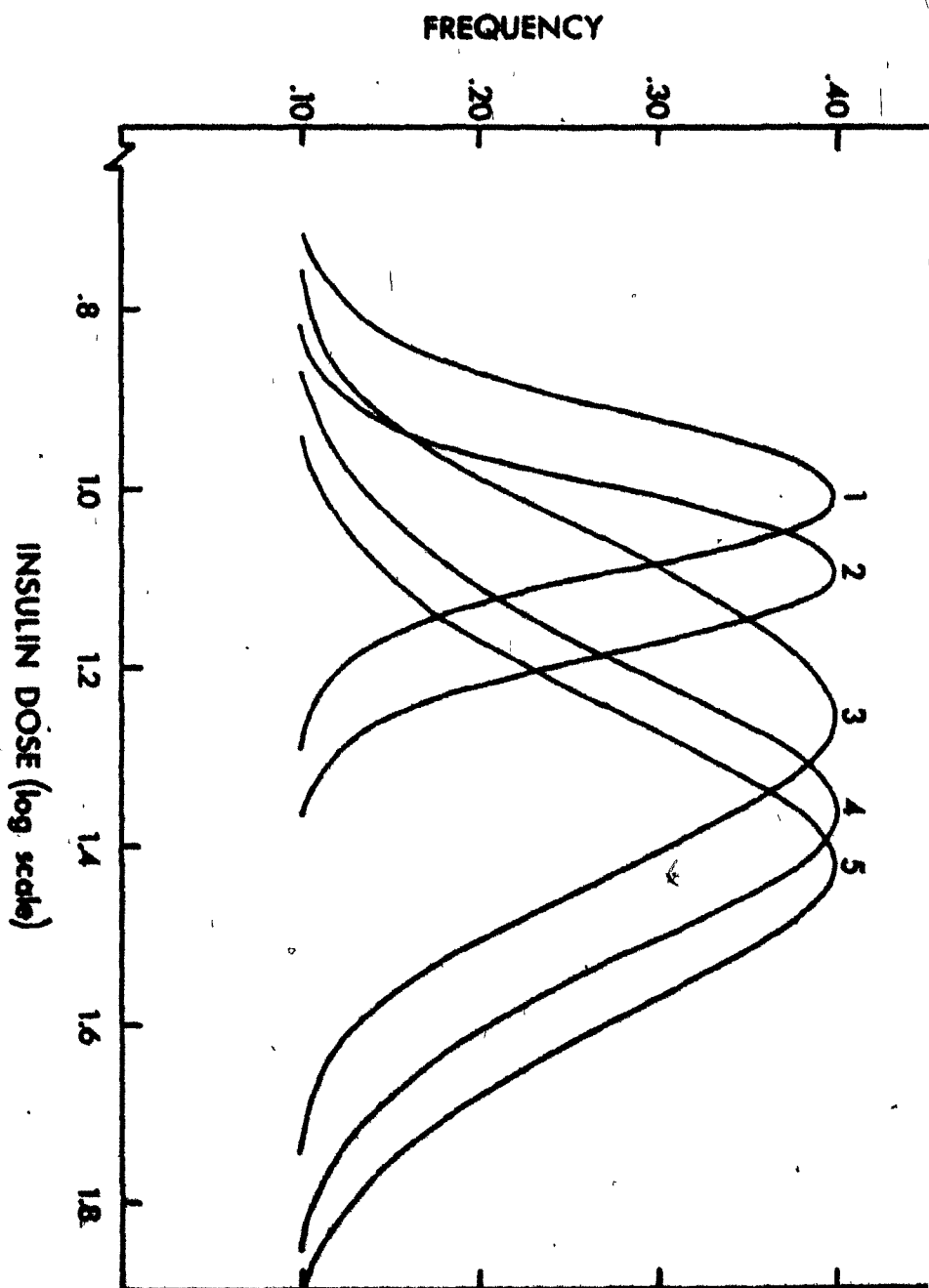


Figure D1. Dosage-tolerance distributions of insulin-induced exencephaly for the crosses with the A/J dams.

1-A x B6/+
 2-A x Cd/+
 3-A x +/+^m
 4-A x A
 5-A x +/+^{cd}

these distributions are converted to a linear representation, the smaller variances are seen as steeper slopes of the lines. Thus the probit regression lines for the mutant crosses possessed steeper slopes, and the common slope was significantly different from the one for the regression lines of the nonmutant crosses, as determined by a statistical procedure.

In biological terms, this meant that the embryos from the mutant crosses responded to the insulin treatment by developing exencephaly by a mechanism that was different from the one acting on the embryos from the nonmutant crosses. The mutant crosses, having heterozygote males as sires, generated a population of both wild-type and heterozygote offspring. To postulate the presence of a gene-teratogen interaction it had to be maintained that the heterozygote embryos were the ones responding to the teratogen by a mechanism different from the one present in the affected wild-type embryos. As exencephaly was induced in the embryos of the nonmutant crosses, it follows that some of the exencephalic embryos from the mutant crosses were wild-type. However, if a true interaction exists, a significantly larger proportion of the exencephalics from the mutant crosses should also carry one of the mutant genes. The Crooked-tail (Cd) and Rib fusions (Rf) mutant genes in their heterozygous form both affect skeletal development. Cd/+ mice possess fused, small, or irregular shaped vertebral centra, and Rf/+ mice have fused ribs. After clearing

and staining the skeletons of the embryos from the SWV crosses of the dose-response study it was determined that, in fact, a significantly greater number of the embryos with the rib or vertebral defects were also exencephalic. This suggested that the Rf and Cd genes had interacted with the teratogen.

The Insulin-induced resorption data were also fitted to probit regression lines for each of the crosses. For the crosses with the SWV females, the slopes of the probit lines for both the mutant and nonmutant crosses could be fitted to a common slope. Therefore these regression lines were all parallel to one another. For the crosses with the A/J females, the probit regression lines for the mutant crosses were parallel, as were the lines for the nonmutant crosses. However, the common slope for the probit lines of the mutant crosses differed significantly from the one for the probit lines of the nonmutant crosses. Furthermore, for the mutant crosses, the common slope for the induced resorption regression lines did not differ significantly from the one for the induced exencephaly regression lines. When this comparison was repeated with the common slopes of the regression lines for induced exencephaly and resorption in the nonmutant crosses the same results were found. For the SWV crosses, on the other hand, the common slope of the parallel regression lines for the resorption data did not differ significantly from the common slope of the induced exencephaly regression lines for the nonmutant crosses. If the slope characterizes the nature of the response, and since these slopes are not significantly different, it is then

tempting to speculate that, for the SWV crosses, the underlying biological mechanism evoked by the insulin administration and acting on the embryos from the nonmutant crosses to produce the brain malformation is the same mechanism responsible for the resorption of the embryos from both the mutant and nonmutant crosses. Similarly for the A crosses, the embryos from the mutant crosses resorb and develop exencephaly by the actions of the same mechanism, a mechanism that is distinct from the one acting on the embryos from the nonmutant crosses. More specifically, the mechanism acting on the heterozygote embryos from the mutant crosses to resorb and develop exencephaly should be distinct from the one acting on the wild-type embryos from both the mutant and nonmutant crosses. Yet, several factors argue against this concept.

The embryos from insulin treated crosses were also collected and examined during the period of neural tube closure and early brain formation (D8-D10). When the frequencies of exencephaly of these embryos were compared to the frequencies from the dose-response study, in which embryos had been collected at a later gestational age, the A crosses showed significantly higher frequencies of exencephaly among the younger embryos. The SWV crosses did not show significant changes in the frequencies. Also, approximately 30% of the embryos from the treated mutant crosses, collected on D9 and D10, exhibited a severe twisting of the body shape. For reasons to be expanded upon in the latter part of this chapter these embryos were believed to be Cd4 and

Rf/4 embryos. The older embryos (D14 or D18) collected for the dose-response work never demonstrated these extreme external body shape abnormalities. One possible explanation for the decreased frequencies of exencephaly in the mutant crosses (A/J females) composed of the older embryos could involve a mechanism in which these abnormal body shaped embryos were selectively resorbed between days 9 and 14. Yet, the high frequency of exencephalics collected from the mutant crosses for the dose-response study, whose fused ribs or abnormal centra marked them as heterozygotes, argues against the existence of such a mechanism. Also, it does not explain the decrease in frequencies among the nonmutant crosses (A/J females) composed of the older embryos, where the mutant genes were not present.

Thus it was not possible to relate two different responses (exencephaly and resorption) of the embryo to one another by a common biological mechanism. Furthermore, if the slope represents the rate of some developmental process, finding two different responses with the same rate may very well not be a valid reason to propose that the underlying biological mechanisms at work must be the same for the two processes. The argument that the processes of induced resorption and induced exencephaly are related is, at best, a weak one.

It is far more interesting to compare the dose-response curves for the A/J crosses to those of the SWV crosses. The same type of response, i.e. brain malformation, could be compared. However, the slope of a probit regression line is representative of the response only over the range of doses used. Unfortunately, it was necessary to administer higher concentrations of insulin to the SWV females, which eliminated the opportunity to conduct a bona fide comparison. Keeping this in mind, it is nevertheless intriguing to note that the common slope of the regression lines for the mutant A crosses did not differ significantly from that for the mutant SWV crosses. A comparison of the common slopes of the regression lines for the nonmutant A and SWV crosses also found nonsignificant differences between the values. It might indicate that the gene-teratogen interaction was independent of the genetic background on which the mutant genes were placed. However, this could only be conclusively established by outcrossing these genes to other inbred strains whose tolerances for insulin fell within one of the range of doses used in this study.

2. The teratogenicity of insulin

Extensive work has been done in an attempt to determine the teratogenicity of insulin. One of the major questions surrounding the issue has been whether insulin acts directly on the developing embryonic tissue, or whether

the hypoglycemia caused by the insulin treatment is the agent of action.

Most of the studies have involved the use of chick embryos. Landauer (1945) had noted that preincubated chick embryos injected in the yolk sac with insulin developed a high frequency of rumplessness. This malformation is characterized by the absence of the tail vertebrae. Such a response to the insulin treatment could be elicited up to the thirtieth hour of incubation, followed by a decline in the frequency to 0% by 96 hours (Landauer and Bliss, 1946). Such a decrease in the frequency was well correlated with the establishment of circulation in the embryos. At this time, however, injections of insulin produced micromelia, a defect of the long bones of the appendicular skeleton, and parrot beak, a shortening of the maxillary bones. Landauer had shown, therefore, that the treatment affected different tissues at different periods in development, but still had not conclusively demonstrated that the insulin was acting directly on these tissues.

Moseley (1947) studied the development of insulin treated chicks during the first six days of incubation. Insulin had been injected into the yolk sac prior to incubation, and the embryos were examined for the progression of rumplessness. The caudal abnormalities began to appear at D2.5 of incubation, when the tissue of the tail was still mostly undifferentiated. Circulation was not

yet established, and the gut cavity was still exposed to the fluid of the yolk sac. It was concluded that the insulin could directly reach the embryonic tissue, causing a disruption of cell division and the subsequent degeneration of the tissue. The disruption of carbohydrate metabolism after insulin treatment was demonstrated by Zwilling (1951). He injected insulin into the yolk sac on day five of incubation, inducing micromelia. Total carbohydrate, free sugar, and glycogen were assayed in both the yolk sac and the embryonic membranes. Compared to the control values, the insulin treated yolk sac showed a significant increase in total glycogen and total carbohydrate concentrations, while the blood from the vitelline vein of the chick embryo showed a decrease in total carbohydrate and free sugar levels. It was felt that the insulin acted on the yolk sac membranes, causing an inhibition of glycogenolysis, which in turn prevented the release of glucose needed by the embryo to maintain growth and differentiation.

Once the upset in carbohydrate metabolism was established, it next became necessary to determine if the defect was due to insufficient amounts of substrate, i.e. glucose loss due to hypoglycemia, or due to the blockage of a specific pathway in the process of respiration. When insulin treatment was supplemented with α -ketoglutaric acid (Zwilling, 1949) or sodium pyruvate (Landauer, 1948), it was found that the occurrence of rumpleness was absent. Nicotinamide did not offer protection against insulin-induced rumpleness, but

did prevent insulin-induced micromelia (Landauer and Rhodes, 1952). These agents, in combination with insulin, prevented the occurrence of the defect in the presence of a decreased blood sugar level. The injection of sulfanilamide, which has no effect on the blood sugar level, into the yolk sac of day 4 chick embryos also produced the micromelia, muscle hypoplasia, and parrot beak seen after insulin treatment (Zwilling and DeBell, 1950). Barron and McKenzie (1962) performed in vitro experiments with the explants of days 2 - 4 chick embryos. The insulin-treated tissue was grown on media supplemented with diphosphopyridine nucleotide (DPN, also known as NAD), or the reduced form of the coenzyme (DPNH). DPN protected the tissue from induced micromelia, its reduced form did not. They also determined that most of the nicotinamide in the chick embryonic tissue was present as DPN. They concluded that insulin effectively blocked the DPN-mediated pathways of carbohydrate metabolism. The inability of the DPNH to offer protection suggested that the reoxidation of reduced DPN, regenerating the coenzyme in its active form, could be the metabolic step blocked by insulin.

Sulphonamides, known for their ability to disrupt the functioning of DPN-linked dehydrogenases, also caused insulin-like malformations whose frequencies were diminished when nicotinamide was given as well (Landauer and Wakasugi, 1968).

Thus, the effect of insulin on carbohydrate metabolism was not simply one of substrate depletion. Loss of available glucose was secondary to the effect of insulin on the DPN-mediated pathways. A loss of functional DPN would close down not only the Krebs cycle, but also the transfer of hydrogen atoms to the electron transport chain, from which the largest proportion of cellular ATP is derived. The expenditure of ATP is involved in many energy requiring processes, including cell division, and loss of this major energy source could only lead to severe disruption of cell activities.

In mammals, the situation is complicated by the presence of a placenta. Defects in brain, vertebral, and rib development have been established after insulin treatment in mice (Smithberg and Runner, 1963). Tolbutamide, which also lowers the blood sugar level, produced malformations similar to those of insulin, and nicotinamide supplements did not protect against the effects of tolbutamide or insulin. Therefore the authors concluded that the hypoglycemia produced by the treatments was the active teratogenic agent. Previous experiments with mice in which fasting on D9 led to substrate depletion, indicated by decreased blood sugar levels, also produced exencephaly and vertebral defects (Smithberg et al, 1956; Runner, 1959). The defects were eliminated if glucose was administered to prevent the drop in blood sugar. It had also been shown that labeled insulin, when injected into pregnant rats, did not cross the placental barrier (Goodner et al, 1969).

In the present study, exencephaly was found in the offspring of female mice treated with insulin on day 8 of gestation. Rib and vertebral malformations were also present in some of the treated embryos. Analysis of the frequencies of the rib and vertebral malformations in offspring of both the mutant and nonmutant crosses, treated and untreated, showed that these abnormalities were due to the presence of one of the mutant genes, Cd. or Rf, and were not caused by the treatment. Treatment with glucose shortly after the injection of insulin avoided hypoglycemia by maintaining the blood sugar level of the treated female within normal limits. Yet the frequencies of exencephaly were not significantly altered by the administration of glucose after the insulin treatment. In this experiment, a decrease in substrate availability was not the main factor disrupting carbohydrate metabolism. Further studies, using nicotinamide to suppress the action of insulin, are needed to determine if the disturbance involves the NAD-mediated pathways of oxidative phosphorylation, as suggested by the work on chick embryo metabolism.

It is highly possible that the insulin acted directly on the embryonic tissues of the affected offspring from the treated crosses. The embryo relies on nutrients from the yolk sac for several days after implantation before the establishment of true placenta late D8 or early D9 (Green, 1966). Degenerative changes occur in the endometrium after implantation in the uterine wall. This causes the rupture

of blood-filled sinusoids in the tissue surrounding the embryo, filling the cavity around the embryo with blood from the maternal circulatory system. Though the yolk sac surrounds the embryo, a true filtering process is established only when the placenta later forms. Therefore, if the placenta has not been firmly established by mid D8, the insulin could reach the differentiating tissues of the developing embryo and disrupt normal cellular activity.

3. The underlying biological mechanism of the interaction

The study of mitosis in the neural tube was first undertaken by Sauer (1935). The closure of the neural tube in chick embryos was examined. It was found that, as the tissue on either side of the neural groove is pushed up to form neural folds, the neuroectoderm becomes characterized by columnar epithelial type cells layered three or four deep. The basal ends (opposite the side lining the lumen) of the cells were highly uneven and totally detached from one another, as opposed to the apical ends. The latter side possessed numerous terminal bars attaching the cells to each other at their free surface. As the neural folds approached fusion, the cells became more elongated, with many more layers of nuclei seen at the luminal surface.

In a later study Langman et al (1966) elaborated on the behavior of the neuroectodermal cells during the fusion of the neural folds. Chick embryos from

18 to 32 hours of age were treated with tritium-labelled thymidine to examine the duration of the cell cycle and migration of the cell nucleus during neural tube closure. It was noted that the neuroectoderm was a pseudostratified layer of columnar cells. During the cycle of DNA synthesis prior to division, the nuclei of these cells were located near the basal surface in the outer zone of the neuroectoderm; with the cytoplasmic processes extending towards the luminal surface. This gave the neuroectodermal cells an overall wedge shape, with the narrow apex lining the lumen. When the nucleus was ready to divide it migrated towards the apical end of the cell, which was the surface of the cell in contact with the lumen of the developing neural tube. During mitosis the cell became quite large and round and, in doing so, reversed the orientation of the cell's wedge shape. After completion of mitosis, the nuclei of the daughter cells migrated back to their original position in the outer zone, returning the cell to its initial appearance. Langman exposed the cells to vincristine, which arrests the cells in metaphase, and noted that the neural folds failed to close, but instead grew in the everted manner characteristic of exencephaly. Examination of the cells showed that the nuclei, in arrested mitosis, were accumulated in the inner zone and depicted as a higher than normal proportion of dividing cells along the luminal surface. Corresponding to this, the wedge shape of many of the cells was oriented so that the broad base lined the surface of the lumen. Therefore, it was concluded that the wedge shape of the cells guided the

direction of movement. In the normal situation, the broad base of the wedge was located on the outer surface for many of the cells, forcing these cells of the neural folds to turn inward, as their direction of movement, and fuse. In the case of arrested mitosis, an abnormally high proportion of the large, round nuclei were located at the inner surface. The broad base of these cells lined the lumen, causing the direction of movement of the neuroectodermal cells to be reversed, and leading to everted growth of the neural folds. This model is especially attractive for determining the cause of neural tube nonclosure when, as with insulin treatment, a large loss in volume of the neuroectodermal tissue was not present. One cannot then propose insufficient amounts of the tissue as the reason for the failure of the neural folds to meet and fuse.

In the present study, the control data indicated that the pattern of mitotic activity in the neuroectoderm consisted of a twofold increase in the rate by D10/6, when compared to the rate at D8/12. The rate of mitosis in the neuroectoderm appeared to be affected by the administration of insulin, while the rate in the underlying mesoderm seemed to be unaltered by the treatment. The normal embryos from the treated mutant and nonmutant crosses followed the trend of mitotic activity seen in the control groups. The exencephalic embryos from the treated nonmutant crosses and the exencephalic embryos with the normal body shape from the treated mutant crosses showed, by D10/6, a twofold decrease from the D8/12 value in the rate of mitosis in the neuroectoderm. In fact, the D10/6 values of the mean mitotic indices for these two groups of affected embryos were not significantly different from one another.

This decrease in the rate of mitosis after treatment may have occurred as a direct effect of the insulin on the carbohydrate metabolism of the cell. A lack of substrate availability was eliminated as a potential cause, but the possibility that insulin successfully blocked some enzyme-mediated pathway of oxidative phosphorylation still existed. The resulting depletion of ATP stores would bring to a halt all energy-requiring cell processes, of which cell division was one. The disruption of cell division may have, as in the case of vincristine treatment, resulted in an abnormally large proportion of cells possessing the reverse wedge shape present during mitosis, which in turn forced the neuroectodermal cells of the folds to grow in an outwards direction. The turning process of the embryo, from an S to a C-shaped configuration was seen to be delayed in up to 37% of the embryos from the treated mutant and nonmutant crosses. The lack of available ATP after insulin treatment could also explain the lag in this energy-dependent process.

The embryos demonstrating the decrease in neuroectodermal cell activity were probably not the ones heterozygous for one of the mutant genes. The exencephalics whose neuroectoderm showed a twofold decrease in mitotic rate were from the treated nonmutant crosses, making them clearly wild-type, or were the normal body shaped ones from the treated mutant crosses, again suggesting that they did not possess one of the mutant genes. The mutant crosses produced wild-type and heterozygous offspring in a 1:1 ratio. Thus, knowing that exencephaly was


Induced in the offspring of the treated nonmutant crosses, some of the embryos from the mutant crosses responding to the insulin treatment were of the wild-type genotype. The large decrease in the rate of mitosis in the cells of the neuroectoderm after insulin treatment may therefore be limited to the wild-type embryos.

This concept is further supported if one looks at mitosis in the neuroectoderm of the exencephalic embryos with the abnormal hindbody shape from the treated mutant crosses. It is suggested that these embryos were heterozygous for one of the mutant genes, for reasons to be dealt with later in this discussion. Approximately 30% of the embryos from each of the treated mutant crosses exhibited extensive twisting and kinking of the lower body region. These embryos were always exencephalic. The rate of mitosis in the neuroectoderm of these embryos appeared to differ from those of the untreated embryos, the exencephalic embryos from the treated nonmutant crosses, and the exencephalic embryos with the normal hindbody shape from the treated mutant crosses. The rate of mitosis did not decrease below the D8/12 value, but instead followed the trend, shown by the control data, to undergo a gradual and continuous increase during the period of neural tube closure and early brain formation. However, the D10/6 value of the mean mitotic index never reached a value that was twice the magnitude of the D8/12 value, suggesting that the increase seen in these exencephalic embryos was not as large as that in the control embryos. The D10/6 mean mitotic index of these embryos differed significantly from that of both the normal shaped exencephalics from the treated mutant crosses and the exencephalics from the treated nonmutant crosses. Thus the insulin treatment appeared

to slow the increase in the rate of mitosis in the neuroectoderm of these embryos, but was not able to greatly decrease the rate, as had been seen in the exencephalic embryos with the normal body shape from both the nonmutant and mutant crosses. The progression of the increase in the rate of neuroectodermal mitosis had been slowed, but not stopped, and certainly not reversed. It cannot be conclusively proven or disproven at this time that this slowing down of the increase in the mitotic rate after insulin treatment was, by itself, sufficient to cause exencephaly in the embryos with the abnormal body shape. The fact that the other exencephalics showed a marked decrease, by D10/6, in the rate of mitosis, compared to the D8/12 value, argues that a very severe change is necessary for damage to the neuroectoderm, sufficient to cause exencephaly, to occur. Yet, if one considers a threshold effect, then the exencephalic embryos with the abnormal body shape could be demonstrating the minimal amount of damage needed for the production of exencephaly. The other exencephalics with the severe decrease in the neuroectodermal mitotic rate are simply expressing a more severe form of the damage, over and above that needed to cause the brain malformation. Several factors argue against the latter. Assuming, as before, that the normal body shaped exencephalic embryos are of the wild-type genotype, the latter idea suggests the wild-type embryos to be more susceptible to the teratogenic effects of insulin. The lower frequencies of exencephaly among the nonmutant crosses as determined by the dose-response study does not support such a concept.

It has also been assumed that the abnormal body shaped embryos were heterozygous for one of the mutant genes. These Rf/+ and Cd/+ individuals were carrying genes that, in their homozygous form, produced spontaneous exencephaly. Rf/+ x Rf/+ and Cd/+ x Cd/+ matings were set up and the litters were examined for spontaneous exencephaly. The exencephalic embryos collected possessed a kinking and twisting of the hindbody that closely resembled the abnormal body shape seen in the exencephalic embryos from the treated mutant crosses. Histological analysis of the affected embryos from the treated mutant crosses indicated areas of somite disorganization in the thoracic and lumbar regions of the neural tube. Abnormal somite development had been isolated as one of the characteristics of both the Cd and Rf homozygous mutants (Morgan, 1954; Thaller and Stevens, 1960). These homozygotes often were resorbed by D9 or D10, yet both the exencephaly and the abnormal kinking of the body shape could still be recognized. In the heterozygous form, the effect of the mutant genes on the developing axial mesoderm led to fused ribs (Rf genotype) and small, fused vertebral centra (Cd genotype), defects that, while serving as markers for the presence of the genes, did not cause fatal disruptions in development.

The similarity of the twisted body shape of the exencephalic embryos, from the treated mutant crosses, to the body shape of the untreated exencephalic embryos homozygous for one of the mutant genes argues for the former being



heterozygous for one of the genes. The insulin interacted with the mutant genes to produce phenocopies of the homozygous state. The insulin disrupted the somite organization of the developing heterozygote, mimicking the condition as it occurs spontaneously in the homozygotes. The somite disorganization led to extensive kinking and twisting of the body, causing a distortion of the normal C - shaped configuration. The mechanical stress exerted on the developing neural tube by the abnormal body shape could thus exert a force sufficient to prevent the neural folds from fusing.

Thus the formation of exencephaly in the gene-carrying embryos of the mutant crosses may be separated from its development in the wild-type embryos by postulating two distinct mechanisms. The wild-type embryos may have developed exencephaly by a disruption of mitosis in the cells of the neuroectoderm. The severe interruption in the rate of mitosis was due to a blockage of carbohydrate metabolism that extended beyond a mere decrease in substrate availability. The subsequent loss of ATP resulted in a cessation of mitotic activity. As the cells were prevented from initiating or completing the division process, the accumulation of large, round nuclei, ready to divide, along the surface of the lumen distorted the spatial orientation of the neuroectodermal cells, forcing them to move in an outwards direction. Thus, the neural folds did not fuse, but instead grew apart in an everted manner.

The mutant crosses produced both wild-type and heterozygote offspring. The exencephalic embryos with the normal body shape from the treated mutant crosses were wild-type embryos, and the apparent decrease in the rate of mitosis in the neuroectoderm could have caused exencephaly in the manner described above.

The exencephalic embryos with the abnormal body shape were thought to be heterozygous for one of the mutant genes. The constant increase in the rate of mitosis in the neuroectoderm, as seen in the control data, seemed to be slowed by the insulin, but never decreased to the point where the value fell below the D8/12 value. This effect of the insulin may therefore be considered as secondary to the effect on the developing somites. It is hypothesized that the insulin treatment disrupted the somite organization in a manner that mimicked the naturally occurring condition among the mutant homozygotes. The presence of either of the mutant genes predisposed the mouse to exencephaly, with the insulin interacting with the genes to produce phenocopies. The subsequent kinking of the body placed severe stress on the neural folds, preventing their fusion and leading to the condition of exencephaly.

E. Summary

The following points are a summary of the main observations and conclusions presented in this thesis.

1. The nonparallelism of the dose-response curves of Insulin-Induced exencephaly for the crosses with the A/J dams indicated the presence of a gene-teratogen interaction. The probit regression lines for the mutant crosses ($Cd/+ \times A$, $Rf/+ \times A$) could be fitted to a common slope that was significantly different from the common slope of the probit regression lines for the nonmutant crosses ($+/+^{Cd} \times A$, $+/+^{Rf} \times A$, $A \times A$).

2. A gene-teratogen interaction was also indicated from a study of the dose-response curves of Insulin-Induced exencephaly for the crosses with the SWV dams. The probit regression lines for the mutant crosses ($Cd/+ \times SWV$, $Rf/+ \times SWV$) were fitted to a common slope, one that was significantly different from the common slope of the regression lines for the nonmutant crosses ($+/+^{Cd} \times SWV$, $+/+^{Rf} \times SWV$, $SWV \times SWV$).

3. For Insulin-Induced resorption, the dose-response curves for the crosses with the A/J dams were also nonparallel. The probit regression lines for the mutant crosses fitted a common slope that was significantly different from the common slope of the regression lines for the nonmutant crosses. Furthermore,

the slope values for these two groups did not differ significantly from those found for the probit regression lines of insulin-induced exencephaly.

4. The dose-response curves of insulin-induced resorption for the crosses with the SWV dams could be fitted to one common slope, and the slope value for these parallel lines was not significantly different from the one found for the probit regression lines of insulin-induced exencephaly for the nonmutant crosses.

5. Examination of the skeletal structure of D18 embryos from the treated SWV crosses indicated that a significantly higher frequency of exencephalic embryos from the mutant crosses possessed rib and vertebral malformations. Analysis of the data indicated this to be due to the expression of the mutant genes, and not due to the administration of insulin, suggesting that many of the exencephalic embryos, from the mutant crosses, were heterozygous for either the Cd or the Rf gene.

6. Morphological examination of embryos during the period of neural tube closure revealed that some of the exencephalic embryos, from the treated mutant crosses only, also possessed an abnormal twisting of the hindbody structure that mimicked the abnormal configuration occurring spontaneously among exencephalic embryos homozygous for either of the mutant genes. Log-linear

analysis of the data showed significant relationships to exist among the patterns of turning and neural tube closure, treatment, and origin (the cross) of the embryo.

7. Histological examination of control and treated tissue indicated that the neuroectoderm of exencephalic embryos (with a normal body shape) from the treated nonmutant crosses undergoes a reduction in the rate of mitosis after treatment. The neuroectoderm of exencephalic embryos, with an abnormal body shape, from the treated mutant crosses did not show this decreased rate, although the rate also did not increase to the control values. Mitosis in the mesoderm of both groups appeared to be unaltered by the treatment. Somites in the thoracic and lumbar regions of exencephalic embryos with the abnormal body shape were seen to be poorly developed, with some disorganization and misalignment of the tissue.

8. An underlying biological mechanism for the gene-teratogen interaction is postulated, in which wild-type embryos developed exencephaly after insulin treatment due to decreased mitotic activity in the neuroectoderm. In the exencephalic embryos with the abnormal hindbody shape, believed to be heterozygous for one of the mutant genes, changes in the mitotic activity of the neuroectoderm were secondary to the abnormal body configuration. This placed a stress on the developing neural folds, preventing their fusion and leading to exencephaly.

Appendix 1: List of genotypes of the embryos comprising the mitotic index analysis.

	<u>gestational age</u>					
	8/12	8/18	9/6	9/12	9/18	10/6
<u>normal</u>	2 Cd/+ x A	2 Cd/+ x A	2 Cd/+ x A	2 Cd/+ x A	2 Cd/+ x A	2 Cd/+ x A
	2 RE/+ x A	2 RE/+ x A	2 RE/+ x A	2 RE/+ x A	2 RE/+ x A	2 RE/+ x A
<u>mutant</u>	2 Cd/+ x SWV	2 Cd/+ x SWV	2 Cd/+ x SWV	2 Cd/+ x SWV	2 Cd/+ x SWV	2 Cd/+ x SWV
<u>and</u>	2 RE/+ x SWV	2 RE/+ x SWV	2 RE/+ x SWV	2 RE/+ x SWV	2 RE/+ x SWV	2 RE/+ x SWV
<u>nonmutant</u>	2 +/+ ^{RE} x SWV	2 +/+ ^{Cd} x SWV	2 +/+ ^{RE} x SWV	2 +/+ ^{RE} x SWV	2 +/+ ^{Cd} x SWV	2 +/+ ^{RE} x SWV
(control	1 +/+ ^{Cd} x SWV	1 SWV x SWV	2 SWV x SWV	2 SWV x SWV	2 +/+ ^{RE} x SWV	1 SWV x SWV
<u>and</u>	2 SWV x SWV	2 +/+ ^{RE} x A	1 +/+ ^{RE} x A	1 +/+ ^{Cd} x A	1 SWV x SWV	2 +/+ ^{Cd} x A
<u>treated</u>)	1 +/+ ^{RE} x A	2 +/+ ^{Cd} x A	1 +/+ ^{Cd} x A	1 +/+ ^{RE} x A	1 +/+ ^{Cd} x A	1 +/+ ^{RE} x A
	2 +/+ ^{Cd} x A	1 A x A	2 A x A	2 A x A	1 +/+ ^{RE} x A	2 A x A
					1 A x A	
<u>encephalic</u>				2 Cd/+ x A	2 Cd/+ x A	2 Cd/+ x A
<u>mutant</u>				2 RE/+ x A	2 RE/+ x A	2 RE/+ x A
				2 Cd/+ x SWV	2 Cd/+ x SWV	2 Cd/+ x SWV
<u>and</u>				2 RE/+ x SWV	2 RE/+ x SWV	2 RE/+ x SWV
<u>nonmutant</u>				2 +/+ ^{Cd} x SWV	1 +/+ ^{RE} x SWV	1 +/+ ^{RE} x SWV
				1 SWV x SWV	1 +/+ ^{Cd} x SWV	2 SWV x SWV
(treated				2 +/+ ^{RE} x A	2 SWV x SWV	2 +/+ ^{RE} x A
<u>only</u>)				1 +/+ ^{Cd} x A	2 +/+ ^{Cd} x A	1 +/+ ^{Cd} x A
				2 A x A	2 +/+ ^{RE} x A	2 A x A

BIBLIOGRAPHY

- Adelmann, H. B. 1925. The development of the neural folds and cranial ganglia of the rat. J. Comp. Neurol. 39: 19 - 172.
- Adinolfi, M., Beck, S., Embury, S., Polani, P. E., and Seller, M. J. 1976. Levels of alpha-fetoprotein in amniotic fluids of mice (curly-tail) with neural tube defects. J. Med. Genet. 13: 511-513.
- Allen, J. R., Marlar, R. J., Chesney, C. F., Helgeson, J. P., Kelman, R., Weckel, K. G., Traisman, E., and White, J. W. 1977. Teratogenicity studies on late blighted potatoes in nonhuman primates (Macaca mulatta and Saguinus labiatus). Terat. 15: 17 - 24.
- Auerbach, R. 1954. Analysis of the developmental effects of a lethal mutation in the house mouse. J. Exp. Zool. 127: 305-327.
- Barber, A. L. 1957. The effects of maternal hypoxia on inheritance of recessive blindness in mice. Am. J. Opthath. 44: 94-101.
- Barron, P., and McKenzie, J. 1962. The inhibitory action of insulin in the early chick embryo. J. Embryol. Exp. Morph. 10: 88-98.
- Beaudoin, A. R. 1969. Serum protein and diazo dye teratogenesis. Terat. 2: 85-90.
- Beaudoin, A. R. 1974. Teratogenicity of sodium arsenate in rats. Terat. 10: 153-158.
- Beck, S. 1963. Frequencies of teratologies among homozygous normal mice compared with those heterozygous for anophthalmia. Nature 200: 810-811..
- Beck, S. 1964. Sub-line differences among C57 black mice in response to trypan blue and outcross. Nature 204: 403-404.
- Bergquist, H. 1959. Experiments on the "overgrowth" phenomenon in the brain of chick embryos. J. Embryol. Exp. Morph. 7: 122-127.
- Biddle, F. G. 1977 a. 6-aminonicotinamide-induced cleft palate in the mouse: the nature of the difference between the A/J and C57Bl/6J strains in frequency of response and its genetic basis. Terat. 16: 301-312.

- Biddle, F. G. 1977b. Can we discriminate between mechanism of cleft palate induction. Terat. 15: 21A (Abst.)
- Biddle, F. G., and Fraser, F. C. 1976. Genetics of cortisone-induced cleft palate in the mouse-embryonic and maternal effects. Genet. 84: 743-754.
- Biddle, F. G., and Fraser, F. C. 1977. Genetic independence of the embryonic reactivity difference to cortisone and 6-aminocaproamide induced cleft palate in the mouse. Terat. (In press)
- Blanc, R., and Child, G. P. 1940. Somatic effects of temperature on development in Drosophila melanogaster II. Phys. Zool. 13: 65-72.
- Blanc, R., and Villee, C. L. 1942. The effect of x-irradiation upon bristle pattern in Drosophila melanogaster. Univ. Cal. Publ. Zool. 49: 51-60.
- Bonnevie, K. 1934. Embryological analysis of gene manifestation in Little and Bagg's abnormal mouse tribe. J. Exp. Zool. 67: 443-520.
- Bonnevie, K. 1936. Pseudencephaly als spontane recessive mutation bei der hausmaus. Skr. Norske. Vidensk-Akad Oslo. 9: pp. 39.
- Brock, D. J., and Sutcliffe, R. O. 1972. Alpha-fetoprotein in the antenatal diagnosis of anencephaly and spina bifida. Lancet 2: 197-199.
- Brown, K. S., and Hame, L. C. 1973. Recessive anencephalus in the oel strain of mice. Genet. 74: 531-532 (abst.)
- Bruch, R. M. 1967. Congenital head and brain malformations in mice homozygous for a recessive mutation. Anat. Rec. 157: 220-221 (abst.)
- Bundt, V., Vare, A. M., and Monte, I. W. 1976. Craniospinal defects and hydrocephalus in rat fetuses following intra-amniotic injection of cadmium sulphate solution. Terat. 14: 18A (abst.).
- Burda, D. 1968. Studies on the experimental induction of overgrowth in chick embryos. Anat. Rec. 161: 419-426.
- Butler, J., and Lyon, M. F. 1967. Homozygotes and heterozygotes for bent-tail (Bn). MNL 36: 36.
- Cardell, E. L., and Langman, J. 1977. Light and electronmicroscopic studies on cell death in the embryonic mouse brain. Terat. 15: 15A (abst.).

- Carpenter, S. J., and Fern, V. 1977. Early stages in the development of exencephaly in arsenic-treated hamster embryos. *Terat.* 15: 23A (abst.).
- Carter, T. C. 1959. Embryology of the Little and Bagg X-rayed mouse stock. *J. Genet.* 56: 401-435.
- Carter, C. O., and Evans, K. 1973. Spina bifida and anencephalus in Greater London. *J. Med. Genet.* 10: 209-234.
- Carter, C. O., Laurence, K. M., and David, P. A. 1967. The genetics of the major central nervous system malformations, based on the South Wales socio-genetic investigation. *Dev. Med. Child. Neurol.* 9: 30-34.
- Chaube, S., and Murphy, M. L. 1969. Fetal malformations produced in rats by N-Isopropyl-d- (2-methyl hydrazino)-p-tolluamide hydrochloride (procarbazine). *Terat.* 2: 23-32.
- Chaurasia, B. D., and Singh, T. B. 1976. The medial dorsal opening in human anencephaly. *Terat.* 14: 237A (abst.).
- Chesley, P. 1935. Development of the short-tailed mutant in the house mouse. *J. Exp. Zool.* 70: 429-455.
- Child, G. P., Blanc, R., and Plough, H. 1940. Somatic effects of temperature on development in *Drosophila melanogaster* I. Phenocopies and reversal of dominance. *Phys. Zool.* 13: 56-64.
- Cockraft, D., and Coppola, P. 1977. Teratogenic effects of excess glucose on head-fold rat embryos in culture. *Terat.* 16: 141-146.
- Coffey, V. P., and Jessop, W. J. E. 1957. A study of 137 cases of anencephaly. *Br. J. Prev. Soc. Med.* 11: 174-180.
- Collman, R. D., and Stoller, A. 1968. The occurrence of anencephalus in the state of Victoria, Australia. *J. Ment. Defic. Res.* 12: 22-35.
- Corbett, T. H., Beaudoin, A. R., and Cornell, R. G. 1975. Teratogenicity of polybrominated biphenyls. *Terat.* 11: 15A (abst.).

- Coulombre, A. J., and Coulombre, J. L. 1958. The role of mechanical factors in brain morphogenesis. *Anat. Rec.* 130: 289-290.
- Crowley, K., Geelan, J., and Langman, J. 1978. Repair mechanisms in the embryonic spinal cord after a chemical insult. *Terat.* 17: 1-12.
- Dagg, C. P. 1967. Combined action of fluorouracil and two mutant genes on limb development in the mouse. *J. Exp. Zool.* 164: 479-489.
- Daniels, E., and Moore, K. 1972. A direct analysis of early chick embryonic neuroepithelial responses following exposure to EDTA. *Terat.* 6: 84-97.
- David, T. J., and Nixon, R. 1976. Congenital malformations associated with anencephaly and lencephaly. *J. Med. Genet.* 13: 263-265.
- Degenhardt, K. H., Franz, J., and Yamamura, H. 1968. A model in comparative teratogenesis: dose response to 5-fluoro-2-deoxycytidine in organogenesis of mice of strains C57Bl/6J Han Ffm and C57Bl/10J Ffm. *Terat.* 1: 311-334.
- Dencker, L. 1977. Trypan blue accumulation in the embryonic gut of rats and mice during the teratogenic phase. *Terat.* 15: 179-184.
- Desesso, J. 1976. Teratogenic effects of concanavalin A in the New Zealand white rabbit. *Terat.* 13: 20A (abst.).
- Desmond, M. E., and Jacobson, A. G. 1977. Embryonic brain enlargement requires cerebrospinal fluid pressure. *Devel. Biol.* 57: 188-196.
- Duraiswami, P. K. 1950. Insulin-induced skeletal abnormalities in developing chickens. *Br. Med. J.* 2: 384-390.
- Edwards, M. J. 1968. Congenital malformations in the rat following induced hyperthermia during gestation. *Terat.* 1: 173-178.
- Elwood, J. M. 1974. Anencephalus in Canada: 1943-1970. *Am. J. Epidemiology.* 100: 288-296.
- Elwood, J. M. 1977. Anencephalus and drinking water composition. *Am. J. Epidemiology* 105: 460-468.

- Elwood, J. H., and Nevin, N. C. 1973. Factors associated with anencephalus and spina bifida in Belfast. Br. J. Prev. Soc. Med. 27: 73-80.
- Enzmann, E., and Haskins, C. 1939. Note of modification in the morphogenesis of *Drosophila melanogaster* occurring under neutron bombardment. Am. Nat. 73: 470-472.
- Fedrick, J. 1974. Anencephaly and maternal tea drinking: evidence for a possible association. Proc. Roy. Soc. Med. 67: 356-360.
- Fern, V. H. 1958. Teratogenic effects of trypan blue on hamster embryos. J. Embryol. Exp. Morph. 6: 284-287.
- Fern, V. H. 1971. Developmental malformations induced by cadmium. Biol. Neonate 19: 101-107.
- Finney, P. J. 1971. Probit Analysis, 3rd ed., Cambridge University Press, Cambridge, U. K.
- Forthoefel, P. 1972. The effects on mouse development of interactions of 5-fluorouracil with Strong's luxoid gene and its plus and minus modifiers. Terat. 6: 5-18.
- Forthoefel, P., and Williams, M. L. 1975. The effects of 5-fluorouracil and 5-fluorodeoxyuridine used alone and in combination with normal nucleic acid precursors on development of mice in lines selected for low and high expression of Strong's luxoid gene. Terat. 11: 1-20.
- Freeman, R. B., and Hughes, A. F. W. 1975. Analysis of overgrowth in chick embryos with neuraxial anomalies. Terat. 11: 18A (abst.).
- Gardner, W. J. 1961. Rupture of the neural tube, the cause of myelomeningocele. Arch. Neurol. 4: 1-7.
- Geelen, J., and Langman, J. 1977. Fusion of the neural walls in the cephalic region of the mouse embryo and abnormalities in the closure process. Terat. 15: 16A (abst.).
- Gibson, J. E., and Becker, B. A. 1968. Effects of phenobarbital and SKF525-A on the teratogenicity of cyclophosphamide in mice. Terat. 1: 393-398.

- Gilani, S. 1974. Teratogenic effects of methylmercury in the chick embryo. *Terat.* 9: 17A (abst.).
- Giroud, A., and Martinet, M. 1957. Morphogénèse de l'anencéphalie. *Arch. Anat. Microsc. Morph. Exp.* 46: 247-264.
- Gluecksohn-Schoenheimer, S. 1945. The embryonic development of mutants of the Sd strain in mice. *Genet.* 30: 29-38.
- Goldschmidt, R. 1917. A preliminary report on some genetic experiments concerning evolution. *Am. Nat.* 52: 28-50.
- Goldschmidt, R. 1935. Gen und ausseneligen schaft (untersuchungen an Drosophila) I und II. *Zeitschr. f. Ind. Abst. u vererb.* 69: 38-131.
- Goldschmidt, R. 1945. Additional data on phenocopies and genic action. *J. Exp. Zool.* 100: 193-201.
- Goodner, C. J., Conway, M. J., and Werrbach, J. H. 1969. Relation between plasma glucose levels of mother and fetus during maternal hypoglycemia; hyperglycemia, and fasting in the rat. *Pediat. Res.* 3: 121-127.
- Greenhouse, G., and Hamburgh, M. 1968. Analysis of trypan-blue induced teratogenesis in Rana pipiens embryos. *Terat.* 1: 61-74.
- Grossman, E., and Smith, T. 1933. Genic modifications in Drosophila melanogaster induced by heat irradiation. *Am. Nat.* 67: 429-436.
- Hamburgh, M. 1952. Malformations in mouse embryos induced by trypan blue. *Nature.* 169: 27-36.
- Hamburgh, M. 1954. The embryology of trypan blue-induced abnormalities in mice. *Anat. Rec.* 119: 409-429.
- Hamburgh, M., Herz, L., and Landa, W. 1970. Effect of trypan blue on expressivity of brachyury gene 'T' in mice. *Terat.* 3: 111-118.

- Hamburgh, M., Mendiza, L., Rader, M., Lang, A., Silverstein, H., and Hoffman, K. 1974. Malformations induced in offspring of crowded and parabiotically stressed mice. Terat. 10: 31-38.
- Hannah, R. S., and Moore, K. L. 1971. Effects of fasting and insulin on skeletal development in rats. Terat. 4: 135-410.
- Hayes, A. W., Hood, R. D., and Lee, H. L. 1974. Teratogenic effects of ochratoxin A in mice. Terat. 9: 93-98.
- Hersh, A. H., and Ward, E. 1932. The effect of temperature on wing size in reciprocal heterozygotes of vestigial in Drosophila melanogaster. J. Exp. Zool. 61: 223-244.
- Hickey, E. D., and Klein, N. W. 1971. Changes in DNA, RNA, and protein content of regions of explanted chick embryos following insulin treatment. Terat. 4: 453-460.
- Horejsi, J., Jelinek, R., Laznicka, M., and Losticky, C. 1973. Effects of histone on morphogenesis of chick embryonic constituents I. The teratogenic range. Terat. 7: 73-84.
- Horowitz, I., and McDonald, A. D. 1969. Anencephaly and spina bifida in the province of Quebec. Can. Med. Ass. J. 100: 748-755.
- Hoshino, K., Nakane, K., and Kaneyama, Y. 1972. Effects of the maternal administration of trypan blue during pregnancy on the manifestation of genetic microphthalmia in mouse fetuses. Terat. 6: 105A (abst.).
- Inouye, M., and Murakami, U. 1975. Teratogenicity of N-methyl-N'-nitro-N-nitrosoguanidine in mice. Terat. 12: 198A (abst.).
- Ives, P. T. 1939. The effects of high temperature on bristle frequencies in scute and wild-type males of Drosophila melanogaster. Genet. 24: 315-331.
- Jaffee, O. C. 1974. The effects of moderate hypoxia and moderate hypoxia plus hypercapnea on cardiac development in chick embryos. Terat. 10: 82-97.
- Inouye, M. 1976. Differential staining of cartilage and bone in fetal mouse skeleton by Alcian blue and alizarin Red S. Congenital Anomalies 16: 171-173.

- James, A., and Novak, K. 1977. Cerebrospinal fluid production in experimentally communicated hydrocephalus. *Exp. Brain Res.* 27: 553-562.
- Jelinek, R., Kyzlink, V., and Blatny, C. 1976. An evaluation of the embryotoxic effects of blighted potatoes on chick embryos. *Terat.* 14: 335-342.
- Johnson, D. R. 1967. Extra-toes: a new mutant gene causing multiple abnormalities in the mouse. *J. Embryol. Exp. Morph.* 17: 543-564.
- Johnson, D. R. 1970. Trypan blue and extra-toes locus (Xt^J). *Terat.* 3: 114-125.
- Jurilloff, D. M. 1978. Genetics of spontaneous and 6-aminonicotinamide-induced cleft lip in mice. Ph.D. Thesis. McGill University.
- Kasirsky, G., and Tansy, M. D. 1971. Teratogenic effects of methamphetamine in mice and rabbits. *Terat.* 4: 131-134.
- Kilham, L., and Fern, V. 1976. Exencephaly in fetal hamsters following exposure to hyperthermia. *Terat.* 14: 323-326.
- Kochhar, D. M. 1968. Studies on vitamin A-induced teratogenesis: effects on embryonic mesenchyme and epithelium, and on incorporation of H^3 -thymidine. *Terat.* 1: 299-310.
- Knox, E. G. 1970. Fetus-fetus interaction, a model aetiology for anencephalus. *Dev. Med. Child Neurol.* 12: 167-177.
- Knox, E. G. 1974. Anencephalus and dietary intakes. *Proc. Roy. Soc. Med.* 67: 355-356.
- Kvist, T. N. 1975. The teratogenic effect of vitamin A on brain formation and head flexion in the chick embryo. *Terat.* 11: 26A-27A (abst.).
- Landauer, W. 1945. Rumplessness of chicken embryos produced by the injection of insulin and other chemicals. *J. Exp. Zool.* 98: 65-77.
- Landauer, W. 1948. The effect of nicotinamide and -ketoglutaric acid on the teratogenic action of insulin. *J. Exp. Zool.* 109: 283-290.

- Landauer, W. 1954. On the chemical production of developmental abnormalities and of phenocopies in chicken embryos. *J. Cell. Comp. Phys.* 43: 261-305.
- Landauer, W. 1957. Niacin antagonists and chick development. *J. Exp. Zool.* 136: 509-530.
- Landauer, W. 1960. Nicotine-induced malformations of chick embryos and their bearing on the phenocopy problem. *J. Exp. Zool.* 143: 107-122.
- Landauer, W. 1965. Gene and phenocopy: selection experiments and tests with 6-aminonicotinamide. *J. Exp. Zool.* 160: 345-354.
- Landauer, W., and Bliss, C. I. 1946. Insulin-induced rumplessness of chickens. III. The relationship of dosage and of developmental stage at time of injection to response. *J. Exp. Zool.* 102: 1-22.
- Landauer, W., and Rhodes, M. B. 1952. Further observations on the teratogenic nature of insulin and its modification by supplementary treatment. *J. Exp. Zool.* 119: 221-261.
- Landauer, W., and Wakasugi, N. 1968. Teratological studies with sulphonamides and their implications. *J. Embryol. Exp. Morph.* 20: 261-284.
- Langman, J., Guerrant, R. L., and Freeman, B. G. 1966. Behavior of neuroepithelial cells during closure of the neural tube. *J. Comp. Neurol.* 127: 399-412.
- Lary, J., and Hood, R. 1977. Developmental interactions between T-2 toxin and the brachyury gene in mice. *Terat.* 15: 19A (abst.).
- Leck, I. 1966. Changes in the incidence of neural tube defects. *Lancet* 2: 791-793.
- Leck, I. 1974. Causation of neural tube defects: clues from epidemiology. *Br. Med. Bull.* 30: 158-163.
- Lee, H. Y., Hikida, R., and Levin, M. 1976. Neural tube defects caused by 5-bromodeoxyuridine in chicks. *Terat.* 14: 89-98.

- Lemire, R. J., Beckwith, J. B., and Warkany, J. 1978. Anencephaly. Raven Press; New York.
- Lewontin, R. C. 1974. The analysis of variance and the analysis of causes. *Am. J. Hum. Genet.* 26: 400-411.
- Lichtenstein, H., Guest, G., and Warkany, J. 1951. Abnormalities in offspring of white rats given protamine zinc insulin during pregnancy. *Proc. Soc. Exp. Biol. Med.* 78: 398-402.
- Little, C. C., and Bagg, H. G. 1923. The occurrence of two heritable types of abnormality among the descendants of X-rayed mice. *Am. J. Roentgenol.* 10: 975-989.
- Marín-Padilla, M. 1966. Mesodermal alterations induced by hypervitaminosis A. *J. Embryol. Exp. Morph.* 15: 261-269.
- Marín-Padilla, M. 1970. Morphogenesis of anencephaly and related malformations. *Curr. Top. Path.* 51: 145-162.
- Marín-Padilla, M., and Fern, V. 1965. Somite necrosis and developmental malformations induced by vitamin A in the golden hamster. *J. Embryol. Exp. Morph.* 13: 1-8.
- McCallion, D. J. 1972. Teratogenic action of heterologous kidney antisera in mice. *Terat.* 5: 11-18.
- McDonald, A. D., Williams, M. C., and West, R. 1974. Neural tube defects and herpes virus type 2 - test of a hypothesis. *Terat.* 10: 13-16.
- Mercier-Porot, L., and Tuchmann-Duplessis, H. 1974. Action of diphenylhydantoin in pregnant rats and mice. *Terat.* 9: 28A (abst.).
- Müller, J. 1962. Teratogenic effect of maternal fasting in the house mouse. *Can. J. Genet. Cytol.* 4: 69-78.
- Morgan, W. 1954. A new crooked tail mutation involving distinct pleiotropism. *J. Genet.* 52: 354-373.
- Morris, G. M., and Steele, C. E. 1977. Comparison of the effects of retinol and retinoic acid on postimplantation rat embryos in vitro. *Terat.* 15: 109-120.

- Maseley, H. R. 1947. Insulin-induced rumpleness of chickens
IV. Early embryology. J. Exp. Zool. 105: 279-316.
- Murakami, U., Hoshino, K., and Inoue, M. 1972. An experimental
observation on the morphogenesis of reopening the cranium.
Cong. Anom. 12: 157-171.
- Naggar, L. 1971. Anencephaly and spina bifida in Israel. Pediat.
47: 577-586.
- Naggar, L., and MacMahon, B. 1967. Ethnic differences in the prevalence
of anencephaly and spina bifida in Boston, Massachusetts.
N. Engl. J. Med. 277: 1119-1123.
- Nakano, K. K. 1973. Anencephaly: a review. Dev. Med. Child
Neurol. 15: 383-400.
- Patten, B. M. 1952. Overgrowth of the neural tube in young human
embryos. Anat. Rec. 113: 381-393.
- Patten, B. M. 1968. Human Embryology. 3rd ed., McGraw Hill;
New York. pp. 74-79.
- Pederson, L., Tygstrup, I., and Pederson, J. 1964. Congenital
malformations in newborn infants of diabetic women. Lancet.
1: 1124-1136.
- Pierro, L. J., and Haines, J. S. 1977. Maternal genotype and cadmium-
induced exencephaly and eye defects in the mouse. Terat.
15: 23A (abst.).
- Pierro, L. J., Haines, J. S., and Oaman, S. F. 1977. Teratogenicity and
toxicity of purified -chaconine and -solanine. Terat.
15: 23A (abst.).
- Plough, H. 1933. Heat-induced mutations in *Drosophila* and their evolutionary
significance. Am. Nat. 67: 83-84 (abst.).
- Plough, H., and Ives, P. 1935. Induction of mutations by high temperature
in *Drosophila*. Genet. 20: 42-69.

- Plunkett, C. R. 1926. The interaction of genetic and environmental factors in development. *J. Exp. Zool.* 46: 181-244.
- Rajchgot, H. 1971. 6-aminonicotinamide-induced cleft lip and embryonic face shape in mice. M. Sc. thesis, McGill University.
- Ream, J. R., Weingarten, P. L., and Pappas, A. M. 1970. Evaluation of the prenatal effects of massive doses of insulin in rats. *Terat.* 3: 29-32.
- Recklinghausen, von F. 1886. Untersuchungen über die spina bifida. Bruck und Verlag von Georg Reimer, Berlin. pp.170.
- Renwick, J. 1973. Prevention of anencephaly and spina bifida in man. *Terat.* 8: 321-324.
- Rohlf, F. J., and Sokal, R. R. 1969. Statistical Tables. W. H. Freeman and Co. San Francisco.
- Runner, M. 1959. Inheritance of susceptibility to congenital deformity. Metabolic clues provided by experiments with teratogenic agents. *Pediat.* 23: 245-252.
- Sadler, T. W. 1977. In vitro development of mouse embryos during early stages of tissue and organ differentiation: a model for teratological research. *Terat.* 15: 27A (abst.).
- Sauer, F. 1935. Mitosis in the neural tube. *J. Comp. Neurol.* 62: 377-405.
- Scott, F. W., de La Hunte, A., Schultz, R. D., Blumer, S. I., and Rills, R. C. 1975. Teratogenesis in cats associated with griseofulvin therapy. *Terat.* 11: 79-86.
- Shenefelt, R. E. 1972. Morphogenesis of malformations in hamsters caused by retinoic acid: relation to dose and stage of treatment. *Terat.* 5: 103-118.
- Shepard, T., and Greenaway, J. 1977. Teratogenicity of cytochalasin D in the mouse. *Terat.* 16: 131-136.
- Shimada, M., Yamano, T., Nakamura, T., Morikawa, T., and Kuwatsuki, T. 1977. Effect of maternal malnutrition of matrix cell proliferation in the cerebrum of mouse embryo: an autoradiographic study. *Pediat. Res.* 11: 728-731.

- Singh, S., and Singh, J. 1974. The teratogenic effect of mitomycin C in chick embryos. *Terat.* 10: 98A (abst.).
- Skalko, R. G., Packard, D. S., Schwendimann, R. N., and Raggio, J. F. 1971. The teratogenic response of mouse embryos to 5-bromodeoxyuridine. *Terat.* 4: 87-94.
- Smith, C. J., and Kelleher, P. 1977. Alpha-fetoprotein and albumin in experimentally-induced exencephaly in the rat. *Terat.* 16: 71-78.
- Smithberg, M., and Runner, M. N. 1963. Teratogenic effects of hypoglycemic treatments in inbred strains of mice. *Am. J. Anat.* 113: 479-489.
- Smithberg, M., Sanchez, H. W., and Runner, M. N. 1956. Congenital deformity in the mouse induced by insulin. *Anat. Rec.* 126: 441 (abst.).
- Snell, G. D., Fekete, E., Hummel, K. P., and Law, L. W. 1940. The relation of mating, ovulation and the estrous smear in the house mouse to time of day. *Anat. Rec.* 76: 39-54.
- Sokal, R., and Rohlf, F. J. 1969. Biometry: the principles and practice of statistics in biological research. W. H. Freeman and Co., San Francisco.
- Spiers, P., Pietrzyk, K. J., Piper, J., and Glebati, S. 1974. Human potato consumption and neural tube malformation. *Terat.* 10: 125-128.
- Stanley, W. 1935. The effect of temperature upon wing size in *Drosophila*. *J. Exp. Zool.* 69: 459-495.
- Strong, L. C., and Hollander, W. F. 1949. Hereditary loop-tail in the house mouse. *J. Hered.* 40: 329-334.
- Swinyard, C., and Chaube, S. 1973. Are potatoes teratogenic for experimental animals? *Terat.* 8: 349-358.
- Theiler, K. 1972. The House Mouse. Springer-Verlag, New York.

- Theiler, K., and Stevens, L. 1960. The development of rib fusions, a mutation in the house mouse. *Am. J. Anat.* 106: 171-181.
- Theodosius, D. T. 1974. Pathogenesis of vitamin A-induced exencephaly in mice. Ph. D. Thesis, McGill University.
- Trimble, B., and Baird, L. 1978. Congenital anomalies of the central nervous system: incidence in British Columbia, 1952-1972. *Terat.* 17: 43-50.
- Turbow, M. M., Clark, W. H., and Dipaulo, C. 1971. Embryonic abnormalities in hamsters following intrauterine injection of 6-aminonicotinamide. *Terat.* 4: 427-432.
- Wallace, M. 1976. Report on the exencephaly (xn) mouse. *MNL* 55: 10.
- Warkany, J. 1971. Congenital Malformations. Notes and Comments. Year Book Medical Publ., Chicago.
- Warkany, J., and Petering, H. G. 1971. Congenital malformations of the central nervous system in rats produced by maternal zinc deficiency. *Terat.* 5: 319-334.
- Warkany, J., and Takacs, E. 1959. Experimental production of congenital malformations in rats by salicylate poisoning. *Am. J. Pathol.* 35: 315-331.
- Watney, M., and Miller, J. 1964. Prevention of a genetically determined congenital eye anomaly in the mouse by the administration of cortisone during pregnancy. *Nature.* 202: 1029-1031.
- White, P. 1949. Pregnancy complicating diabetes. *Am. J. Med.* 7: 609-614.
- Wilson, D. B. 1974. Proliferation in the neural tube of the splash mutant mouse. *J. Comp. Neurol.* 154: 249-256.
- Wilson, D. B., and Michael, S. D. 1975. Surface defects in ventricular cells of brains of mouse embryos homozygous for the loop-tail gene: scanning electron microscopic study. *Terat.* 11: 87-98.

- Wilson, J., and Vallance-Owen, J. 1966. Congenital deformities and insulin antagonism. *Lancet* 2: 940-942.
- Winfield, J. B., and Bennett, D. 1971. Gene-teratogen interactions: potentiation of ACM-D teratogenesis in the house mouse by the lethal gene brachyury. *Terat.* 4: 157-170.
- Yamamura, H., Deguchi, H., and Sawano, J. 1972. Some histological findings in developing exencephalous brain of mouse embryos induced by a cadmium salt. *Terat.* 6: 124A (abst.).
- Yen, S., and MacMahon, B. 1968. Genetics of anencephaly and spina bifida. *Lancet* 2: 623-626.
- Zwilling, E. 1949. Association of hypoglycemia with insulin micromelia in chick embryos. *J. Exp. Zool.* 109: 197-214.
- Zwilling, E. 1951. Insulin-induced hypoglycemia and rumplessness in chick embryos. *J. Exp. Zool.* 117: 65-73.
- Zwilling, E., and DeBell, J. T. 1950. Micromelia and growth retardation as independent effects of sulfanilamide in chick embryos. *J. Exp. Zool.* 115: 59-81.